EFFECTS OF SULFURIC AND NITRIC ACIDS ON CATION LEACHING FROM AN ULTISOL

By

LEWIS A. GASTON

A DISSERTATION PRESENTED TO THE GRADUATE SCHOOL
OF THE UNIVERSITY OF FLORIDA IN
PARTIAL FULFILLMENT OF THE REQUIREMENTS
FOR THE DEGREE OF DOCTOR OF PHILOSOPHY

UNIVERSITY OF FLORIDA

1987

ACKNOWLEDGEMENTS

I would like to express my appreciation to Dr. R. S. Mansell for his support and guidance during this research. Through my association with Dr. Mansell I have gained insight and improved scholarship. I would also like to thank the rest of my supervisory committee, Dr. R. D. Rhue, Dr. P. S. C. Rao, Dr. A. R. Overman, and Dr. W. W. McFee, and also Dr. P. Nkedi-Kizza for their advice and critical review of this dissertation. I would further like to thank a former committee member, Dr. B. G. Volk, now at the University of Missouri, for his advice and assistance during the early stages of this project. I must also thank Dr. S. A. Bloom for his invaluable assistance in preparing the many figures included in this work. An expression of gratitude is always due one's family. I would, therefore, like to formally thank my wife, C. F. Gaston, for her support and encouragement. Although she may have grown weary of being a virtual single parent, she did not, to my knowledge, start dating again.

This work was supported in part by the U.S. Environmental Protection Agency under Project A0457-06 entitled "Effects of Acid Deposition on Ion Mobilities in Selected Soils."

TABLE OF CONTENTS

PAGE

ACKNOWLEDGEMENTS ii

ABSTRACT v

CHAPTERS

1 INTRODUCTION 1

2 LITERATURE REVIEW 4

- Factors Affecting Anion Mobility 5
- Sorption Mechanisms 11
- Chemical Models 14
- Transport Models 17

3 MATERIALS AND METHODS 21

- Column Leaching Experiments 21
- Soil Analyses 23
- Soil Minerals and Texture 27
- Tracer Breakthrough Curves 27

4 RESULTS AND DISCUSSION 29

- Anion Sorption Isotherms 29
- Leaching Experiments 32
  - Application of pH 3.0 Acids to Column of Topsoil 32
  - Application of pH 3.7 Acids to Column of Topsoil 46
  - Application of pH 4.7 Acids to Column of Topsoil 48
  - Application of pH 3.0 Acids to Columns of Subsoil 54
  - Application of pH 3.7 Acids to Column of Subsoil 62
  - Application of pH 4.7 Acids to Columns of Subsoil 67

Charge Balance 69
Topsoil 70
Subsoil 70
Precipitation Reactions of Sulfate and Aluminum Solubility 72
Simulation Models and Results 78
Transport Model 78
Chemical Equilibrium Model 79
Comparison of Transport Model Results to an Analytical Solution for Cation Transport Involving Binary, Homovalent, Non-preference Exchange 90
Equilibrium Model Results 93
Use of pH-dependent Anion Sorption Isotherms 102
NonEquilibrium Model 107

5 CONCLUSIONS 118

Leaching Experiments 118
Leaching Simulations 119

BIBLIOGRAPHY 122

APPENDICES

A ANION SORPTION DATA 128

B COLUMN LEACHING DATA 129

C COMPUTER PROGRAMS 152

BIOGRAPHICAL SKETCH 162

Abstract of Dissertation Presented to the Graduate School
of the University of Florida in Partial Fulfillment of the
Requirements for the Degree of Doctor of Philosophy

EFFECTS OF SULFURIC AND NITRIC ACIDS ON CATION LEACHING FROM AN ULTISOL

By

LEWIS A. GASTON

August 1987

Chairman: R. S. Mansell
Cochairman: R. D. Rhue
Major Department: Soil Science

Packed columns of Cecil series (Typic Hapludult) topsoil and subsoil materials were leached with either HNO_3 or H_2SO_4 solutions at pH 3.0, 3.7, and 4.7. Effluent was fractionally collected and analyzed for basic cations and sulfate. Breakthrough curves for ion concentrations in effluent from columns receiving pH 3.0 H_2SO_4 showed retarded losses of Ca, Mg, H, and Al compared to the case when pH 3.0 HNO_3 was applied. Differences due to type of acid applied were greater for the subsoil than for the topsoil. Similar effects, though much reduced, were produced when pH 3.7 acids were applied to subsoil columns. Acid type produced no differences in leaching rates for pH 4.7 solutions. Breakthrough curves were integrated, corrected for soluble salts, and compared to amounts of H input. Net retention of cations for the subsoil leached with pH 3.0 H_2SO_4 was marked

relative to that observed when pH 3.0 HNO_3 was applied. All other treatments showed net losses of cations. Net losses occurred for the pH 3.7 treatments. Apparent net losses were greatest for the pH 4.7 treatments. Small net losses from the topsoil leached with pH 3.0 H_2SO_4 were likely due to overestimation of the charge borne by Al. Retention or loss of cations appeared related to SO_4^{2-} sorption-desorption.

A simple mixing-cell transport model coupled with a chemical equilibrium submodel that included anion sorption was used to describe H^+-induced cation leaching. Although the model predicted later cation breakthroughs for leaching with H_2SO_4 than with HNO_3, predicted breakthroughs were later than experimentally observed. Due to wide variations in soil pH, the Freundlich isotherms used were inadequate to describe SO_4^{2-} sorption. Modification of the chemical submodel to include time-dependent cation exchange and explicit pH-dependence of anion sorption are apparently needed to achieve agreement of model results with experimental data.

CHAPTER 1

INTRODUCTION

Soil acidification results from any regime of processes that results in net removal of basic and addition of acidic cations. The natural process of leaching that tends to occur as water moves through soil may effect soil acidification if the losses of bases are not offset by inputs by atmospheric deposition or nutrient recycling or releases by mineral weathering. Biologic processes within the soil tend to generate H^+ ions. Oxidation of N and S liberates H^+ and respiration releases CO_2 which combines with H_2O to form the weak acid, H_2CO_3. Some nutrient uptake by plants is also acidifying.

Natural acidifying processes may be aggravated by soil management practices. Nutrient recycling is interrupted by removal of ions during harvesting. Amendments of oxidizable N fertilizers tend to accelerate H^+ production in the soil.

Soil acidification is also effected by anthropogenic (i.e., man-made) deposition of sulfuric and nitric acids. The effect of this additional acidifying process, however, has been estimated to be small compared to that due to amendments of N fertilizers (McFee et al., 1983). Furthermore, management practices of agricultural soils regularly include application of limestone. McFee et al (1983) concluded that for an unmanaged forest soil, however, the effect of acid deposition on base leaching and acidification, particularly the mobilization of Al, may be deleterious to plant growth.

One factor which would seem to mitigate these potentially adverse effects is sorption of anions from the acidic leaching solution. If input anion species are sorbed to a greater extent than native anions are desorbed, cation leaching must be retarded. Furthermore, if different anions exhibit different tendencies for sorption, the anionic composition of the input solution would affect cation leaching rates. Thomas (1960) has demonstrated such effects for anion-sorbing soils.

The anion species, NO_3^- and SO_4^{2-}, are dominant components in acid rain (Bubenick et al., 1983; Jacks et al., 1984). Differences in the extent of sorption of these species would effect differences in cation leaching, acidification, and mobilization of Al caused by H^+ loading. The principal objective of this investigation was to discern differences in leaching rates for several common cation species from an anion-sorbing soil leached with either HNO_3 or H_2SO_4. Since pH is known to affect anion sorption, these acids were applied at three different pHs. Another objective was to evaluate a predictive model for describing the effects of pH and anion sorption upon cation leaching. The intent here was to assess the applicability of simple transport and chemical equilibrium models for the complicated system of physical and chemical processes which occur during the transport of acid solutions through soil. The transport model used was a mixing-cell model. This model simulates hydrodynamic dispersion by a simple algorithm. Accordingly, computational time is reduced and the code is simple. The principal advantage of the chemical equilibrium model used is that cation exchange selectivities are estimated from solution and sorbed phase concentrations of the unaltered soil. Detailed studies of binary exchange reactions are not required.

CHAPTER 2

LITERATURE REVIEW

Thomas (1960) compared experimentally determined breakthrough curves (BTCs) for concentrations of Ca^{2+} in effluent from columns of Ca^{2+}-saturated Yolo, Cecil, Lloyd, and Davidson series soils, leached with various Al^{3+} and K^+ salts, with predicted BTCs based on a simple chromatographic theory. Agreement was good for the Yolo soil but poor for the three Piedmont soils (Cecil, Lloyd, and Davidson). For the latter group of soils, actual breakthrough for Ca^{2+} was later than predicted. These deviations were attributed to electrolytic imbibition which is the combined retention of anions and cations That author also investigated anionic effects on electrolytic imbibition. While Cl^- and NO_3^- salts effected some retardation of Ca^{2+} with respect to theory, $SO_4{}^{2-}$ salts resulted in greater retardation for Ca^{2+} movement. Retardation was greatest when H_2PO4^- salts were used Chlorides and NO_3^- anions tend to be sorbed by soil to a lesser extent than are $SO_4{}^{2-}$ or $H_2PO_4{}^-$ anions. The results of this study have an important implication for the problem of accelerated leaching of cations from soils subjected to acid deposition. For soils that exhibit anion sorption, the nature and relative amounts of the anions deposited will affect the rate of H^+-induced cation leaching. According to Johnson et al. (1982), forest soils can be acidified by infiltrating acid rain without being leached of Al and basic cations if the anion of the acid is immobilized in the soil. Lee (1985) irrigated lysimeter boxes containing Bohannon (Typic Haplumbrept) soil, a SO_4^{2-} sorbing soil, and planted with either young red alder (Alnus rubra Bong.) or sugar maple (Acer saccharum Marsh.) with H_2SO_4 solutions of several pHs. After three-and-one-half years, Ca^{2+} and Mg^{2+} had been leached to a depth of only 15 to 30 cm for the pH 3.0 treatment. This depth coincided with that at which SO_4^{2-} was being removed from solution by sorption. Huete and McColl (1984) found that smaller amounts of cations were leached from an Alfisol subsoil and an Oxisol topsoil when H_2SO_4, rather than HNO_3, was applied.

Cation mobility is clearly dependent upon anion mobility. Accordingly, this study was undertaken to determine the effects of differences in the mobilities of NO_3^- and SO_4^{2-}, components in acid rain, upon cation leaching rates from an anionic sorbing soil. Factors affecting the mobilities of these anions are subsequently discussed.

Factors Affecting Anion Mobility

Anion movement is determined by the combined effects of convective-dispersive transport and sorption-desorption processes. For 1-dimensional transport, reversible sorption, and steady water flow the transport equation for a given species may be expressed as

$$\frac{\partial C}{\partial t} + \frac{\rho}{\theta}\frac{\partial S}{\partial t} = D\frac{\partial^2 C}{\partial x^2} - V\frac{\partial C}{\partial X} \pm P \qquad [1]$$

where C is solute concentration (mole m^{-3}), S is sorbed phase concentration (mole kg^{-1}), P is a sink or source term (mole m^{-3} s^{-1}) for removal or addition of a species by precipitation/dissolution, irreversible sorption, or microbial activity, θ is volumetric water content, ρ is bulk density (kg m^{-3}), D is the hydrodynamic dispersion coefficient (m^2 s^{-1}), v is the pore water velocity (m s^{-1}), x is distance (m), and t is time (s).

Generally the greater the extent of sorption, the greater is the retardation of an anionic sorbing species relative to a non-sorbing species. Several factors influence the amount sorbed per unit mass of soil as well as its time rate of change. Major factors affecting SO_4^{2-} sorption include 1) solution concentration, 2) pH, 3) nature of sorbent, and 4) nature of other ionic species present (Gaston et al., 1986). These factors likewise influence NO_3^- sorption and, consequently, its mobility.

Sulfate sorption has been observed variously to either conform to the Langmuir isotherm,

$$\frac{S}{b} = \frac{KC}{1+KC} \qquad [2]$$

in which a maximum in sorption is reached with increasing solution concentration, or to the Freundlich isotherm,

$$S = kC^n \qquad (3)$$

in which no sorption maximum occurs. In these equations C is solute concentration (mole m^{-3}), S is sorbed phase concentration (mole kg^{-1}), b is the sorption maximum (mole kg^{-1}) and K (m^3 $mole^{-1}$), k ($mole^{1-n}$ m^{3n} kg^{-1}) and n are empirical constants. Kinjo and Pratt (1971) found the Langmuir equation, (2), better described NO_3^- sorption for the subsoils of two Andepts, an Alfisol, and an Oxisol.

Models used for predicting effects of acid deposition on soil chemistry have commonly assumed reversible isotherms for SO_4^{2-} sorption. Sulfate sorption may not always be reversible, however (Aylmore et al., 1966). Apparent non-singularity due to irreversible sorption in SO_4^{2-} isotherms would affect leaching rates for soil cations in the situation where heavy inputs of SO_4^{2-} to a soil were followed by low levels of SO_4^{2-} input. As pointed out by Reuss and Johnson (1986), non-singularity in this case would diminish H^+-induced leaching of cations.

Sulfate sorption generally increases with decreasing pH. Nitrate sorption behaves similarly (Kinjo & Pratt, 1971; Sieck & Waring, 1979). Although this behavior is consistent with the increase in positive sites for anion adsorption with decreasing pH and accounts for the effect of pH on NO_3^- sorption (Hingston et al., 1972), SO_4^{2-} adsorption may also occur at neutral sites (Rajan, 1978, 1979). In these investigations, Rajan observed an increase in surface negative charge due to SO_4^{2-} adsorption. Couto et al. (1979) also found that SO_4^{2-} sorption slightly increased the CEC. Hingston et al. (1972), however, claim that no evidence exists for SO_4^{2-} adsorption at neutral sites. Sulfate adsorption proceeded with neutralization of positive sites so that the limit of SO_4^{2-} adsorption at a given pH was the same as the maximum amount of non-specifically adsorbed anion at that pH. If SO_4^{2-} sorption occurs only by adsorption and, on an equivalent basis, cannot exceed the maximum of non-specifically adsorbed anions, then cations would be leached from an anion-sorbing soil just as effectively by H_2SO_4 as by HNO_3. As Singh et al. (1980) pointed out, immobilization of input anion will result in retarded leaching of cations only if a less than equivalent amount of native soil anions is simultaneously displaced. In light of the leaching studies by Thomas (1960) and Huete and McColl (1984), which demonstrated retarded cation losses when SO_4^{2-}, rather than the non-specifically adsorbed NO_3^-, was the major anion in the system, the mechanism proposed by Hingston et al. (1972) is not solely responsible for SO_4^{2-} sorption. (Proposed mechanisms for SO_4^{2-} sorption are discussed later.)

Among inorganic sorbents, aluminum and iron oxide materials and kaolinitic minerals exhibit the greatest capacity to sorb SO_4^{2-} (Gaston et al., 1986). These same inorganic materials were responsible for NO_3^- sorption (Kinjo & Pratt, 1971; Black & Waring, 1979). The effect of organic matter on SO_4^{2-} sorption is unclear. Although several authors found that organic matter contributed to SO_4^{2-} sorption, some found that it exerted a negative influence on SO_4^{2-} sorption (Gaston et al., 1986). Black and Waring (1979) found that organic matter tended to reduce NO_3^- sorption. According to these studies, anionic effects on cation leaching should be expected for soils containing appreciable amounts of 1:1 clays (kaolinite, for example) and aluminum and iron oxide materials.

Competition of other sorbing anion species for sorption sites tends to reduce the extent of SO_4^{2-} sorption. Phosphate has been shown to decrease SO_4^{2-} sorption (Ensminger, 1954; Kamprath et al., 1956; Chao, 1964). Chloride (Chang & Thomas, 1963; Gebhardt & Coleman, 1974) and NO_3^- species (Chao, 1964) are poorly competitive with SO_4^{2-}. Khanna and Beese (1978) in West Germany showed that a pulse application of Cl^- and NO_3^- to columns of an acid podzolic brown soil saturated with SO_4^{2-} did not desorb SO_4^{2-}. It may be conversely concluded that NO_3^- adsorption is restricted in the presence of SO_4^{2-}. Preferential sorption of SO_4^{2-} is at least partially understood in terms of differences in surface binding of these species. Nitrate is nonspecifically bound to positive surface sites (Hingston et al., 1972) by Coulombic attraction. Sulfate, on the other hand, is specifically bound to surface Al or Fe by displacement of H_2O (Hingston et al., 1972) and/or OH^- (Rajan, 1978 and 1979). Serna et al. (1977) presented spectroscopic evidence for such weak binding for NO_3^- compared to SO_4^{2-}.

In addition to anionic effects on SO_4^{2-} sorption, Chao et al. (1963) demonstrated that the composition of the cationic milieu affects SO_4^{2-} sorption. The higher the valence of the predominant cation in the system, the greater was the extent on SO_4^{2-} sorption. The authors suggested this effect could be due to either the formation of a bridging complex in which a trivalent or divalent cation links SO_4^{2-} to a negative exchange site or to reduced anion repulsion when the diffuse double layer contains such cations.

In addition to the four major factors discussed above, SO_4^{2-} sorption is also affected by time and temperature. Rajan (1978) found that although SO_4^{2-} sorption onto hydrous alumina was about 90% complete within 10 min. reaction time, equilibrium was not reached until three hours. Chang and Thomas (1963) found that SO_4^{2-} sorption on 2 Cecil soils and a Georgia kaolinite coated with Fe oxide continued over several days. Barrow and Shaw (1977) found that the removal of SO_4^{2-} from solution, availability of SO_4^{2-} to plants, and desorption each decreased with increasing contact time between solution and sorbed phases. Singh (1984) described the kinetics of SO_4^{2-} sorption for B horizon material of a

Typic Udipsamment and a Typic Dystrochrept using a 2-rate constant and multiple-order rate equations.

On the basis of thermodynamics, anion sorption should be affected by changes in temperature. Barrow and Shaw (1977) and Singh (1984) showed that SO_4^{2-} sorption increased slightly with increasing temperatures near ambient temperature.

On the basis of these factors affecting NO_3^- and SO_4^{2-} sorption it can be generally concluded that the mobility of these anions will be least (i.e., sorption should be greatest) in a soil composed of 1:1 clays or aluminum and iron oxide materials, having a distinctly acid pH, and containing low amounts of a preferentially sorbed anion.

Results of studies by Thomas (1960) and Huete and McColl (1984) indicate that for soils in which a difference in mobilities of these anions exists NO_3^- is more mobile than SO_4^{2-}. The lower mobility of SO_4^{2-} occurs because, for the same sorbent material and pH, a greater portion of the total amount of the anion exists in the sorbed phase. The mechanisms whereby SO_4^{2-} is retained by the soil, compared to that by which NO_3^- is adsorbed, account for this greater sorption of SO_4^{2-}.

Sorption Mechanisms

Sorption of NO_3^- is by Coulombic attraction to positively charged sites on aluminum and iron oxides and kaolinitic minerals (Hingston et al., 1972). Sorption of SO_4^{2-} may occur by any of three general mechanisms (Harward & Reisenaur, 1966): These are 1) coordination with aluminum or iron in oxide materials via displacement of coordinated H_2O or OH^- and a similar exchange on the edges of 1:1 type clays, 2) a mechanism whereby SO_4^{2-} and cation are both retained (termed "molecular adsorption"), and 3) chemical precipitation reactions.

In the ligand exchange mechanism, SO_4^{2-} may be adsorbed as a monodentate ligand displacing H_2O from positive sites (Hingston et al., 1967, 1972). Sulfate may also be adsorbed as binuclear bridging complex displacing H_2O or OH^- from adjacent metal atoms (Rajan, 1978, 1979). Parfitt and Smart (1978) presented spectroscopic evidence for bidentate SO_4^{2-} adsorption. Their overall reaction for SO_4^{2-} adsorption on iron oxide materials, analogous to that proposed by Rajan, is

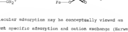

[4]

Molecular adsorption may be conceptually viewed as concurrent specific adsorption and cation exchange (Harward & Reisenaur, 1966). According to Chang and Thomas (1963), an adsorbed acidic cation hydrolyzes, releasing H^+, allowing for the adsorption of SO_4^{2-} co-ion, and SO_4^{2-} displaces OH^-. Neutralization of H^+ and OH^- drives the reaction. Another form of molecular adsorption is the physical entrapment of SO_4^{2-} salts in soil micropores (Harward and Reisenauer, 1966).

Several authors have suggested that, while SO_4^{2-} is adsorbed by a host of materials, it may also be precipitated in the presence of these materials as basaluminite, $Al_4(OH)_{10}SO_4 \cdot 5H_2O$, or alunite, $KAl_3(OH)_6(SO_4)_2$ (Gaston et al., 1986). Whether these minerals control soil solution SO_4^{2-} is unclear. Adams and Rawajfih (1977) found that basaluminite might be controlling SO_4^{2-} solubility in a K_2SO_4 amended sandy loam. The data of Wolt (1981) suggest that alunite, in conjunction with gibbsite or kaolinite, might control SO_4^{2-} in solution. Khanna and Beese (1978) could not demonstrate that either mineral was controlling the solution concentration of SO_4^{2-}. Gebhardt and Coleman (1974) found that in the soil solution of B horizon material of an Andept ion products for basaluminite spanned a range from supersaturation to undersaturation.

These mechanisms by which SO_4^{2-} is sorbed render it more tightly and preferentially bound than the non-specifically bound NO_3^-. These mechanisms, influenced by solution concentration, pH, and ionic environment, account for the reduced mobility of SO_4^{2-} relative to NO_3^-.

Not treated here are biological influences upon the mobility of these anions. Differential uptake of these species by plants affects the relative mobilities of these anions as do differences in the rates of microbially mediated immobilization and oxidation.

Some models for the chemical effects of acid deposition on groundwater and streamwater quality have included estimates for these sinks and sources. Selected chemical models are discussed below. These models were developed for use in conjunction with hydrologic models. Flow models appropriate to the leaching experiments in this study are discussed subsequently to the chemical models.

Chemical Models

Among the simpler models is that of Reuss and Johnson (1986). Among the several cation exchange reactions occurring in soils that receive acid rain, these authors consider only the Ca^{2+}-Al^{3+} cation exchange reaction because Ca^{2+} is quite similar to Mg^{2+} in selectivity with respect to Al^{3+} and these divalent species are generally more abundant in the soil than the monovalent bases. Solution concentration of Al^{3+} is controlled by acidic hydrolysis of Al-bearing minerals. Equilibria involving monomeric Al hydroxides are included. Sulfate sorption and desorption influence the total positive charge in solution. Simple carbonate equilibria are also considered in this model. For specified inputs of SO_4^{2-}, NO_3^-, and Cl^-, known initial amount of Ca^{2+} adsorbed, and partial pressure of CO_2, equilibrium concentrations of these various species are calculated.

The Model of Acidification of Groundwater in Catchments (MAGIC) of Cosby et al. (1985) is conceptually similar to that of Reuss and Johnson. Their MAGIC model, however, includes several cation exchange reactions and Al-fluoride and Al-sulfate monomers. Sink/source terms, due to nutrient uptake, microbial transformations, or weathering release, are included in mass balance equations for the basic cations and strong acid anions. Sulfate sorption is presumed governed by the Langmuir equation, [2]

The Integrated Lake Watershed Acidification Study (ILWAS) model was applied to two watersheds by Cheng et al. (1986). The chemical submodel of ILWAS includes the inorganic reactions 1) cation exchange among NH_4^+, Ca^{2+}, H^+, K^+, Mg^{2+}, and Na^+, 2) weathering of primary minerals, 3) dissolution of Al and complexation with OH^-, F^-, SO_4^{2-} and organic ligands, 4) simple carbonate equilibria, and 5) anion sorption and desorption. Aluminum may either be in equilibrium with gibbsite or kinetically derived from it. Phosphate and SO_4^{2-} sorption and desorption are described with linear isotherms. This model also considers biologic processes including 1) mineralisation of nutrient species via decomposition of organic matter, 2) nutrient uptake, 3) respiratory release of CO_2, and 4) oxidation of N.

Although the latter two models provide considerable detail to the inorganic chemistry, they neglect two additional phenomena which may affect the chemistry of a soil undergoing artificial acidification. Although Al is assumed to exist in solution as any of several monomeric complexes, no allowance is made for adsorption of any form but Al^{3+}. Implicit in the assumption that only Al^{3+} is adsorbed is recognition of the difficulty in obtaining unequivocal estimates of the amounts of the different Al monomers on the exchange complex. Furthermore, the existence of solution and sorbed phase polymeric Al is ignored. Bache and Sharp (1976) have demonstrated that polymeric Al can be desorbed, and desorption increases with increasing concentration and decreasing pH of the extractant. These authors have shown that polymerization reactions are important even at a pH as low as 4.8. Jardine et al. (1985) successfully described Al sorption on Ca^{2+} saturated kaolinite using a 2-site model. Aluminum sorption occurred by equilibrium cation exchange for Ca^{2+} and kinetically controlled polymerization on the solid surface.

The effect of soil solution pH on anion sorption is also neglected by these models. If the extent of sorption of an input strong acid anion is appreciably increased with decreasing pH of the soil solution, then predictive models which only consider the effect of solution concentration on anion sorption would tend to overestimate the rate of cation leaching. The chemical equilibrium model used in this study deferred to the experimental complexity of rigorously treating the Al chemistry. The model does, however, attempt to account for pH effects on anion sorption during soil acidification by use of sorption isotherms derived from experiments obtained from addition of the corresponding strong acid to samples of soil. Descriptions of this model and of the simplified flow model are presented in Chapter 4.

Transport Models

For 1-dimensional, steady flow through a porous medium the time and position dependence of concentration of a reactive species is described by

$$\frac{\partial C}{\partial t} + \frac{\rho}{\theta}\frac{\partial S}{\partial t} = D\,\frac{\partial^2 C}{\partial x^2} - V\,\frac{\partial C}{\partial X} \pm P \qquad [1]$$

The several variables and constants of equation [1] have been previously defined. Analytic solutions exist for a variety of boundary conditions provided the term $\partial S/\partial t$ is directly proportional to the term $\partial C/\partial t$. For a system consisting of several competitively sorbed solutes i, the terms $\partial S_i/\partial t$ are not directly proportional to the terms $\partial C_i/\partial t$. The set of equations for such a system are non-linear and must be solved numerically using finite difference or finite element schemes. Rubin and James (1973) and Valocchi et al. (1981), for example, have modelled transport involving multispecies cation exchange by use of the Galerkin finite element method.

Schweich and Sardin (1981) have presented an alternative formulation that is computationally simpler for such a system. Here, again considering 1-dimensional, steady flow, the medium is imagined divided into several equal length segments or cells. Equation [1] is rewritten as a mass balance relation for each successive pair of cells by omitting the dispersion term and estimating the convection term as a differential. For a finite length soil column divided into J number of cells there are J equations of the form

$$QC_{i-1} = QC_2 + \frac{V}{J}\frac{dC_i}{dt} + \frac{M}{J}\frac{dS_i}{dt} \qquad [5]$$

where the subscript i refers to a particular cell, Q is the volumetric flow rate, V is the pore volume, and M is the mass of soil. Other symbols are as previously defined. By these simplifications the partial differential equation [1] has been reduced to an ordinary differential equation. During the solution of these J equations numerical dispersion occurs. It is possible, therefore, by proper choice of J to mimic the dispersion phenomenon that equation [1] takes into explicit account.

Schultz and Reardon (1983) simulated 2-dimensional transport in an aquifer using a mixing-cell model combined with an analytic solution for a tracer instantaneously released in a flow stream. Their approach seems readily adaptable to 1-dimensional flow. In this approximation the flow medium was conceptually divided into an arbitrary number of cells. At the beginning of a given time step the total solution mass of a solute within a cell was imagined concentrated along the central axis of the cell. During the flow time step 2-dimensional spreading occurred as the solute initially concentrated along the axis moved several cells downstream. The concentration in any cell was then calculated as that derived from its upstream parent plus contributions derived from the two or three longitudinal and transverse neighbors of the parent cell.

One of the simplest of all published approaches is a mixing-cell model described by Tanji et al. (1967) for predicting chemical changes during deep percolation. In this model the profile is conceptually divided into an arbitrary number of segments. Numerical dispersion arises during saturated flow as concentrations along the profile are updated according to the algorithm

$$C_{i,j} = 0.5C_{i-1,j} + 0.5C_{i,j-1} \qquad [6]$$

where $C_{i,j}$ is the solution concentration of a species in the i^{th} segment during the j^{th} time step of flow. The algorithm, [6], is applied for every species for each increment of flow. Changes in solution concentration of the various species, due to chemical reactions, are estimated using an equilibrium model applied after each increment of flow.

In this formulation, more or less dispersion can be computationally introduced by decreasing or increasing, respectively, the number of segments considered. The algorithm, [6], assumes perfect mixing between inflow solution, $C_{i-1,j}$, and resident solution, $C_{i,j-1}$, since the coefficients of both these terms are 0.5. Numerical dispersion can also be effected by varying these coefficients. As discussed by Tanji (1970), increasing or decreasing f in

$$C_{i,j} = fC_{i-1,j} + (1-f)C_{i,j-1} \tag{7}$$

effects decreased or increased numerical dispersion, respectively.

Van Ommen (1985) presented a theoretical basis for proper choice of f based on experimental values of pore water velocity, coefficient of dispersion, and arbitrary choice of the length of a cell. The author's model, applied to flow involving binary cation exchange, produced results in reasonable agreement with an analytical solution.

CHAPTER 3

MATERIALS AND METHODS

Column Leaching Experiments

The soil used was Cecil series (Typic Hapludult) soil taken from a forested site near Clemson, S.C. (Hydraulic conductivity data for Cecil soil from this site are available in Cassel, 1985.) The capacity of this soil to sorb anions is well documented (Ensminger, 1954; Kamprath et al., 1956; Thomas, 1960; Chang and Thomas, 1963). Columns, 10 cm long by 8.32 cm diameter, were uniformly packed with air-dried topsoil or subsoil materials to bulk densities of 1.57 g cm^{-3} and 1.48 g cm^{-3}, respectively. These columns were then wet from the bottom up with either HNO_3 or H_2SO_4 solutions at pH 3.0, 3.7, or 4.7. Input flux was maintained essentially constant and effluent fractions were collected until approximately 40 pore volumes had been collected. Flow and input concentration data for each of the 12 columns are shown in Table 3-1.

Concentrations of HNO_3 corresponding to pH 3.0, 3.7, and 4.7 solutions were calculated using the Davies equation for estimating activity coefficients. Standardized acid was diluted to achieve the target concentrations. The diluted acid solutions were checked for final pH. The H^+ concentration of each solution was taken as the initial

Table 3-1. Flow data and input concentrations of H^+ for twelve columns of Cecil soil.

Topsoil

Treatment	H^+ concentration (mol/m^3)	Pore volume (l)	Darcy flux (cm/hr)	Pore velocity (cm/hr)
HNO_3, pH 3.0	1.036	0.2238	1.02	2.48
H_2SO_4, pH 3.0	1.040	0.2260	0.97	2.33
HNO_3, pH 3.7	0.203	0.2260	0.98	2.36
H_2SO_4, pH 3.7	0.203	0.2204	1.00	2.47
HNO_3, pH 4.7	0.020	0.2159	1.00	2.52
H_2SO_4, pH 4.7	0.020	0.2239	1.02	2.48

Subsoil

Treatment	H^+ concentration (mol/m^3)	Pore volume (l)	Darcy flux (cm/hr)	Pore velocity (cm/hr)
HNO_3, pH 3.0	1.036	0.2447	1.02	2.27
H_2SO_4, pH 3.0	1.040	0.2529	0.98	2.11
HNO_3, pH 3.7	0.203	0.2444	1.01	2.25
H_2SO_4, pH 3.7	0.203	0.2441	0.99	2.20
HNO_3, pH 4.7	0.020	0.2518	0.99	2.14
H_2SO_4, pH 4.7	0.020	0.2463	0.99	2.19

concentration times the appropriate dilution factor. Preparation of H_2SO_4 solutions was similar. Owing to the incomplete second dissociation of the dibasic acid, the H^+ concentration in the input solution was less than the normality of the acid. However, based on a pK_a for HSO_4^- of 1.96 (Adams, 1971), H_2SO_4 was approximately 97% dissociated at the highest concentration used. The remaining 3% of H^+ tied up in HSO_4^- was presumed readily released once the acid entered the soil. Hence, input H^+ concentration was taken equal to the normality of the acid solution

Samples of effluent were subsequently analyzed for 1) Al, colorimetrically using Eriochrome Cyanine R (McLean, 1965); 2) NH_4^+, colorimetrically by the indophenol blue method (Keeney and Nelson, 1982); 3) Ca^{2+} and Mg^{2+}, by atomic absorption spectroscopy; 4) H^+, by specific ion electrode, 5) K^+ and Na^+, by atomic emission spectroscopy; and 6) SO_4^{2-}, turbidimetrically The method of SO_4^{2-} analysis was a modification of that described by Rhoades (1982) in which reagents were proportionally reduced to the small aliquot of sample available.

Soil Analyses

Water extractable and sorbed phase concentrations of the above ions and Cl^- were determined for the unaltered Cecil topsoil and subsoil materials. The soil was prepared by drying, grinding, and sieving with a 2 mm sieve. Ten-gram samples of soil were extracted with 25 ml H_2O by shaking for 1 hr, centrifuging, and vacuum filtering. Soil samples including residual aqueous solutions were then extracted for sorbed ions. In each extraction, the soil and residual solution were shaken with 25 ml of the extracting solution for 1/2 hr, centrifuged, and vacuum filtered. This extraction sequence was repeated three times. To remove interferences of organic matter in the topsoil on SO_4^{2-} determinations, 0.1 g of activated charcoal was added to the samples prior to the water extraction. Calcium, K^+, Mg^{2+}, and Na^+ were extracted with 1N NH_4OAc buffered at pH 7.0. Aluminum and NH_4^+ were extracted with 1N KCl. Chloride and SO_4^{2-} were extracted with 0.016 M KH_2PO_4. Total acidity was determined using the $BaCl_2$-TEA method (Thomas, 1982). The difference between total acidity and extracted Al^{3+} was assumed to represent exchangeable H^+. Corrections were made for the retained aqueous solutions. Analysis for Cl^- was by the mercuric thiocyanate method (Rhus and Kidder, 1983). All other analyses were as above. Standards for SO_4^{2-} (topsoil) were similarly exposed to the activated charcoal. Each extraction was replicated four times. Data from these extractions were used for soluble salts, total initial amounts of each species (Table 3-2), and for estimating Gaines-Thomas type selectivity coefficients used in the simulation model. This formulation for exchange selectivity coefficient is given by

$$K_{gt} = \frac{(X_i)^{z_j} (a_j)^{z_i}}{(X_j)^{z_i} (a_i)^{z_j}} \qquad [9]$$

where X is the equivalent fraction of a species on the exchanger, a is the solution activity of a species, and z is the valence (Gaines and Thomas, 1953). The selectivity coefficients are presented in Table 4-7, Chapter 4. The CEC of the soil was assumed to be equal to the sum of extracted sorbed phase positive charge, corrected for sorbed anionic charge (This point is discussed in Chapter 4.)

Anion Sorption Isotherms

Data for SO_4^{2-} sorption isotherms with pH dependence were obtained by equilibrating 10 g samples of topsoil or subsoil with 25 ml portions of H_2SO_4 of varied concentrations. Soil samples and acid were shaken for 1 hr, centrifuged, measured for pH, and vacuum filtered. The filtrate was then analyzed for SO_4^{2-}. Knowing the initial amount of SO_4^{2-} present (native plus added) and the amount in solution, the amount sorbed was calculated by difference. Here, as above, interference by organic matter in the topsoil samples was eliminated by the addition of activated charcoal. Acid blanks with charcoal were run. Each equilibration was duplicated.

It was assumed that the concentration dependence of SO_4^{2-} sorption during soil acidification with H_2SO_4 or HCl

Table 3-2 Initial soil chemical data. All ionic quantities are given in cmol (+)/kg soil.

Topsoil

	NH_4^+	Al^{3+}	Ca^{2+}	H^+	K^+	Mg^{2+}	Na^+	SO_4^{2-}	Cl^-	Total (+)
Solution phase	0.076	0.012	0.039	0.012	0.019	0.015	0.012	0.040	0.012	0.167
Sorbed phase	0.034	0.828	0.143	3.60	0.017	0.019	0.017	0.099	0.014	4.66
Total	0.112	0.084	0.182	3.61	0.036	0.034	0.029	0.139	0.026	4.64

Principal minerals kaolinite, vermiculite (with interlayer aluminum), quartz

Texture Sandy loam (76.9% sand, 14.0% silt, 9.1% clay)

Subsoil

	NH_4^+	Al^{3+}	Ca^{2+}	H^+	K^+	Mg^{2+}	Na^+	SO_4^{2-}	Cl^-	Total (+)
Solution phase	0.021	0.002	0.050	0.005	0.006	0.017	0.014	0.041	0.008	0.115
Sorbed phase	0.072	0.668	0.622	4.61	0.036	0.160	0.018	0.367	0.014	6.19
Total	0.093	0.670	0.672	4.62	0.042	0.177	0.032	0.406	0.022	6.30

Principal minerals kaolinite, vermiculite (with interlayer aluminum), quartz, gibbsite

Texture Sandy clay loam (61.6% sand, 13.7% silt, 24.7% clay) could be described with the Freundlich equation [3]. The constants in the Freundlich equation were estimated by a least squares procedure applied to the logrithmic form of the Freundlich equation

$$\ln(S_i) = \ln(k_i) + s\ln(C_i) \qquad [9]$$

Similar isotherms for Cl^-, rather than NO_3^-, were determined. The sorption behavior of non-specifically adsorbed Cl^- is essentially identical to that of NO_3^- (Hingston et al , 1972; Thomas, 1960) and Cl^- is more easily and reliably determined.

Soil Minerals and Texture

The mineralogy of the Cecil topsoil and subsoil was determined by x-ray diffraction methods and the texture was determined by the pipette method (Table 3-2). Mineralogical and textural data were obtained from Liu (in preparation).

Tracer Breakthrough Curves

In order to establish values for input parameters of the numerical model applied in this study, tracer BTCs were needed for both soils. Chloride was used here as the tracer. To prevent sorption or desorption of Cl^-, which would otherwise be expected for these soils, the experiments were run at constant pH and in the presence of a preferentially sorbed anion. Air-dried, uniformly packed columns of topsoil and subsoil were wet from the bottom with a 0.025M KH_2PO_4 + 0.025M Na_2HPO_4 solution containing 0.00282M Cl^-. Steady output flux of Cl^- at pH 6.82 was established. The input solution was then changed to the same buffer, but containing 0.000282M Cl^-, and the effluent fractionally collected over the ensuing three pore volumes. Although anion exclusion was a potentially confounding problem, no patent exclusion of Cl^-, manifested by early breakthrough, was observed when relative concentration was plotted against the number of pore volumes of column effluent. The fairly low negative charge of these soils probably reduced the expression of this effect. The model parameters derived from these tracer experiments are discussed later. Experimental and simulated Cl^- BTCs for the topsoil and subsoil are shown in Figs. 4-22 and 4-23, respectively.

CHAPTER 4

RESULTS AND DISCUSSION

Anion Sorption Isotherms

Figures 4-1 and 4-2 show the effect of solution concentration on SO_4^{2-} and Cl^- (considered to represent all weakly sorbed anions, including NO_3^-) sorption by the Cecil topsoil and subsoil, respectively. The Freundlich isotherms describing sorption are shown as well as the experimental data. Values for the constants in the isotherm equations are given in Table 4-1.

Table 4-1. Freundlich isotherm constants for SO_4^{2-} and Cl^- sorption in Cecil topsoil and subsoil.

	k	m
Topsoil		
SO_4^{2-} sorption	0.26	0.39
Cl^- sorption	0.068	0.50
Subsoil		
SO_4^{2-} sorption	0.98	0.38
Cl^- sorption	0.12	0.61

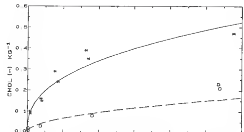

Figure 4-1. Freundlich sorption isotherms for SO_4^{2-} (———) and Cl^- (— — —) and experimental sorption data for SO_4^{2-} (*) and Cl^- (O) in Cecil topsoil

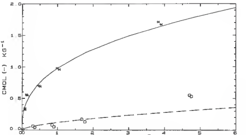

Figure 4-2. Freundlich sorption isotherms for SO_4^{2-} (———) and Cl^- (— —) and experimental sorption data for SO_4^{2-} (*) and Cl^- (O) in Cecil subsoil.

Data in Figures 4-1 and 4-2 show that in both the topsoil and subsoil SO_4^{2-} was sorbed to a greater extent than was Cl^-. Accordingly, leaching of either soil with H_2SO_4 may be expected to result in a lower rate of cation loss than leaching with HNO_3. As will be presently shown, however, occurrence of anionic effects on cation leaching is strongly influenced by the pH of the input acid.

Leaching Experiments

Application of pH 3.0 Acids to Columns of Topsoil

Breakthrough curves for Ca^{2+} in effluent from columns of Cecil topsoil that received 3.0 acid (Fig. 4-3) show a slight retardation for the H_2SO_4 treatment compared to the HNO_3 treatment. Also, peak concentration was less and initial tailing was greater for H_2SO_4 than for HNO_3. Total amounts of each species leached were estimated by integrating the BTCs with respect to numbers of pore volumes. Table 4-2 shows these totals.

Table 4-3 shows the ratios of the amount of each basic cation leached to the amount initially present in the soil. These fractions were calculated from data presented in Tables 3-2 and 4-2 and the known mass of soil per column. Acidic cations are not included since there were sources for these species during leaching. Soil columns received inputs of H^+ and Al^{3+} was liberated by acidic dissolution of soil minerals. Assuming neither K^+ nor Mg^{2+} was generated by acidic dissolution of soil minerals, the values for the

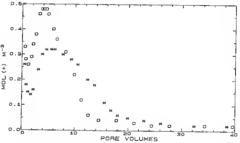

Figure 4-3: Calcium breakthrough curves for Cecil topsoil leached with nitric (O) and sulfuric (*) acids at pH 3.0.

Table 4-2. Total quantities of soil cations leached by 40 pore volumes of acid solutions. All data in mmol(+)

Topsoil

Treatment	Al^{3+}	NH_4^+	Ca^{2+}	H^+	K^+	Mg^{2+}	Na^+	Total Charge
HNO_3, pH 3.0	6.88	1.20	1.36	1.72	0.32	0.32	0.12	11.92
H_2SO_4, pH 3.0	6.70	1.16	1.37	1.52	0.32	0.33	0.12	11.52
HNO_3, pH 3.7	0.77	1.20	0.84	0.32	0.30	0.29	0.09	3.71
H_2SO_4, pH 3.7	0.71	1.12	0.80	0.32	0.29	0.27	0.09	3.60
HNO_3, pH 4.7	0.81	0.98	0.49	0.12	0.26	0.23	0.11	3.00
H_2SO_4, pH 4.7	0.94	1.07	0.48	0.13	0.25	0.24	0.12	3.23

Subsoil

Treatment	Al^{3+}	NH_4^+	Ca^{2+}	H^+	K^+	Mg^{2+}	Na^+	Total Charge
HNO_3, pH 3.0	3.29	0.54	4.27	0.63	0.33	1.10	0.09	10.25
H_2SO_4, pH 3.0	1.76	0.63	3.55	0.28	0.33	0.91	0.11	7.57
HNO_3, pH 3.7	0.25	0.59	1.87	0.03	0.21	0.49	0.09	3.53
H_2SO_4, pH 3.7	0.23	0.56	1.57	0.02	0.23	0.38	0.10	3.09
HNO_3, pH 4.7	0.13	0.42	1.09	0.04	0.21	0.28	0.10	2.27
H_2SO_4, pH 4.7	0.18	0.38	1.01	0.04	0.21	0.31	0.10	2.23

Table 4-3 Fractions of initial quantities of basic cations leached by 40 pore volumes of acid solutions

Topsoil

Treatment	NH_4^+	Ca^{2+}	K^+	Mg^{2+}	Na^+
HNO_3, pH 3.0	1.26	0.85	1.04	1.10	0.48
H_2SO_4, pH 3.0	1.21	0.88	1.04	1.14	0.48
HNO_3, pH 3.7	1.15	0.54	0.98	1.00	0.38
H_2SO_4, pH 3.7	1.17	0.51	0.94	0.93	0.36
HNO_3, pH 4.7	1.03	0.32	0.85	0.79	0.44
H_2SO_4, pH 4.7	1.12	0.31	0.81	0.83	0.48

Subsoil

Treatment	NH_4^+	Ca^{2+}	K^+	Mg^{2+}	Na^+
HNO_3, pH 3.0	0.72	0.79	0.98	0.77	0.35
H_2SO_4, pH 3.0	0.84	0.66	0.98	0.84	0.43
HNO_3, pH 3.7	0.79	0.35	0.82	0.34	0.35
H_2SO_4, pH 3.7	0.75	0.29	0.68	0.27	0.39
HNO_3, pH 4.7	0.56	0.20	0.62	0.20	0.39
H_2SO_4, pH 4.7	0.51	0.19	0.82	0.22	0.39

ratios of these species leached from the topsoil with respect to the amounts initially present are obviously overestimated. Reference to Table 3-2 shows that in the topsoil there was little of either K^+ or Mg^{2+} initially present. Although errors in measurement of extractable K^+ and Mg^{2+} were small in absolute value, such experimental errors (along with experimental errors in measurement of effluent concentration) probably account for the apparent leaching of somewhat more K^+ and Mg^{2+} than were initially present.

The ratio of the amount of NH_4^+ leached to that initially extractable from the topsoil exceeds one for all acid treatments used. Mineralization of soil organic matter N may have been a source of NH_4^+ during these leaching experiments. Also, K^+ is not a completely efficient extractant for NH_4^+ in soils that exhibit the capacity to fix NH_4^+ (Keeney and Nelson, 1982). Although, in a study by Rich (1960), Al interlayering in vermiculite greatly reduced the capacity of the material to fix NH_4^+, the Al interlayered vermiculite apparently retained some capacity to fix added NH_4^+. It is not known, however, if the Cecil soil exhibits any such capacity to fix either NH_4^+ or K^+.

Although the initial quantity of Ca^{2+} removed by HNO_3 was greater than that removed by H_2SO_4, by 40 pore volumes of effluent, these quantities were equal. The initial steep decreases in effluent Ca^{2+} concentration were caused by flushing soluble salts initially present in the soil from the column. Extensive tailing in the low concentration range after about 10 pore volumes suggests there was a slow release of Ca^{2+}. This slow release could have been due to changes in exchange selectivity as the fraction of Ca^{2+} on the exchange complex approached zero. It could also have been due to slow diffusion in/out of regions of immobile water within small aggregates or interlamellar spaces of the aluminumhydroxy interlayered vermiculite

Breakthrough curves for Mg^{2+} (Fig. 4-4) are similar to those for Ca^{2+}. However, since Mg^{2+} was less preferentially adsorbed than Ca^{2+} and was present in a lower quantity, breakthrough was earlier for Mg^{2+} ions. Equal amounts of Mg^{2+} were leached by the two treatments

Hydrogen ion BTCs (Fig. 4-5) for the H_2SO_4 treatment show a slightly slower rate of concentration increase with number of pore volumes than for the HNO_3 treatment. For each of the two acids, however, even after 40 pore volumes, the H^+ concentration was only about 25% of the input concentration (1.04 mol(+)/m^3).

This buffering by the soil was due not only to cation exchange of H^+ for adsorbed Al^{3+} or basic cation but also to H^+ reaction with a soil mineral. Table 4-4 shows the sums of leached plus residually extractable Al^{3+} for each acid treatment compared to the initially extractable Al^{3+}. These data indicate that there was substantial Al production when

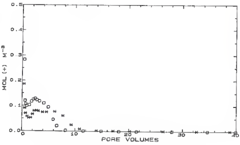

Figure 4-4. Magnesium breakthrough curves for Cecil topsoil leached with nitric (o) and sulfuric (*) acids at pH 3.0.

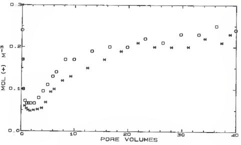

Figure 4-5. Hydrogen ion breakthrough curves for Cecil topsoil leached with nitric (0) and sulfuric (*) acids at pH 3.0.

Table 4-4 Comparison of amount of Al leached plus the amount of Al extractable at the end of the experiment to the amount of Al initially extractable. All data in mmol(+)

Topsoil

Treatment	Leached	Residual	Sum	Initial
HNO3, pH 3.0	6.88	8.75	15.63	8.01
H2SO4, pH 3.0	6.70	9.28	15.98	8.01
HNO3, pH 3.7	0.77	8.19	8.96	8.01
H2SO4, pH 3.7	0.71	8.08	8.79	8.01
HNO3, pH 4.7	0.81	7.73	8.54	8.01
H2SO4, pH 4.7	0.94	7.61	8.55	8.01

Subsoil

Treatment	Leached	Residual	Sum	Initial
HNO3, pH 3.0	3.29	9.31	12.60	5.04
H2SO4, pH 3.0	1.76	9.87	11.63	5.04
HNO3, pH 3.7	0.25	5.33	5.58	5.04
H2SO4, pH 3.7	0.23	5.76	5.99	5.04
HNO3, pH 4.7	0.13	4.40	4.53	5.04
H2SO4, pH 4.7	0.18	4.92	5.10	5.04

columns of topsoil and subsoil were leached with pH 3.0 acids.

This buffering, therefore, can be accounted for on the basis of H^+ reaction with an Al-bearing mineral. If, for example, kaolinite dissolved and equilibrium was maintained, then the ion product $(Al^{3+})(Si(OH)_4)(OH^-)^3$ would be constant. Furthermore, if (OH^-) were expressed in terms of (H^+) and the dissociation constant for water and if $(Si(OH)_4)$ were constant, then the activity ratio $(Al^{3+})/(H^+)^3$ would be constant. Accordingly, for leaching of the Cecil soil with acid, as the output concentration of bases approached zero, the effluent concentration of H^+ would have approached a concentration less than the input level. Effluent concentrations from the Cecil topsoil suggest that dissolution of kaolinite, in conjunction with the dissolution of quartz (controlling the activity of $Si(OH)_4$), controlled the activity ratio $(Al^{3+})/(H^+)^3$. If Al^{3+} and H^+ were the only cations in the effluent and local equilibrium occurred, the output concentration of H^+ should approximately reach 0.22 mol(+)/m^3 (for input pH 3.0 and based on solubility constants adapted from Marion et al., 1976). This value is very close to observed values toward the end (approximately 40 pore volumes of effluent) of the leaching experiments.

Breakthrough curves for Al^{3+} (Fig. 4-6) show somewhat retarded breakthrough for the H_2SO_4 treatment. Maximum concentrations exceeded, however, the value predicted on the

---

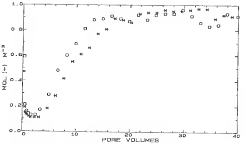

Figure 4-6. Aluminum breakthrough curves for Cecil topsoil leached with nitric (0) and sulfuric (*) acids at pH 3.0.

basis of a kaolinite-quartz system. This value is about 0.82 mol(+)/m^3.) (Input concentration, 1.04 mol(+)/m^3, minus the above calculated final concentration of H$^+$ in the effluent, 0.22 mol(+)/m^3.) These discrepancies do not disprove the hypothesis that the kaolinite-quartz system controlled Al solubility. Although BTCs for Al are written in terms of Al^{3+}, the quantity actually measured was total Al. Not only did the Al measured include Al^{3+}, but also several other monomers, polymers, and complexes.

Potassium breakthroughs (*Fig.* 4-7) show monotonic decreases in concentration throughout the runs. Initial rate for K$^+$ leaching loss was somewhat greater for the HNO$_3$ treatment but by 40 pore volumes equal amounts of K$^+$ had been leached by the two treatments. Breakthrough curves for the other monovalent cations are similar to those for K$^+$.

Sulfate breakthrough curves are shown in Fig. 4-8. The BTC for SO$_4^{2-}$, H$_2$SO$_4$ treatment, shows that the input level concentration of SO$_4^{2-}$ was reached in the effluent after about 15 to 20 pore volumes. Attainment of SO$_4^{2-}$ sorption capacity coincided with only nominal increases in H$^+$ concentration (Fig. 4-5). Differences in Al^{3+} concentrations in the effluent vanished between 15 to 20 pore volumes of effluent showing that SO$_4^{2-}$ sorption was no longer affecting retardation of cation leaching. The BTCs for SO$_4^{2-}$ leached by HNO$_3$ show an early peak reflecting a slightly retarded loss of SO$_4^{2-}$ as the wetting front passed

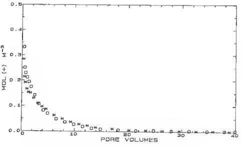

Figure 4-7. Potassium breakthrough curves for Cecil topsoil leached with nitric (O) and sulfuric (*) acids at pH 3.0.

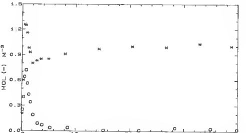

Figure 4-8 Sulfuric breakthrough curves for Cecil topsoil leached with nitric (O) and sulfuric (*) acids at pH 3.0.

through the column. For the HNO_3 treatment, the rate of SO_4^{2-} loss was low for pore volumes beyond the early peak. Nitrate is a poor desorbing agent for SO_4^{2-}. Furthermore, SO_4^{2-} sorption was enhanced by the low pH of the influent solution.

In general, differences in cation BTCs during leaching produced by H_2SO_4 and HNO_3 at pH 3.0 can be explained by differences in the extent of sorption of the input anion and desorption of the leached anions. Retarded cation BTCs for the H_2SO_4 treatment imply that the difference, quantity of SO_4^{2-} sorbed minus quantity of native anions desorbed, was greater than the corresponding difference for the HNO_3 treatment, NO_3^- sorbed minus native anions desorbed. Effluent concentrations of anions other than SO_4^{2-} were not measured, however.

Application of pH 3.7 Acids to Columns of Topsoil

Somewhat more Ca^{2+} was leached by HNO_3 than by H_2SO_4 in the early stages of acid application to soil columns (Fig. 4-9). Beyond about 10 pore volumes the difference between these treatments was negligible. The BTCs for other cations show no difference between treatments.

The breakthrough curve for Ca^{2+} leached by HNO_3 at pH 3.0 compared to that for Ca^{2+} leached by the acid at pH 3.7 shows that considerably more Ca^{2+} was initially leached by the lower pH treatment (Fig. 4-10). Rates of loss beyond about 20 pore volumes, however, show that more Ca^{2+} was

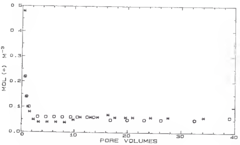

Figure 4-9. Calcium breakthrough curves for Cecil topsoil leached with nitric (O) and sulfuric (*) acids at pH 3.7.

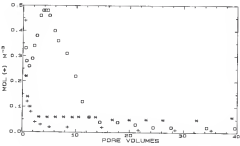

Figure 4-10. Calcium breakthrough curves for Cecil topsoil leached with nitric acid at pH 3.0 (O), pH 3.7 (*), and pH 4.7 (+).

being leached by the pH 3.7 treatment. By 20 pore volumes most of the Ca^{2+} initially present in the soil had been removed from the column leached with pH 3.0 HNO_3. More Ca^{2+} simply remained in the column leached with pH 3.7 HNO_3. Comparison of the BTCs for Al^{3+} at pH 3.0 and pH 3.7, HNO_3 treatment, shows a markedly decreased rate of loss at the higher pH (Fig. 4-11). Reduced leaching at this higher pH occurred for all cations.

Although the effects of differences in SO_4^{2-} and NO_3^- sorption obviously affected cation leaching rates by pH 3.0 acids, there was apparently little effect of differences in SO_4^{2-} and NO_3^- sorption on cation leaching rates by pH 3.7 acids. For the Cecil topsoil, extremely low pH conditions are required for these anionic sorption effects to be manifested. Furthermore, the retardation of cation leaching produced by SO_4^{2-} anions, with respect to NO_3^-, was clearly very much a secondary effect when compared to the principal effect of H^+ concentration upon controlling cation leaching rates.

Application of pH 4.7 Acids to Columns of Topsoil

No differences in cation leaching rates were observed between treatments. Cation leaching rates were least at pH 4.7. Figure 4-10 shows the Ca^{2+} BTC for HNO_3 input at pH 4.7 compared to the Ca^{2+} BTCs for HNO_3 at pH 3.7 and 3.0.

An interesting behavior observed for pH 4.7 acid was that the total concentration of positive charge being

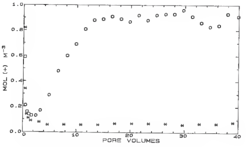

Figure 4-11. Aluminum breakthrough curves for Cecil topsoil leached with nitric acid at pH 3.0 (O) and pH 3.7 (*)

[illegible] exceeded, several times, the concentration of [illegible] H^+. Considering the data from Tables B-1 through B-7, it can be shown that the concentration of positive charge in the effluent [illegible] in the leaching experiments, was approximately [illegible]. The input concentration of H^+ was only about [illegible], however.

As [illegible] mentioned, the microbially mediated oxidation of [illegible] in soil organic matter is an internal source of H^+. Although the columns were water-saturated, [illegible] likely did not limit potential microbial activity [illegible] the input acid solutions were well-[illegible]; furthermore, O_2 was convectively transported [illegible] columns. The H^+ concentration of the acid [illegible] may have limited microbial activity for [illegible] (Alexander, 1977). Accordingly, the amount of H^+ [illegible] produced by microbial oxidation of soil organic [illegible] is likely greatest for the pH 4.7 experiments. The influence of this source of H^+ on the [illegible] leaching of cations (relative to input H^+ concentration) from columns that received pH 4.7 acids cannot here be assessed independently of that due to H^+ generated upon the [illegible]tion of anions. A rough estimate of the relative [illegible] of these processes, however, may be made from the [illegible] organic matter content of the soil and assumed C/N/S [illegible] and rates of oxidation of these organically bound elements. The relation

$$C_X = M(OM\%/100)f(X/C)r(\Delta t/t)(1/EQWT)(1/V) \qquad [10]$$

where M is the mass of the soil in the column (g); OM% is the weight percent of organic matter present in the soil; f is the weight ratio of C to organic matter and is assumed to be 1.7, X/C is the weight ratio of an organically bound element to carbon; r is the annual rate of oxidation of the element; Δt/t is the fraction of a year over which the leaching experiment was conducted; EQWT is the equivalent weight of the element (g eq^{-1}); and V is the total volume of acid solution that entered the column (m^3) can be used to estimate the average solution concentration of an anion (and the corresponding H^+ concentration) derived from the microbial oxidation of an organically bound element. Assuming C/N/S is 1.00/0.10/0.01, r is approximately 2% of the total per year (Alexander, 1977), and that the leaching experiment lasted for about 1/50 of a year, then the average effluent concentration of SO_4^{2-} derived from oxidation of organic S in the topsoil would have been about 0.0002 mol(-) m^{-3}. Similarly, the average effluent concentrations of NO_3^- and H_2CO_3 would have been about 0.003 mol(-) m^{-3} and 0.035 mol m^{-3}, respectively. Since H_2CO_3 is only weakly dissociated, a concentration far less than 0.035 mol(-) m^{-3} HCO_3^- (first dissociation) would have been produced by oxidation of organic C. Considering the equilibrium relation

$$(H^+)(HCO_3^-)/(H_2CO_3) = 10^{6.4} \qquad [11]$$

the concentration of HCO_3^- at pH 5.0 (an approximate value for the effluent from columns that received pH 4.7 acids) would have been about 0.003 mol(-) m^{-3}. It seems reasonable, therefore, that the sum of the average concentrations of SO_4^{2-}, NO_3^-, and HCO_3^- (and the corresponding H^+ concentration) derived from microbial oxidation of soil organic matter was less than about 0.01 mol(-) m^{-3}. This concentration is substantially less than the difference between concentration of effluent positive charge and input concentration of H^+, 0.11 mol(+) m^{-3} minus 0.02 mol(+) m^{-3}. The value for effluent concentration of positive charge is probably inaccurately high, however, since all solution Al was considered to be Al^{3+}. Even if, for the sake of argument, the charge on solution Al is taken to be zero (an unlikely condition at pH 5.0), internal production of H^+ by oxidation of soil organic matter could not alone have accounted for the higher rate of positive charge loss than H^+ input. In this case the solution concentration of positive charge would have been 0.04 mol(+) m^{-3}. Accordingly, it may be concluded that the higher rate of positive charge loss from columns of topsoil that received pH 4.7 acids than rate of H^+ input was, in large part, due to desorption of anions.

Results for the subsoil leaching experiments generally paralleled those for the topsoil. Breakthrough curves when pH 3.0 acid was applied show more marked differences in effects of the treatments. Differences, though small, were exhibited at pH 3.7.

Application of pH 3.0 Acids to Columns of Subsoil

Retardation of Ca^{2+} leached by H_2SO_4 was obvious when compared to Ca^{2+} leached by HNO_3 (Fig. 4-12). The maximum Ca^{2+} concentration in column effluent was also greater for the HNO_3 treatment. Tailing in the Ca^{2+} BTCs occurred for both treatments. Beyond about 18 pore volumes of effluent the rate of Ca^{2+} loss was greater for the H_2SO_4 treatment. However, by 40 pore volumes the quantity of Ca^{2+} leached by HNO_3 still exceeded that leached by H_2SO_4.

Breakthrough curves for Mg^{2+} (Fig. 4-13) are similar to those for Ca^{2+}. Breakthrough occurred later for the H_2SO_4 treatment and the concentration maximum was less. Tailing occurred and the rate of Mg^{2+} leaching was greater for the H_2SO_4 treatment beyond about 14 pore volumes.

More K^+ was initially leached by HNO_3 than by H_2SO_4 (Fig. 4-14). The BTC for K^+ leached by HNO_3 shows a monotonic decrease with increasing number of pore volumes. For the H_2SO_4 treatment, however, the BTC shows a small peak at about eight pore volumes. Equal quantities of K^+ had been leached by the two acids by 40 pore volumes. Effluent concentrations of NH_4^+ and Na^+, for both acid treatments, steadily decreased.

Beyond early minima, concentrations of H^+ in the effluent were greater for the HNO_3 treatment (Fig. 4-15).

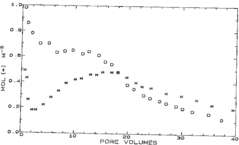

Figure 4-12. Calcium breakthrough curves for Cecil subsoil leached with nitric (O) and sulfuric (*) acids at pH 3.0.

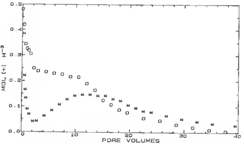

Figure 4-13. Magnesium breakthrough curves for Cecil subsoil leached with nitric (O) and sulfuric (*) acids at pH 3.0.

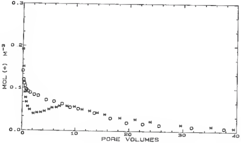

Figure 4-14. Potassium breakthrough curves for Cecil subsoil leached with nitric (○) and sulfuric (*) acids at pH 3.0.

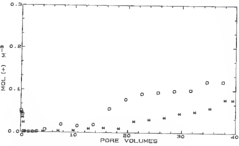

Figure 4-15. Hydrogen ion breakthrough curves for Cecil subsoil leached with nitric (O) and sulfuric (*) acids at pH 3.0.

For the two acids, H^+ concentrations in the effluent were no more than about 12% of the input concentration. This buffering in the subsoil was likely due to reaction with gibbsite controlling the activity ratio, $(Al^{3+})/(H^+)^3$. If Al^{3+} and H^+ were the only cationic species and the outflow concentration of charge equalled input H^+ concentration, the effluent concentration of H^+ would be about 0.14 mol(+)/m^3 (for pH 3.0 acid input concentration 1.04 mol(+)/m^3 and based on the solubility constant for gibbsite adapted from Marion et al., 1976). A comparable value was being approached experimentally by 40 pore volumes of effluent.

Similar to the H^+ ion BTCs, Al^{3+} breakthroughs (Fig. 4-16) show steady increases in concentration as leaching progressed. Outflow Al^{3+} concentrations were greater for the HNO_3 treatment than for H_2SO_4. Even by 40 pore volumes of effluent, however, the Al^{3+} concentrations were well below the maximum of 0.90 mol(+)/m^3 predicted for the gibbsite system.

The BTC for SO_4^{2-} anions for the H_2SO_4 treatment (Fig. 4-17) shows substantial retardation of the input SO_4^{2-}. Input concentration of SO_4^{2-} was not reached in the column effluent even by 40 pore volumes. The SO_4^{2-} BTC for leaching with HNO_3 shows a low, decreasing loss of SO_4^{2-}. Apparently, the low pH conditions effected by introducing HNO_3 at pH 3.0 into the column largely offset the increased tendency to desorb SO_4^{2-} anions by decreased concentration

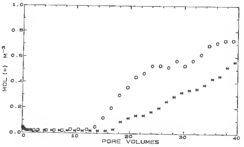

Figure 4-16. Aluminum breakthrough curves for Cecil subsoil leached with nitric (O) and sulfuric (*) acids at pH 3.0.

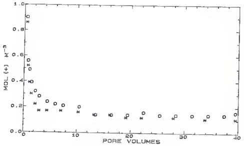

Figure 4-17. Sulfate breakthrough curves for Cecil subsoil leached with nitric (O) and sulfuric (*) acids at pH 3.0.

Also, NO_3^- is a poor competitor with SO_4^{2-} for soil sorption sites.

As with the topsoil, the explanation for the comparative retardation of Ca^{2+}, Mg^{2+}, Al^{3+}, H^+, and K^+ breakthroughs when the subsoil was leached with H_2SO_4 is that sorption of SO_4^{2-} was dominant over desorptive losses of other anions whereas for leaching with HNO_3 no such dominance of NO_3^- sorption occurred over SO_4^{2-} desorption and desorption of other native anions.

Application of pH 3.7 Acids to Columns of Subsoil

For pH 3.7 acids differences in cation leaching rates were observed between the acid treatments. Leaching rates of Ca^{2+} (Fig. 4-18) were initially greater for the HNO_3 treatment but decreased to a rate only nominally greater than that for the H_2SO_4 treatment. Small differences in leaching rates of Mg^{2+} (Fig. 4-19) were effected by the different acids. Leaching rate of Mg^{2+} remained somewhat greater throughout the run for the HNO_3 treatment. Differences between treatments for the other cations were negligible.

Comparison of Ca^{2+} BTCs for subsoil columns leached with pH 3.0 and pH 3.7 HNO_3 (Fig. 4-20) shows substantially less Ca^{2+} was leached by the higher pH acid solution. By 40 pore volumes, however, effluent concentrations of Ca^{2+} were the same. The effect of input pH was more dramatic for Al^{3+} (Fig. 4-21). Nitric acid solution at pH 3.7 produced a

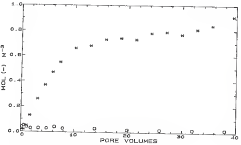

Figure 4-18. Calcium breakthrough curves for Cecil subsoil leached with nitric (O) and sulfuric (*) acids at pH 3.7.

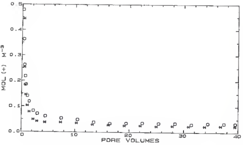

Figure 4-15. Magnesium breakthrough curves for Cecil subsoil leached with nitric (O) and sulfuric (*) acids at pH 3.7.

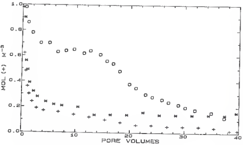

Figure 4-20. Calcium breakthrough curves for Cecil subsoil leached with nitric acid at pH 3.0 (O), pH 3.7 (*), and pH 4.7 (+).

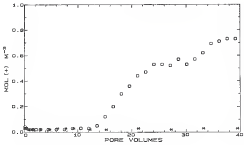

Figure 4-21. Aluminum breakthrough curves for Cecil subsoil leached with nitric acid at pH 3.0 (O) and pH 3.7 (*).

steady, low Al^{3+} concentration in the effluent, equal to that from the pH 3.0 treatment up to about 12 pore volumes. Beyond this point, Al^{3+} concentration in the effluent from the column leached with pH 3.0 HNO_3 substantially increased. By 40 pore volumes of effluent, the Al^{3+} concentration from the column leached with pH 3.7 acid was only about 1/20 of that for the lower pH treatment.

As with the topsoil, the effect of SO_4^{2-} sorption, relative to NO_3^- sorption, on cation leaching appears limited to input pHs of about 3.7 and lower. At such low pH values the retardation of cation leaching by interaction between SO_4^{2-} anions and soil components is small compared to the greatly enhanced leaching produced by high concentrations of H^+.

Application of pH 4.7 Acids to Columns of Subsoil

No differences in cation leaching by HNO_3 and H_2SO_4 solutions were observed for pH 4.7 solutions. Cation leaching was least for this pH. Leaching patterns of Ca^{2+} in column effluent for pH 4.7 HNO_3 treatment relative to the Ca^{2+} BTCs for pH 3.0 and 3.7 acid solutions are given in Fig. 4-20.

Summing data for positive charge concentration in the effluent near the end of the leaching experiments (from Tables B-9 through B-15) gives an approximate positive charge concentration of 0.08 mol(+) m^{-3}. This value exceeds the concentration of H^+ that was concurrently input. By applying the relation [10] for microbial oxidation of organic matter in the subsoil columns it can be shown that the average negative charge concentration in the effluent derived from oxidation of organic matter was about 0.01 mol(-) m^{-3}. As with the topsoil, desorption of anions apparently was more important than organic matter decomposition in effecting the higher rate of loss of positive charge than rate of H^+ input.

Such desorption of anions likely does not occur naturally under forest conditions, however. Atmospheric inputs of acid rain are commonly enriched with basic cations and accompanying anions. The acid solution reaching uppermost portion of the topsoil is further concentrated with such ion species as it passes through the forest canopy and the litter layer. Under forest conditions, the solution reaching the subsoil is the resultant leachate from the topsoil which has been buffered and changed in ionic composition. In these experiments acid solutions were applied directly to columns of topsoil. Nevertheless, experimentally observed effects from the soil columns demonstrate the sensitivity of the soil to substantial changes in the composition of the soil solution. As discussed below, accelerated leaching of soil cations by acid solutions of low pH may be mitigated by concurrent net sorption of input anion. In this case, the input of a quantity of H^+ results in the leaching loss of a less than equivalent amount of native cations.

Effluent concentrations, by pore volume of leachate, for all species and all treatments are tabulated in Appendix B.

Charge Balance

A cursory look at data in Table 4-2 reveals that though cation leaching increased as the pH of the leaching solution was decreased, there is no equivalent relation between input quantities and leaching losses of soil cations. This was especially true for the subsoil. For example, the approximately 50-fold increase in H^+ concentration of the leaching solution, for pH 3.0 compared to 4.7 H_2SO_4 solutions, resulted in less than a 4-fold increase in cations leached. Data from Table 4-2 can be combined with known amounts of input acid and measured outflow amounts of $SO_4{}^{2-}$ anion to identify which treatments resulted in net retention or loss of cations and show the relation of such retention or loss to the retention or loss of $SO_4{}^{2-}$.

For H^+ flow into columns of air-dried soil in which no reactions other than cation exchange and acid-induced dissolution of kaolinite or gibbsite occur, the amount of positive charge leached should exceed the total amount of H^+ input by the amount of soluble salts initially present. If anion sorption-desorption occurs, however, the difference given as (positive charge out minus soluble salts) minus positive charge input will tend to be either negative or positive depending upon whether or not net sorption or desorption of anions occurs. Table 4-5 indicates those treatments for which net retention or loss of positive charge occurred. Values for amounts of soluble salts in the topsoil and subsoil were obtained from Table 3-2.

Topsoil

No treatment resulted in net retention of positive charge for columns of topsoil. For the pH 3.0 H_2SO_4 treatment, however, the loss of positive charge was small compared to the charge on Al leached. Since this value for Al is an overestimation, it seems likely that positive charge actually accumulated. Retention of SO_4^{2-} occurred in the topsoil for this treatment. Leaching with pH 3.7 acids caused minor net losses of positive charge. Leaching with pH 4.7 acids resulted in appreciable net losses of charge. Net desorption of anions must have occurred since overestimation of charge borne by Al cannot account for these losses. Losses of SO_4^{2-} were greatest at this highest input pH.

Subsoil

Leaching Cecil subsoil with pH 3.0 HNO_3 or H_2SO_4 produced a net retention of positive charge and this effect was especially pronounced for the H_2SO_4 treatment. Concurrent retention of nearly 40% of the SO_4^{2-} input also

Table 4-5. Comparison of total effluent to influent positive charge as related to retention or loss of SO_4^{2-} Data is expressed in mmol(+). Negative values indicate retention of charge and positive values indicate loss of charge.

Topsoil

Treatment	Al^{3+}Out	(+)Out	(+)Out-Salts	(+)In	((+)Out -Salts) -(+)In	SO_4^{2-}Out	SO_4^{2-}In	(SO_4^{2-}Out -SO_4^{2-}In)
HNO_3, pH 3.0	6.88	11.92	10.42	9.51	0.91	0.47	0.00	0.47
H_2SO_4, pH 3.0	6.70	11.52	10.02	9.67	0.35	8.76	9.67	-0.94
HNO_3, pH 3.7	0.77	3.71	2.21	1.88	0.33	0.62	0.00	0.62
H_2SO_4, pH 3.7	0.71	3.60	2.10	1.84	0.36	1.97	1.84	0.13
HNO_3, pH 4.7	0.81	3.00	1.50	0.18	1.32	0.65	0.00	0.65
H_2SO_4, pH 4.7	0.94	3.23	1.73	0.18	1.55	0.73	0.18	0.55

Subsoil

Treatment	Al^{3+}Out	(+)Out	(+)Out-Salts	(+)In	((+)Out -Salts) -(+)In	SO_4^{2-}Out	SO_4^{2-}In	(SO_4^{2-}Out -SO_4^{2-}In)
HNO_3, pH 3.0	3.29	10.25	9.34	10.39	-1.05	0.25	0.00	0.25
H_2SO_4, pH 3.0	1.76	7.57	6.66	10.82	-4.16	6.80	10.82	-4.02
HNO_3, pH 3.7	3.53	3.53	2.62	2.03	0.59	0.61	0.00	0.61
H_2SO_4, pH 3.7	3.09	3.09	2.18	2.04	0.14	1.52	2.04	-0.52
HNO_3, pH 4.7	2.27	2.27	1.36	0.21	1.15	0.91	0.00	0.91
H_2SO_4, pH 4.7	2.23	2.23	1.32	0.20	1.12	0.77	0.20	0.57

occurred. The small discrepancy between net retained cations and net retained SO_4^{2-} probably occurred because no correction was made for native soluble SO_4^{2-} in the estimation of SO_4^{2-} leached. Small net losses of positive charge occurred at pH 3.7. Despite some retention of SO_4^{2-} for the pH 3.7 H_2SO_4 treatment, desorption and leaching of other anions apparently occurred to a greater extent. Leaching with pH 4.7 acids resulted in greater net losses of positive charge and net desorption of anions occurred. Sulfate losses were greatest at input pH 4.7.

From Table 4-5 it is clear that the net retention of cations at low pH of acid applied or net loss of cations was related to the retention or loss of SO_4^{2-}. As discussed earlier, SO_4^{2-} sorption occurs by specific adsorption but may also occur by precipitation reactions. The possible occurrence of such precipitation reactions during these acid leaching experiments is examined below. Dissolution of kaolinite and gibbsite is also considered.

Precipitation Reactions of Sulfate and Aluminum Solubility

Precipitation as a basic aluminum sulfate is one of the possible mechanisms of SO_4^{2-} sorption. Two such compounds cited in the literature as possibly contributing to SO_4^{2-} sorption are basaluminite, $Al_4(OH)_{10}SO_4 \cdot 5H_2O$, and alunite, $KAl_3(OH)_6(SO_4)_2$. To investigate if either of these compounds may have been controlling SO_4^{2-} solubility in these leaching experiments, effluent concentration of Al^{3+}, H^+,

K^+, and $SO_4{}^{2-}$, corrected to activities using the Davies equation, were combined to give the ion products, $(Al^{3+})^4(SO_4{}^{2})/(H^+)^{10}$, and $(K)(Al^{3+})^3(SO_4{}^{2-})^2/(H^+)^6$. These alternative formulations of the ion products were written assuming the ion product for water, $(H^+)(OH^-)$, to be 10^{-14}. Since the measured value for Al overestimated Al^{3+} by virtue of the coexistence of several monomeric and polymeric species, values for Al^{3+} used in these calculations were corrected to account for a portion of the error by considering the mono- meric species, Al^{3+}, $Al(OH)^{2+}$, $Al(OH)_2{}^+$, $Al(OH)_3$, and $AlSO_4{}^+$, to be in equilibrium. Sulfate concentrations were corrected for the species, $AlSO_4{}^+$. The solubility products for basaluminite and alunite, expressed in the above forms, are $10^{22.4}$ and $10^{-1.4}$, respectively (adapted from Adams and Rawajfih, 1977). The logarithms of the calculated ion products, across a range of effluent collected, are shown in Tables 4-6 and 4-7. Calculations were based on interpolated effluent data from four selected columns: topsoil that received pH 3.0 HNO_3; topsoil that received pH 3.0 H_2SO_4; subsoil that received pH 3.0 HNO_3; and subsoil that received pH 3.0 H_2SO_4.

Compared to literature values, the average ion product for basaluminite for each of the selected columns was low, indicating undersaturation with respect to basaluminite. Except for the subsoil column leached with H_2SO_4, undersaturation increased as leaching progressed. Effluent

Table 4-6 Logarithms of selected ion products from the leachate from topsoil columns leached with pH 3.0 HNO_3 or H_2SO_4. The data were calculated from interpolated concentrations.

Ion product	$(Al^{3+})^4(SO_4^{2-})/(H^+)^{10}$		$(K^+)(Al^{3+})^3(SO_4^{2-})^2/(H^+)^6$		$(Al^{3+})/(H^+)^3$	
pore volume	HNO3	H2SO4	HNO3	H2SO4	HNO3	H2SO4
2.0	18.87	19.91	-0.95	0.25	7.81	8.00
4.0	16.10	19.92	-2.28	0.22	7.69	7.96
6.0	17.60	18.91	-2.93	-0.35	7.58	7.60
8.0	17.20	18.89	-3.27	-0.38	7.40	7.55
10.0	17.30	18.94	-3.44	-0.43	7.44	7.54
12.0	17.16	18.76	-3.88	-0.64	7.43	7.47
14.0	16.85	18.70	-4.55	-0.81	7.39	7.44
16.0	16.57	18.52	-5.10	-1.00	7.36	7.38
18.0	16.52	18.31	-5.24	-1.23	7.35	7.31
20.0	16.47	17.99	-5.37	-1.60	7.34	7.21
22.0	16.31	17.90	-5.47	-1.71	7.27	7.18
24.0	16.48	18.05	-4.95	-1.67	7.25	7.23
26.0	16.81	18.14	-4.57	-1.69	7.30	7.25
28.0	16.76	18.13	-4.58	-1.76	7.24	7.25
30.0	16.59	18.13	-4.70	-1.84	7.19	7.25
32.0	16.56	18.03	-4.86	-2.00	7.17	7.21
34.0	16.23	17.78	-5.17	-2.20	7.12	7.14
36.0	16.96	17.74	-5.44	-2.25	7.05	7.13
38.0	16.10	17.68	-5.45	-2.47	7.11	7.11
40.0	16.09	17.47	-5.56	-2.70	7.13	7.06
Mean	16.83	18.40	-4.39	-1.31	7.33	7.38

Table 4-7 Logarithms of selected ion products from the leachate from subsoil columns leached with pH 3.0 HNO3 or H2SO4. The data were calculated from interpolated concentrations.

Ion product	$(Al^{3+})^4(SO4^{2-})/(H^+)^{10}$		$(K^+)(Al^{3+})^3(SO4^{2-})^2/(H^+)^6$		$(Al^{3+})/(H^+)^3$	
pore volume	HNO3	H2SO4	HNO3	H2SO4	HNO3	H2SO4
2.0	20.91	20.80	-4.03	-4.02	9.62	9.58
4.0	19.62	21.38	-3.56	-1.85	8.60	9.21
6.0	18.70	21.24	-3.50	-1.28	8.32	9.00
8.0	18.31	21.08	-3.73	-1.08	8.17	8.88
10.0	18.93	20.96	-3.39	-0.99	8.35	8.79
12.0	18.56	20.43	-3.46	-1.07	8.32	8.54
14.0	19.76	20.20	-2.63	-1.14	8.47	8.43
16.0	19.50	20.42	-2.55	-0.96	8.27	8.46
18.0	19.39	22.56	-2.64	0.53	8.20	9.01
20.0	19.13	22.36	-2.92	0.79	8.11	8.81
22.0	19.04	21.87	-2.97	0.60	8.07	8.62
24.0	19.08	21.99	-2.98	0.71	8.07	8.62
26.0	18.98	22.17	-3.09	0.86	8.04	8.64
28.0	18.98	22.19	-3.12	0.89	8.03	8.62
30.0	18.88	22.00	-3.24	0.76	8.00	5.55
32.0	18.88	21.88	-3.27	0.70	8.00	8.50
34.0	18.59	21.73	-3.47	0.63	7.90	8.44
36.0	18.56	21.42	-3.53	0.45	7.89	8.32
38.0	18.57	20.95	-3.57	0.16	7.89	8.16
40.0	18.62	21.07	-3.60	0.20	7.90	8.19
Mean	19.06	21.43	-3.26	-0.26	8.22	8.67

concentrations from this column gave relatively constant ion products which were smaller by about one order of magnitude than the K_{sp} for basaluminite.

Average ion products for effluent from columns of topsoil and subsoil leached with HNO_3 were less than the literature value for alunite. On the other hand, average ion products for effluent from the H_2SO_4 leached soils showed slight supersaturation with respect to alunite. Leachate collected early in the runs using topsoil showed supersaturation regardless of the type of acid applied. The degree of supersaturation was greater for the H_2SO_4 treatment. By 40 pore volumes effluent from topsoil columns was undersaturated. An opposite effect occurred during leaching of subsoil columns. Initial leachate for both acid treatments showed undersaturation. As leaching proceeded, leachate from the column treated with HNO_3 became less undersaturated and the leachate from the H_2SO_4 treated column became supersaturated with respect to alunite after only five pore volumes.

These calculations fail to determine conclusively that either basaluminite or alunite was controlling SO_4^{2-} in solution. Since it is possible that chemical equilibrium did not exist locally in the columns under the flow conditions that prevailed (i.e., small contact times), these ion product calculations do not preclude the occurrence of these minerals or their control of SO_4^{2-} solubility. Within the limitations of the estimations of Al^{3+} concentration, however, similar calculations for the activity ratio, $(Al^{3+})/(H^{+})^{3}$, tend to confirm the earlier suppositions that kaolinite and quartz controlled this ratio in the topsoil but in the subsoil this ratio was controlled by gibbsite.

From Marion et al. (1976), assuming quartz was controlling the solution activity, (H_2SO_4), during acidic dissolution of kaolinite, the calculated value for $(Al^{3+})/(H^{+})^{3}$ is $10^{7.25}$. Average values for this ratio from topsoil leachate are $10^{7.33}$, for the HNO_3 treatment, and $10^{7.38}$, for the H_2SO_4 treatment (Table 4-6). These calculated values include corrections for effect of ionic strength on activity coefficients and for hydrolysis and ion pair formation described above. For both acid treatments this ratio decreased as leaching continued. High values early in the leaching process may have been due to organic complexes or polymeric forms, neither of which were considered in the calculations. Average values for the subsoil were $10^{8.22}$, for the HNO_3 treatment, and $10^{8.67}$, for the H_2SO_4 treatment (Table 4-7). For gibbsite, $(Al^{3+})/(H^{+})^{3}$ is $10^{7.97}$ (Marion et al., 1976). By about 20 pore volumes of effluent the activity ratio for leachate from the HNO_3 treatment had closely approached this theoretical value. Values for the H_2SO_4 treatment decreased with pore volumes of effluent but remained higher than $10^{7.97}$. Based on these calculations, as well as experimental BTCs, it appears that kaolinite and quartz were controlling Al solubility in the Cecil topsoil and that gibbsite was controlling Al solubility in the subsoil. The mathematical transport model assumed these relations.

Simulation Models and Results

Transport Model

The flow simulation model used was essentially that of Tanji (1970). Transient flow into initially air-dried soil was approximated by assuming a sharp wetting front separating saturated soil contiguous with dry soil. Dispersion was simulated in the saturated zone during the wetting phase. The algorithm used to approximate convective-dispersive transport was

$$C_{i,j} = fC_{input_i} + (1-f)C_{i,j-1} \qquad [12]$$

$$C_{input_{i+1}} = (1-f)C_{input_i} + fC_{i,j-1} \qquad [13]$$

where $C_{i,j}$ is the molar concentration in the i^th^ cell for the j^th^ time step of flow, C_{input_i} is the concentration of replacing solution introduced into the i^th^ cell from the cell immediately upstream, and the factor, f, controls numerical dispersion. The larger the value of f, the more piston-like the solute movement and vice versa.

Conservation of mass requires the input solution from the i^{th} cell to the cell downstream to be given by [13]:

During the wetting phase the concentration in the cell at the wetting front was equal to the input concentration from its upstream neighbor plus the concentration of soluble salts dissolved in the cell as it was saturated. Exit concentrations during saturated flow were the input concentrations from the terminal cell.

Assignment of a value for f was made on the basis of a least squares comparison of simulated tracer BTCs to experimental breakthrough of Cl^-. When 10 segments were used per column, the best-fit value for f was 0.64 for the topsoil and 0.62 for the subsoil. Figures 4-22 and 4-23 show tracer simulations compared to experimental Cl^- breakthroughs for Cecil topsoil and subsoil, respectively.

Chemical Equilibrium Model

For each cell in the flow domain and after each flow time step, the chemical model was evoked. The chemical model required inputs of initial solution and sorbed phase concentrations of all species. Using several equilibrium relations and making certain assumptions concerning the reactions involved, the model solved for equilibrium concentrations of these species. The solution procedure is described below:

1. Knowing the initial solution and sorbed phase concentrations for all species, the total quantity, in

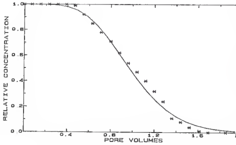

Figure 4-22. Comparison of tracer simulation (continuous line) to experimental C^- breakthrough for Cecil topsoil

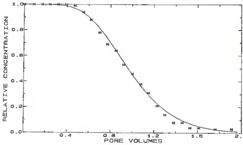

Figure 4-23 Comparison of tracer simulation (continuous line) to experimental C^- breakthrough for Cecil subsoil.

equivalents, of each species is calculated, for basic cations, by

$$T_i = e_i C_i V + X_i Q \qquad [14]$$

where T_i is the total amount in equivalents of species i in the cell, C_i is the molar concentration, z_i is the charge on the species, X_i is the equivalent fraction on the exchanger, V is the volume of the cell, and Q is the CEC for soil in the cell.

The total quantity of an anion is that in solution plus that sorbed. Neither total H^+ nor Al^{3+} are calculated since the total quantity of each of these changes during the equilibration process. During acidic dissolution of an Al bearing mineral, H^+ is consumed. Precipitation of Al^{3+} releases H^+ to solution. Anion sorption and desorption, as discussed below, respectively remove from or release to the soil solution one or the other of these acidic cations. The total acidity, TA, however, does not change and it is this quantity which is calculated. Total acidity is assumed to be

$$TA = (C_{H^+} + 3C_{Al^{3+}})V + (X_{H^+} + X_{Al^{3+}})Q + (S_{SO_4^{2-}} + S_{NO_3^-}) \qquad [15]$$

The variables of the first two terms are analogous to those previously defined. The variables, $S_{SO_4^{2-}}$ and $S_{NO_3^-}$, are the total equivalents of these anions sorbed in the cell. Two points need to be explained here.

First, the model considers all Al in the soil to be Al^{3+}. This is not strictly true as previously discussed, but is a simplifying assumption for the model. Second, it is assumed that for every equivalent of anion sorbed there is an associated equivalent of either H^+ or Al^{3+} For non-specifically adsorbed NO_3^- this must be true since NO_3^- is bound by Coulombic attraction to a protonated site Furthermore, for specifically adsorbed SO_4^{2-} either a proton was consumed during positive charging of a site followed by ligand exchange for H_2O or was subject to consumption by liberation of OH^- anions upon adsorption at a neutral site. Desorption of SO_4^{2-} anions requires displacement by OH^- anions, presumably derived from H_2O, such that H^+ consumed during adsorption of SO_4^{2-} is regenerated during the desorption process. Consequently any adsorbed SO_4^{2-} represents the same equivalent quantity in potential H^+. For instances where SO_4^{2-} adsorption yields a negative site the resultant charge may be balanced by adsorption of any cation. However, in a system which is principally acidic, the fraction of such sites occupied by either H^+ or Al^{3+} is probably large For SO_4^{2-} removal from the solution phase by precipitation as a basic aluminumsulfate (if such occurs) an approximately equal quantity of Al^{3+} is also precipitated. If basaluminite is precipitated, the equilibrium reaction is

$$4Al^{3+} + SO_4^{2-} + 10H_2O = Al_4(OH)_{10}SO_4 + 10H^+ \qquad [16]$$

The net reaction requires that two equivalents of acid be precipitated for each two equivalents of SO_4^{2-} precipitated. The other basic aluminumsulfate cited is alunite. The stoichiometry here is not exact,

$$K^+ + 3Al^{3+} + 2SO_4^{2-} + 6H_2O = KAl_3(OH)_6(SO_4)_2 + 6H^+ \qquad [17]$$

differing from equal quantities of SO_4^{2-} and acid precipitated by the quantity of K^+ precipitated.

2. Anion sorption or desorption is calculated. Parameters used in the Freundlich equation are given in Table 4-1. As applied in the model, the values for the proportionality constant, k, were scaled to allow for expression of S in terms of equivalents per mass of soil in a cell and C as molar concentration. A 1/2-interval search is used to determine values for sorbed and solution concentrations knowing the total quantity of the anion in the cell.

In such a trial and error procedure, an initial estimate is made for a variable. This estimate lies halfway between the established theoretical maximum and minimum. Depending on whether a calculated value, using this estimate, is too large or too small, a new maximum (equal to the initial estimate) or a new minimum (equal to the initial estimate) is selected. A second estimate of the independent variable, lying halfway between the updated extremes, is made and a second value is calculated from the new estimate. This process is repeated, narrowing the possible range of solutions, until satisfactory agreement is obtained.

3. Solution concentration of positive charge is set equal to solution concentration of negative charge determined above. Knowing the concentration of positive charge in solution, it is a fairly simple matter to determine the estimated equilibrium sorbed and solution concentration for the cations species. The procedure used is to first calculate the equivalent fraction of H^+ on the exchange complex corresponding to a guessed concentration of H^+ in solution. These values, together with the total quantity of each base, then allow for calculation of the solution concentration of each base. Equilibrium values for solution concentrations are those for which the sum of equivalents is equal to the total concentration. Sorbed phase concentrations are then calculated by subtracting solution concentrations from total concentrations for each species. The method is illustrated below.

a. The maximum solution concentration of H^+ possible is that for which the only cations present are H^+ and Al^{3+}. The minimum concentration of H^+ is zero. The search for equilibrium solution concentrations of the cations is begun by calculating the maximum concentration of H^+. This value is that which solves

$$C_{H^+}\ 3C_{Al^{3+}} = C_{total} \qquad [18]$$

but

$$C_{Al^{3+}} = kC_{H^+}^{3} \qquad [19]$$

where

$$k = a_{Al^{3+}}/(a_{H^+})^{3} \qquad [20]$$

It is assumed that the ratio of activities, $a_{Al^{3+}}/(a_{H^+})^3$, is constant and equal to that associated with the mineral controlling Al^{3+} solubility. Concentrations throughout this procedure are related to activities through activity coefficients derived from the Davies equation. It is assumed that the ionic strength varies only slightly during the equilibration process so that activity coefficients calculated on the basis of initial solution concentrations in the cell are applicable despite subsequent calculated changes in these concentrations The substituted expression, using activity coefficients,

$$C_{H^+} + 3kC_{H^+}^{3} = C_{total} \qquad [21]$$

is solved using a Newton-Raphson numerical procedure. The initial guess in the 1/2-interval search is one half this H^+ concentration maximum.

b. For this initial guess for the concentration of H^+ in the solution phase, the corresponding fraction of H^+ on the exchange complex is calculated using

$$X_{H^+} + X_{Al^{3+}} = (TA - (C_{H^+} + 3C_{Al^{3+}})V - (S_{SO_4^{2-}} + S_{NO_3^-}))/Q \qquad [22]$$

where

$$X_{Al^{3+}} = f(X_{H^+})^3 \qquad [23]$$

and

$$f = X_{Al^{3+}}/(X_{H^+})^3 \qquad [24]$$

this ratio having been determined from extractions of the unaltered soil. If the Gaines-Thomas selectivity coefficient for H^+-Al^{3+} exchange is assumed constant and the solution activity ratio, $a_{Al^{3+}}/(a_{H^+})^3$, is constant, then the ratio of equivalent fractions, f, must be constant. This equation is solved using a Newton-Raphson procedure. At this point, solution concentrations of the bases corresponding to the guessed C_{H^+} and calculated X_{H^+} values are determined.

c. Equations of the form

$$C_i = T_i/(z_iV + ((X_{H^+})^{z_i})Q/((\gamma_{H^+})^{z_i}/\gamma_i)K(C_{H^+})^{z_i})) \qquad [25]$$

where

$$K = a_i(X_{H^+})^{z_i}/(X_i(a_{H^+})^{z_i} \qquad [26]$$

is the selectivity coefficient for the specific exchange reaction and e are single-ion activity coefficients calculated from the Davies equation. Values for the Gaines-Thomas selectivity coefficients used in the model are presented in Table 4-8 These coefficients were calculated from the date presented in Table 3-2

In the procedure, corrections are made for the ion pairs, $CaSO_4{}^0$ and $MgSO_4{}^0$, prior to calculating the concentration of Ca^{2+} and Mg^{2+}. The method is shown in the computer program (Appendix C).

d The comparison

$$C_{NH_4}{}^+ + C_{K^+} + C_{Na^+} + 2C_{Ca^{2+}} + 2C_{Mg^{2+}}$$
$$+ 3C_{Al^{3+}} + C_{H^+} = C_{total} \qquad [27]$$

is made. Depending on whether the sum is greater or less than the total, the estimate of C_{H^+} is changed in accordance to the 1/2-interval search scheme and steps b. and c. are repeated. The search is stopped when agreement with equation [27] is satisfactory

4. The equilibrium solution concentrations of the cations are used to calculate equivalent fractions for each species on the exchanger by equations of the form

Table 4-8. Values for Gaines-Thomas selectivity coefficients (for H^+ replacement of indicated species) used in the chemical equilibrium model

Topsoil

Exchange pair:	$H^+-NH_4^+$	H^+-K^+	H^+-Na^+	H^+-Ca^{2+}	H^+-Mg^{2+}	H^+-Al^{3+}
Selectivity coefficient:	7.18×10^2	3.70×10^2	2.11×10^2	6.69×10^5	1.92×10^6	4.62×10^7

Subsoil

Exchange pair:	$H^+-NH_4^+$	H^+-K^+	H^+-Na^+	H^+-Ca^{2+}	H^+-Mg^{2+}	H^+-Al^{3+}
Selectivity coefficient:	2.81×10^2	1.55×10^2	7.57×10^2	1.38×10^6	1.92×10^6	3.58×10^8

$$X_i = (T_i - z_i C_i V)/Q \qquad [28]$$

From initial values of solution and sorbed phase concentrations this computational model will estimate equilibrium values for the variables.

Comparison of Transport Model Results to an Analytical Solution for Cation Transport Involving Binary, Homovalent, Nonpreference Exchange

It was of interest to compare the performance of the mixing-cell transport model to an analytical solution for a simple case. Such a case is binary, homovalent, nonpreference cation exchange occurring during steady, saturated flow. Equation [1], with the term, P, set equal to zero, describes such a flow system. In this case $\partial S/\partial t$ is directly proportional to $\partial C/\partial t$ and equation [1] reduces to

$$\frac{\partial C}{\partial t} = \frac{D}{R}\frac{\partial^2 C}{\partial X^2} - \frac{V}{R}\frac{\partial C}{\partial X} \qquad [29]$$

The retardation factor, R, is given by

$$R = (1 + \frac{Q}{C_t}\frac{\rho}{\theta}) \qquad [30]$$

where Q is the cation exchange capacity of the soil and C_t is the total concentration of cations in solution. Several solutions to equation [29] exist depending on the chosen boundary conditions. For the particular system modeled here (a column of Cecil topsoil, as used in this study) the approximate boundary conditions are flux conditions for a finite length column. The boundary and initial conditions are given by

$$-D\frac{\partial C}{\partial x}(0,t) + v(0,t) = vC_0 \qquad [31]$$

$$\frac{\partial C}{\partial x}(L,t) = 0 \qquad [32]$$

$$C(X,0) = C_1 \qquad [33]$$

where C_1 is the initial solution concentration and C_0 is the input concentration. Brenner (1962) solved this general problem. If

$$A(x,t) = (C(x,t)-C_1)/(C_0-C_1) \qquad [34]$$

then

$$\begin{aligned} A(x,t) = {} & \frac{1}{2}\,\mathrm{erfc}\,\frac{Rx - vt}{2(DRt)^{1/2}} + \left(\frac{v^2t}{DR}\right)^{1/2} \exp - \left[\frac{(Rx - vt)^2}{4DRt}\right] \\ & - \frac{1}{2}\left(1 + \frac{vx}{D} + \frac{v^2t}{DR}\right) \exp(vx/D)\ \mathrm{erfc}\,\frac{Rx + vt}{2(DRt)^{1/2}} \\ & + \left(\frac{4v^2t}{DR}\right)^{1/2} \left[1 + \frac{v}{4D}\left(2L-x + \frac{vt}{R}\right)\right] \exp\left[\frac{vL}{D} - \frac{R}{4Dt}\left(2L-x + \frac{vt}{R}\right)^2\right] \\ & - \frac{v}{D}\left[2L-x + \frac{3vt}{2R} + \frac{v}{4D}\left(2L-x + \frac{vt}{R}\right)^2\right] \exp(vL/D)\ \mathrm{erfc}\,\frac{R(2L-x) + vt}{2(DRt)^{1/2}} \end{aligned} \qquad [35]$$

The value for the dispersion coefficient, D, was estimated from a least squares fitting procedure of the analytical solution (for R = 1) to an experimental Cl^- breakthrough curve. The length of the soil column was 10 cm and the pore water velocity was 2.42 cm/hr. The best-fit value for D was 1.48 cm^2/hr. Values for other input parameters were $Q = 0.04657$ eq/kg, $C_t = 0.10$ eq/l, $\rho = 1.57$ kg/l, and $\theta = 0.4164$.

For the mixing-cell transport model, the soil column was assumed to be divided into 10 equal segments. Least squares best-fit of simulated tracer breakthrough to experimental Cl^- breakthrough was obtained for an f value (in the algorithm, [12] and [13]) of 0.64. The exchange capacity of each segment was 0.003975 eq and the volume was 0.02264 l.

For binary, homovalent, non-preference cation exchange, the chemical submodel was simple. Knowing the initial solution and sorbed phase concentrations for both cation species, total equivalents of each, in a given segment, were calculated from equation [14]. The cation exchange equilibrium expression, analogous to equation [20], was written in terms of the solution concentration and equivalent fraction of one of the two species. The resulting expression was reduced to an equation containing only the solution concentration of that species,

$$C_1 = C_t\, T_1/(Q + VC_t) \qquad [36]$$

Analogous variables have been previously defined. Knowing C_t, C_2 was found by difference. Furthermore, knowing the total equivalents of each species and their solution concentrations, the equivalent fraction of each was calculated from equations similar to [28].

Figure 4-24 shows elution curves for input and leached cations predicted by the analytical and mixing-cell models. With respect to the analytical solutions, the mixing-cell model predicted excessive dispersion. This behavior appears to be characteristic of the model. A possible cause of this discrepancy may be that the numerical model fails to consider input and exit boundary conditions observed by the analytical model. The locations of predicted breakthroughs, however, were essentially the same for both models. Inasmuch as the chemistry of the acid soil systems considered in this research probably exerts a dominant influence on ion leaching rates, the failure of the mixing-cell transport model to accurately describe dispersive effects on solute transport does not limit the use of this model for prediction of ion leaching rates from soil.

Equilibrium Model Results

The predicted elution curve for Ca^{2+} leached from Cecil topsoil by pH 3.0 HNO_3, compared to the experimental leaching data, is shown in Fig. 4-25. Predicted peak emergence was retarded, occurring at about twice the number of pore volumes of effluent as experimentally observed

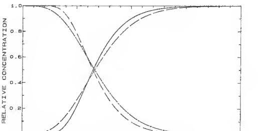

Figure 4-24. Comparison of breakthrough curves of input and leached cations from a binary homovalent, nonpreference exchange system as predicted by analytical and mixing-cell models. Analytical solution, ———, and —— —. Mixing-cell model, - - - -, and ——- -.

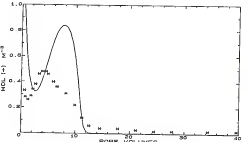

Figure 4-25. Comparison of equilibrium model results (continuous line) to experimental elution of Ca^{2+} from Cecil topsoil leached with pH 3.0 HNO_3

(eight pore volumes compared to about four). The height of the simulated peak was nearly twice that of the experimental peak. Also, the predicted decrease in Ca^{2+} concentration beyond the maximum was abrupt, going to zero by about 13 pore volumes. The experimental data showed extensive tailing.

The simulation model assumed all cation exchange reactions achieved equilibrium. Clearly, this situation did not occur. Nonequilibrium conditions may have been due to any of several causes including 1) variations in cation exchange selectivity with changes in the sorbed phase composition; 2) diffusion in/out of stagnant water regions in aggregates; or 3) cation exchange rate limited by the kinetics of exchange reaction or diffusion to/from exchange sites.

In simulations not discussed here, the author assumed regular variations in exchange selectivities as the composition of the exchanger phase changed. The selectivity coefficients for H^+ replacing $B_i^{z_i+}$ were arbitrarily assumed to hyperbolically decrease with decreasing equivalent fractions of $B_i^{z_i+}$ on the exchanger. These simulation results, with respect to those discussed in this section, showed somewhat earlier breakthroughs, lower concentration peaks and curve tailing. Although this simple type of exchange selectivity variation did improve simulation results, it did not fully account for the experimentally observed breakthrough data. Accordingly, the data may be better accounted for by a mobile/immobile water model or a two-site, equilibrium/kinetic, model.

The existence of isolated micropore regions in the soil matrix, through which flow does not occur, tends to effect an earlier emergence of concentration peaks, lower maximum concentrations, and tailing. Simulations done by Mansell et al. (1986) and Schulin et al. (1986) have demonstrated such effects. Selim et al. (1976) used a two-site, equilibrium and 1st order adsorption, model to describe transport of a pesticide in soil. Jardine et al. (1985) were able to describe Al movement using such a model. Although choice of models is not arbitrary, predicted results may be similar for each model. Nkedi-Kizza et al. (1984), for example, have discussed the mathematical equivalence of combined diffusion/equilibrium sorption and two-site, equilibrium/kinetic sorption, models for transport of a reactive solute.

Figure 4-26 shows predicted SO_4^{2-} effluent concentrations compared to experimental data. Use of the Freundlich sorption isotherm led to the prediction of a gradual decrease in SO_4^{2-} concentration throughout the leaching process. Experimental data show an early peak followed by lower concentrations than predicted. The peak in SO_4^{2-} concentration tended to coincide with the minimum in H^+ effluent concentration. (Compare to experimental data in Figs. 4-5 and 4-8.) Conversely, low concentration leaching of SO_4^{2-} beyond the peak occurred along with higher H^+

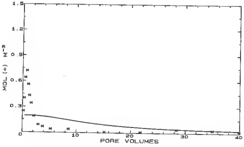

Figure 4-26. Comparison of equilibrium model results (continuous line) to experimental elution of SO_4^{2-} from Cecil topsoil leached with pH 3.0 HNO_3.

effluent concentration values. The effect of solution H^+ concentration on anion sorption has been previously discussed. Apparently, SO_4^{2-} sorption was strongly influenced by solution concentration of H^+. Failing to explicitly include this effect led to underprediction of initial SO_4^{2-} leaching at higher pH values and overprediction of SO_4^{2-} leaching at lower pH values. Overprediction of SO_4^{2-}, in turn, contributed to overestimation of solution concentration of cations.

This effect can be seen in Fig. 4-27 which shows predicted and observed Al^{3+} concentrations. Maximum Al^{3+} concentration was predicted at about 12 pore volumes of effluent, beyond which point the concentration slowly decreased. No similar behavior was experimentally observed. Predicted breakthrough of Al^{3+} was retarded with respect to experimental data. Also, the breakthrough was abrupt. The retarded and steep predicted Al^{3+} breakthrough occurred coincidentally with the predicted Ca^{2+} peak emergence and steep drop in effluent Ca^{2+} concentration.

Figure 4-28 reveals qualitative agreement between predicted and experimental H^+ leaching data. The occurrence and value of the early concentration minimum were reasonably well accounted for by the model. Predicted breakthrough was, however, retarded and abrupt, similar to the predicted behavior for Al^{3+}. The apparent plateau in H^+ concentration beyond about 12 pore volumes of effluent exhibits a slight decrease with increasing effluent volume. As with predicted

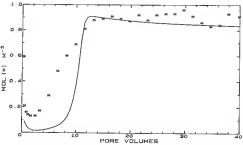

Figure 4-27. Comparison of equilibrium model results (continuous line) to experimental breakthrough of Al^{3+} from Cecil topsoil leached with pH 3.0 HNO_3

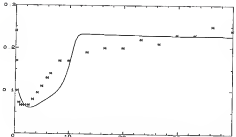

Figure 4-28. Comparison of equilibrium model results (continuous line) to experimental breakthrough of H$^+$ from Cecil topsoil leached with pH 3.0 HNO3.

Al^{3+} elution, the behavior was due to excessive prediction of SO_4^{2-} leaching.

Figure 4-29 shows predicted versus experimentally observed Ca^{2+} concentrations for Cecil topsoil leached with pH 3.0 H_2SO_4. As was the case for Cecil topsoil leached with pH 3.0 HNO_3, the predicted time of peak emergence and concentration maximum were much greater in simulation than experiment. The model failed to account for tailing. Despite these points of discrepancy between simulation results and experimental data, the use of anion sorption isotherms predicted the relative effects of NO_3^- and $SO_4^=$ sorption on cation leaching rates. Peak emergence was predicted to occur later for the topsoil leached with pH 3.0 H_2SO_4 than with pH 3.0 HNO_3. (Compare Figs. 4-25 and 4-29.)

Use of pH-Dependent Anion Sorption Isotherms

Contributing to the above discussed points of discrepancy between experimental data and simulation results was the inapplicability of the Freundlich isotherms for describing anion sorption in a soil subjected to marked changes in pH. If effects of solution concentration for H^+ could be explicitly included in an anion sorption isotherm, better model performance might be expected. It is proposed that a simple empirical analog of the Freundlich equation may offer substantially improved prediction of anion leaching behavior. This analog is

$$S_i = k_i(C_i)^m(C_{H^+})^n \qquad [37]$$

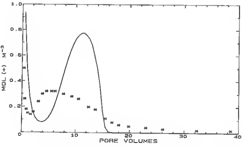

Figure 4-29. Comparison of equilibrium model results (continuous line) to experimental elution of Ca^{2+} from Cecil topsoil leached with pH 3.0 H_2SO_4.

where C_{H^+} is the solution concentration of H^+, n is a constant, and the other variables have been previously defined.

Kampreth et al. (1956) demonstrated that a family of sorption isotherms may be generated for $SO_4{}^{2-}$ over a range of pH values. These pH-dependent sorption isotherms had similar shapes, differing essentially only in increased sorption, at a given solution concentration of $SO_4{}^{2-}$, with increased acidity of the soil solution. It seemed reasonable to the author, therefore, that a single equation might describe $SO_4{}^{2-}$ (or any other anion) sorption over a range of pH values if the form of the equation predicted increased sorption with increased solution concentration of either $SO_4{}^{2-}$ or H^+. A simple functional form having this characteristic is equation [37].

Experimental data used to estimate the parameters of the Freundlich equation [3] could be fitted to equation [37] by a least squares procedure provided values for H^+ concentrations were also known (Anion sorption data is presented in Appendix A.) Thus, by such a fitting procedure it was ascertained that pH-dependent $SO_4{}^{2-}$ sorption and Cl^- sorption (considered representative of the sorption behavior of all weakly sorbed anions, including $NO_3{}^-$) in the topsoil could be described by

$$S_{SO_4{}^{2-}} = 0.29(C_{SO_4{}^{2-}})^{0.26}(C_{H^+})^{0.14} \qquad [38]$$

$$k_{Cl^-} = 1.08(C_{Cl^-})^{0.31}(C_{H^+})^{0.20} \qquad [39]$$

Figure 4-30 shows the predicted SO_4^{2-} elution curve for topsoil leached with pH 3.0 HNO_3 when equations [38] and [39] were used in the model compared to experimentally determined effluent concentrations. Clearly, explicit inclusion of the pH effect on anion sorption improved model predictions. (Compare to Fig. 4-26.) The early peak, due to desorption at low H^+ concentrations, in effluent SO_4^{2-} concentration was predicted. Also, the low concentration leaching subsequent to this peak, due to enhanced SO_4^{2-} retention at higher H^+ concentrations, was accurately described. The position and shape of the SO_4^{2-} peak were not well-described, however. Too much desorption at low H^+ concentration was predicted. Better results might be obtained if better estimates of the parameters, k, m, and n, were available. This would entail inclusion of more data sets (S, C_1, C_{H^+}) in the least squares procedure. Furthermore, it would be desirable to have data from sorption experiments in which C_1 and C_{H^+} were varied in at least more than one systematic way.

Inclusion of the isotherm equations [38] and [39] into the equilibrium model was accomplished by estimating equilibrium sorption of each anion at the initial concentration of H^+ in a cell (at step 2 in the model). Step 3 estimated the equilibrium solution and sorbed phase

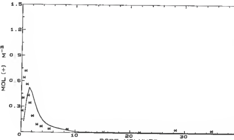

Figure 4-30. Comparison of simulated SO_4^{2-} elution (continuous line) using pH-dependent anion sorption isotherms to experimental data for leaching Cecil topsoil with pH 3.0 HNO_3

concentrations of cations. Steps 2 and 3 were then repeated with a new value for H^+ solution concentration. Somewhat better estimates of equilibrium sorbed and solution phase concentrations might have been obtained by passing through these steps several times but at the expense of more computational time.

Nonequilibrium Model

Possible causes for the failure of the equilibrium model to describe the observed leaching behavior have been discussed. Determination of selectivity variations for each species in a multicomponent system is a formidable task. Determination of certain parameters which appear upon introduction of mobile/immobile water phases or kinetically controlled sites for cation exchange are often not susceptible to unequivocal measurement (Nkedi-Kizza et al., 1984). Despite such difficulties, the relative applicability of the mobile/immobile water and two-site, equilibrium/kinetic, models to describing H^+-induced cation leaching of the Cecil soil is now considered.

Rao et al. (1980) found that tracer BTCs from an aggregated medium could be identically described using either a mobile/immobile water transport model or a mobile water only transport model that employed a dispersion coefficient modified to account for diffusion in/out of aggregates if the aggregate size or pore water velocity were sufficiently small. Therefore, since Cl^- BTCs for the Cecil topsoil and subsoil could be described by the transport model without inclusion of mobile/immobile water regions (see Figs. 4-22 and 4-23), the fitted parameter f adequately accounted for the contribution of diffusion in/out of stagnant regions to the overall dispersion. Failure of the equilibrium model to account for times of peak concentration emergence or breakthrough, however, indicates that some fraction of the exchange complex was not at instantaneous equilibrium with the solution phase. The cause of the observed nonequilibrium condition might have been slow cation exchange reaction kinetics or diffusion to/from sites for exchange. The latter case may be identified with the occurrence of mobile/immobile water phases. Here, however, the volume of immobile water is small and associated with external and internal particle surfaces for cation exchange. Accordingly, diffusion of tracer Cl^- in/out of this volume may have a small effect on observed Cl^- BTCs. An anion tracer is perhaps even largely excluded from this immobile water volume.

Nonequilibrium due principally to reaction kinetics or diffusion to/from exchange sites may be accounted for by evoking a two-site, equilibrium/kinetic, model for cation exchange. The kinetic portion of the model includes equations of the form

$$\frac{dX_{i2}}{dt} = r_i(K_{i2}C_i - X_{i2}) \qquad [40]$$

where X_{i_2} is the equivalent fraction of cation i on the portion of the exchange complex where exchange reactions are not governed by instantaneous equilibrium, C_i is the solution concentration of i, K_{i_2} is the equilibrium sorption coefficient, and r_i is a constant that varies from cation species to cation species

Several new parameters appear in this model: 1) the rates of reaction for kinetically controlled cation exchange, and 2) the fraction of exchange sites associated with such kinetically controlled exchange. (Methods of determining these parameters are discussed later in this section.)

Ogwada and Sparks (1986) have shown that if the rate of cation exchange is limited by diffusion to cation exchange sites, as well as exchange reaction rate, the overall rate coefficient, r, is given by

$$r = \frac{r_{diffusion}\ r_{reaction}}{(r_{diffusion} + r_{reaction})} \qquad [41]$$

Using different methodologies for determining the overall rate coefficient, these authors were able to calculate values for the diffusion and reaction components of the overall rate coefficient. According to their data the overall rate coefficient for K^+-Ca^{2+} exchange on a soil, kaolinite, and vermiculite, differed only slightly from the calculated diffusion component.

Note that equation [40] may be written as

$$\frac{dX_i}{dt} = r_{i_1}C_i - r_{i_{-1}}X_{i_2} \qquad [42]$$

where r_{i_1} and $r_{i_{-1}}$ are, respectively, the rates of the forward and reverse reactions. Accordingly,

$$r_i = \frac{r_{i_1}}{K_{i_2}} \qquad [43]$$

Therefore, the overall rate coefficient r_i, is approximately determined by the rate of diffusion to/from exchange sites and the equilibrium sorption coefficient. For diffusion in/out of interlamellar spaces of vermiculite r_i should vary appreciably depending upon cation size. For the aluminum-hydroxy interlayered material in the Cecil soil these differences may be less. According to Rich (1968), these materials exhibit interlamellar spaces that are propped open in comparison to such spaces in vermiculite. Although appropriate values for r_{i_1} could be determined for each cation species by the methods discussed by Ogwada and Sparks (1986), for the sake of illustrating the applicability of the two-site model to the Cecil soil used in this study a single value was used.

In order to adapt equations of the form [40] to model application these equations must be integrable. Within the framework of the mixing-cell model, C_i, in equation [40], can be expressed in terms of the total equivalents, T_i, of the species present in a cell at any flow step, the solution volume of the cell, V, the CEC of the equilibrium exchange sites, Q_1, the CEC of the nonequilibrium exchange sites, Q_2, and the equilibrium sorption coefficient for sites governed by instantaneous equilibrium, K_{i_1}, giving

$$\frac{dX_{i_2}}{dt} = r_i((T_iK_{i_2}/(V+Q_1K_{i_1}))-(1+(Q_2K_{i_2}/V+Q_1K_{i_1})))X_{i_2}) \qquad [44]$$

If K_{i_1} and K_{i_2} are constant the equation can be integrated to give

$$X_{i_2} = (1/B)(A-(A-BX_{i_{2\,\mathrm{initial}}})\exp(-Br_it)) \qquad [45]$$

where

$$A = T_iK_{i_2}/(V+Q_1K_{i_1}) \qquad [46]$$

$$B = 1+(Q_2K_{i_2}/(V+Q_1K_{i_1})) \qquad [47]$$

and $X_{i_{2\,\mathrm{initial}}}$ is the initial equivalent fraction of the species adsorbed onto type two, kinetically controlled, sites.

For the present soil system, however, K_{i_1} and K_{i_2} are derived from the expression for the Gaines-Thomas selectivity coefficient for H^+ exchange for cation i and are given by

$$K_{i_j} = (1/K_i)(X_{H^+j}/C_{H^+})^{z_i}(\gamma_i/(\gamma_{H^+})^{z_i}) \ , \quad j=1,2 \qquad [48]$$

where X_i is the Gaines-Thomas selectivity coefficient These parameters are not constant, of course. However, since X_{H^+j} and C_{H^+} may be expected to vary only slightly during the adsorption process the integration can be made, using initial values for these variables, introducing only small error.

Equations of the form (45) may be used in a two-site model coupled to a mixing-cell transport model provided the r_i constants are known and Q_2 is known. As mentioned above, no attempt was made in this study to measure the r_i values. Neither was Q_2 estimated. Instead, Q_2 and a single value for r_i were varied to achieve model results in general agreement with experimental results. Although such simulations serve to indicate the potential applicability of the two-site model for explaining the experimental results, these parameters, all r_is and Q_2, are susceptible to measurement (Ogwada and Sparks, 1986; Jardine and Sparks, 1984a).

The logarithmic form of equation (45) can be employed in batch type experiments to determine the appropriate values for the r_is if the CECs of the equilibrium and kinetic sites are known and changes in solution concentrations of the adsorbing species with time are measured. Since the model assumes the existence of equilibrium sites, film diffusion through a stagnant volume of water to surface exchange sites must be ignored. The stirred batch method of Ogwada and Sparks (1986) would appear appropriate for the measurement of rate coefficients for cation exchange limited by interparticular diffusion and reaction rates.

If limited access to interlamellar sites in the aluminohydroxy vermiculite (or interior exchange sites in organic matter) was the cause of nonequilibrium, then the CEC associated with each sites might be determined by first saturating readily accessible exchange sites with a large cationic species such as cetyltrimethylammonium bromide (CTAB) then extracting for interlamellar cations and total acidity. This adsorbate was used by Jardine and Sparks (1984a) to block cation exchange at readily accessible sites while leaving interlamellar sites open for exchange.

A confounding problem in an attempt to model cation exchange in a soil that exhibits different types of sites for exchange is the possibility that the selectivity for exchange is not the same for both types of sites. Jardine and Sparks (1984b), for example, have demonstrated that K^+-Ca^{2+} exchange selectivity for a Paleudult was different when CTAB occluded readily accessible sites than when such sites were available to participate in the exchange reaction. Although such differences in exchange selectivity were not determined here, these differences could be ascertained by use of the CTAB adsorbate. Consistent with the use of single valued selectivity coefficients determined using the unaltered soil (as previously described), quantification of extractable bases, Al, and titratable acidity remaining in a soil sample saturated with CTAB would allow exchange selectivities of the limited accessible exchange sites to be estimated. In the subsequent application of the two-site model it was assumed that exchange selectivities determined for the whole soil were applicable to both readily and limitedly accessible exchange sites.

Kinetically controlled cation exchange was easily included in the mixing-cell transport and chemical equilibrium model. After each flow step, equilibrium distributions of adsorbed and solution phases was calculated. Rate dependent adsorption was calculated. Due to changes in solution concentrations of cations brought about by the kinetic exchange step, the equilibrium solution and adsorbed phase concentrations were subsequently updated to new equilibrium values. Figures 4-31 and 4-32 show predicted elution curves for Ca^{2+} and Al^{3+}, respectively, obtained from a two-site model compared to experimental data. The model treated exchange at one-half of the sites as kinetically controlled ($Q_2 = 0.001988$). The single rate coefficient used, r_1, was 0.25 hr^{-1}. The time over which equation [45] was integrated was (volume of water in a segment)/(volumetric flow rate). The model considered anion sorption to be explicitly pH-dependent by use of equations [38] and [39].

The location and height of the concentration peak for Ca^{2+} was adequately described using this model. Although tailing was predicted,the exact shape of the Ca^{2+} concentration curve was only qualitatively described. Nevertheless,

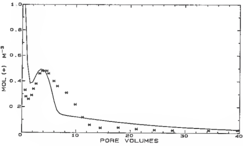

Figure 4-11. Comparison of nonequilibrium model results (continuous line) to experimental elution of Cs^{2+} from Cecil topsoil leached with pH 3.0 HNO_3

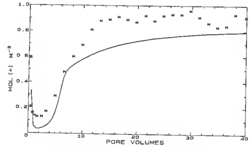

Figure 4-32. Comparison of nonequilibrium model results (continuous line) to experimental breakthrough of Al^{3+} from Cecil topsoil leached with pH 3.0 HNO_3.

the greatly enhanced agreement, compared to results from the equilibrium model, between simulated and experimental results suggests that the two-site model may be adequate for describing H^+-induced cation leaching.

The location of the Al^{3+} breakthrough was described by the model. The steady increase in predicted Al^{3+} effluent concentration beyond about 14 pore volumes of effluent corresponded to the steady decrease in effluent Ca^{2+} concentration. Experimentally measured Ca^{2+} and Al^{3+} concentrations were fairly constant beyond about 12 to 14 pore volumes of effluent. The general discrepancy between the higher experimentally determined concentrations and lower predicted values for Al^{3+} was likely due to overestimation of the charge borne by Al.

CHAPTER 5

CONCLUSIONS

Leaching Experiments

Rates at which basic and acidic cations were leached from columns of Cecil topsoil and subsoil by application of simulated acid rain depended on the nature of the acid. Losses of cations were less if SO_4^{2-}, rather than the weakly sorbed NO_3^-, was the common anion. This effect was more pronounced for the Cecil subsoil. When pH 3.0 acid was applied to columns of subsoil, net retention of positive charge occurred. The small apparent net loss of positive charge from the topsoil leached with pH 3.0 H_2SO_4 solution was likely due to overestimation of charge borne by Al. When pH 3.7 H_2SO_4 solution was applied to columns of subsoil losses of Ca^{2+} and Mg^{2+} were retarded with respect to the case when pH 3.7 HNO_3 was applied. Differences in cation leaching losses due to the type of acid applied for the topsoil were negligible at this pH. For pH 4.7 input acid, however, there were no differences in cation leaching losses due to nature of the acid. At this pH, however, there were appreciable net losses of positive charge from the topsoil and subsoil irrespective of the acid type. These losses, and the smaller net losses at pH 3.7, were largely attributed to desorption of native anions. It is doubtful, however, that such behavior occurs naturally in a forest soil because the leaching solution is typically enriched with salts.

Anionic effects on H^+ induced cation leaching from Cecil soil appear to be limited to pH values less than 3.7, for the topsoil, and about 3.7, for the subsoil. At such low pH values anionic effects on cation leaching were secondary to the principal effect of enhanced leaching by higher concentrations of H^+ ions. The exact range of pH over which these effects can be seen in the natural soil environment is not known. Processes such as unsaturated flow, redistribution, nutrient cycling, and microbial activity could enhance or diminish these effects for acid rain of any pH.

Leaching Simulations

The equilibrium model predicted later breakthroughs than experimentally observed. This model also did not account for tailing of basic cation BTCs. Such behavior could have been due to variations in exchange selectivity as the sorbed phase composition of the exchanger changed. Also, diffusion in/out of regions of immobile water or non-instantaneous rates of cation exchange could have caused the observed nonequilibrium.

The Freundlich isotherms did not adequately account for pH effects on anion sorption/desorption. In turn, errors in estimation of anion concentrations influenced predictions of cation concentrations. Explicit inclusion of pH effects on anion sorption by use of modified Freundlich equations, [38] and [39], improved predictions of SO_4^{2-} concentrations in the leachate.

It was demonstrated that a nonequilibrium model for cation exchange has the potential of describing H^+-induced cation leaching from the Cecil soil. Inasmuch as tracer BTCs could be described by a model which did not include regions of immobile water, it was concluded that diffusion in/out of regions of stagnant water did not significantly contribute to the observed nonequilibrium conditions. Accordingly, a two-site, equilibrium/kinetic, model for cation exchange was applied. Such a model could account for nonequilibrium conditions due to either rate of cation exchange or diffusion to/from limitedly accessible exchange sites in interlamellar positions of the aluminohydroxy interlayered vermiculite present in the Cecil soil.

By varying parameters for fraction of exchange sites which exhibit non-instantaneous exchange and the rate of cation exchange, reasonable agreement between model and experimental results was obtained. The model assumed equal rates of cation exchange for all species. Better agreement between model results and experimental data could probably be obtained by use of different rate coefficients for each cationic species.

Although additional input data would be needed to quantitatively simulate leaching from the Cecil soil, it seems likely that reasonably accurate predictions could be made for a less physically and chemically heterogeneous soil (for example, a sandy soil) without such data. For such a simpler soil system inclusion of the two-site model may not be needed.

BIBLIOGRAPHY

Adams, F. 1971. Ionic concentrations and activities in soil solutions. Soil Sci. Soc. Am. Proc. 35:420-426.

Adams, F., and Z. Rawajfih. 1977. Basaluminite and alunite: A possible cause of sulfate retention by acid soils. Soil Sci. Soc. Am. J. 41:686-692.

Alexander, M. 1977. Introduction to soil microbiology, 2nd ed. John Wiley and Sons, New York.

Alymore, L.A.G., M. Karim, and J.P. Quirk. 1966. Adsorption and desorption of sulfate ions by soil constituents. Soil Sci. 103:10-15.

Bache, B.W., and G.S. Sharp. 1976. Soluble polymeric hydroxyaluminum ions in acid soils. J. Soil Sci. 27:167-174.

Barrow, N.J., and T.C. Shaw. 1977. The slow reactions between soil and anions: 7. Effect of time and temperature of contact between an adsorbing soil and sulfate. Soil Sci. 124:347-354.

Black, A.S., and S.A. Waring. 1979. Adsorption of nitrate, chloride and sulfate by some highly weathered soils from South-east Queensland. Aust. J. Soil Res. 17:271-282.

Brenner, H. 1962. The diffusion model of longitudinal mixing in beds of finite length. Numerical values. Chem. Eng. Sci. 17:229-243.

Bubenick, D.V., J.A. Dirgo, and D.R. Roeck. 1983. Sources affecting acid rain formation. In D.V. Bubenick (ed.) Acid rain information book. National Technical Information Service, U.S. Department of Commerce, Springfield, Va.

Cassel, D.K. 1985. Physical characteristics of soils of the southern region--summary of in situ unsaturated hydraulic conductivity. Southern Cooperative Series Bulletin 303. North Carolina State University, Raleigh, N.C.

Cheng, F.-J., J.W. Delleur, and A.R. Rao. 1986. Implementation, sensitivity analysis and application of the "ILWAS" model of acid precipitation impacts to Panther Lake and Walker Branch watersheds. Technical Report No. 176.

Purdue University, Water Resources Research Center, Lafayette, Ind.

Chang, M.L., and G.W. Thomas. 1963. A suggested mechanism for sulfate adsorption by soils. Soil Sci. Soc. Am. Proc. 27:281-283.

Chao, T.T. 1964. Anionic effects on sulfate adsorption by soils. Soil Sci. Soc. Am. Proc. 28:581-583.

Chao, T.T., M.E. Harward, and S.C. Pang. 1963. Cationic effects on sulfate adsorption by soils. Soil Sci. Soc. Am. Proc. 27:35-38.

Cosby, B.J., R.F. Wright, G.M. Hornberger, and J.N. Galloway. 1985. Modelling the effects of acid deposition: Estimation of long-term water quality responses in a small forested catchment. Water Resour. Res. 21:1591-1601.

Couto, W., D.J. Lathwell, and D.R. Bouldin. 1979. Sulfate sorption by two oxisols and an alfisol of the tropics. Soil Sci. 127:108-116.

Ensminger, L.E. 1954. Some factors affecting the adsorption of sulfate by Alabama soils. Soil Sci. Soc. Am. Proc. 18:259-264.

Gaines, G.L., and H.C. Thomas. 1953. Adsorption studies on clay minerals. II A formulation of the thermodynamics of exchange adsorption. J. Chem. Phys. 21:714-718.

Gaston, L.A., R.S. Mansell, and R.D. Rhue. 1986. Sulfate mobility in acid soils and implications with respect to cation leaching: A review. Soil Crop Sci. Soc. Fla. Proc. 45:67-72.

Gebhardt, H., and N.T. Coleman. 1974. Anion adsorption by allophanic tropical soils: II. Sulfate adsorption. Soil Sci. Soc. Am. Proc. 38:259-262.

Harward, M.E., and H.M. Reisenauer. 1966. Reactions and movement of inorganic soil sulfur. Soil Sci. 101:326-335.

Hingston, F.J., R.J. Atkinson, A.M. Posner and J.P. Quirk. 1967. Specific adsorption of anions. Nature. 215:1459-1461.

Hingston, F.J., A.M. Posner and J.P. Quirk. 1972. Anion adsorption by goethite. I. The role of the proton in determining adsorption envelopes. J. Soil Sci. 23:177-192.

Huete, A.R., and J.D. McColl. 1984. Soil cations leaching by "acid rain" with varying nitrate-to-sulfate ratios. J. Environ. Qual. 13:366-371.

Jacks, G., G. Knutsson, L. Maxe, and A. Fylkner. 1984. Effect of acid rain on soil and groundwater in Sweden. In B. Yaron (ed.) Pollutants in porous media. Springer-Verlag, New York.

Jardine, P.M., J.C. Parker, and L.W. Zelazny. 1985. Kinetics and mechanisms of aluminum adsorption on kaolinite using a two-site nonequilibrium transport model. Soil Sci. Soc. Am. J. 49:867-873.

Jardine, P.M., and D.L. Sparks. 1984a. Potassium-calcium exchange in a multireactive soil system. I. Kinetics. Soil Sci. Soc. Am. J. 48:39-45.

Jardine, P.M., and D.L. Sparks. 1984b. Potassium-calcium exchange in a multireactive system: II Thermodynamics. Soil Sci. Soc. Am. J. 48:45-50.

Johnson, D.W., J. Turner, and J.M. Kelly. 1982. The effects of acid rain on forest nutrient status. Water Resour. Res. 18:449-461.

Kamprath, E.J., W.L. Nelson, and J.W. Fitts. 1956. The effect of pH, sulfate and phosphate concentrations on the adsorption of sulfate by soils. Soil Sci. Soc. Am. Proc. 20:463-466.

Keeney, D.R., and D.W. Nelson. 1982. Nitrogen--inorganic forms. In A.L. Page (ed.) Methods of soil analysis. Part 2. Chemical and microbiological properties, 2nd ed. American Society of Agronomy, Inc., Madison, Wis.

Khanna, P.K., and F. Beese. 1978. The behavior of sulfate on salt input in podzolic brown earth. Soil Sci. 125:16-22.

Kinjo, T., and P.F. Pratt. 1971. Nitrate adsorption: I. In some acid soils of Mexico and South America. Soil Sci. Soc. Am. Proc. 35:722-725.

Lee, J.J. 1985. Effect of simulated sulfuric acid rain on the chemistry of a sulfate-adsorbing forest soil. Water, Air, and Soil Pollution. 25:185-193.

Liu, K.R. In preparation. Leaching of cations during displacement of acid solutions through columns of Cecil soil. Ph.D. Dissertation, University of Florida.

Mansell, R.S., S.A. Bloom, R.M. Selim, and R.D. Rhue. 1986. Multispecies cation leaching during continuous displacement of electrolyte solutions through soil columns. Geoderma. 38:61-75.

Marion, G.M., D.M. Hendricks, G.R. Dutt, and W.H. Fuller. 1976. Aluminum and silica solubility in soils. Soil Sci. 121:76-85.

McFee, W.W., F. Adams, C.S. Cronan, M.K. Firestone, C.D. Foy, R.D. Harter, and D.W. Johnson. 1983. Effects on soil systems. In R.A. Linthurst (ed.) The acid deposition phenomenon and its effects: Critical assessment review papers. EPA-600/8-83-016B. U.S. Environmental Protection Agency, Office of Research and Development, Washington, D.C.

McLean, E.O. 1965. Aluminum. In C.A. Black (ed.) Methods of soil analysis. Part 2. Chemical and microbiological properties. American Society of Agronomy, Inc., Madison, Wis.

Nkedi-Kizza, P., J.W. Biggar, H.M. Selim, M.Th. van Genuchten, P.J. Wierenga, J.M. Davidson, and D.R. Nielson. 1984. On the equivalence of two conceptual models for describing ion exchange during transport through an aggregated Oxisol. Water Resour. Res. 20:1123-1130.

Ogwada, R.A., and D.L. Sparks. 1986. Kinetics of ion exchange on clay minerals and soil: II Elucidation of rate-limiting steps. Soil Sci. Soc. Am. J. 50:1162-1166.

Parfitt, R.L., and R. St. C. Smart. 1978. The mechanisms of sulfate adsorption on iron oxides. Soil Sci. Soc. Am. J. 42:48-50.

Rao, P.S.C., D.E. Rolston, R.E. Jessup, and J.M. Davidson. 1980. Solute transport in aggregated porous media: Theoretical and experimental evaluation. Soil Sci. Soc. Am. J. 44:1139-1146.

Rajan, S.S.S. 1978. Sulfate adsorbed on hydrous alumina, ligands displaced, and changes in surface charge. Soil Sci. Soc. Am. J. 42:39-44.

Rajan, S.S.S. 1979. Adsorption and desorption of sulfate and charge relationships in allophanic clays. Soil Sci. Soc. Am. J. 43:65-69.

Reuss, J.O., and D.W. Johnson. 1986. Acid deposition and the acidification of soils and water. Springer-Verlag, New York.

Rhoades, J.D. 1982. Soluble salts. In A.L. Page (ed.) Methods of soil analysis. Part 2. Chemical and microbiological properties, 2nd ed. American Society of Agronomy, Inc. Madison, Wis.

Rhue, R.D., and G. Kidder. 1983. Procedures used by the IFAS extension soil testing laboratory and interpretation of results. IFAS Fla. Coop Ext. Serv. Circ. 596. University of Florida, Gainesville, Fla.

Rich, C.I. 1960. Aluminum in interlayers of vermiculite. Soil Sci. Soc. Am. Proc. 24:26-32.

Rich, C.I. 1968. Hydroxy interlayers in expansible layer silicates. Clays and Clay Minerals. 16:15-30.

Rubin, J., and R.V. James. 1973. Dispersion-affected transport of reacting solutes in saturated porous media. Galerkin method applied to equilibrium controlled exchange in unidirectional steady water flow. Water Resour. Res. 9:1332-1356.

Schulin, R., H. Fluhler, R.S. Mansell, and H.M. Selim. 1986. Miscible displacement of ions in aggregated soils. Geoderma. 38:311-322.

Schultz, R.D., and E.J. Reardon. 1983. A combined mixing cell/analytic model to describe two-dimensional reactive solute transport for unidirectional groundwater flow. Water Resour. Res. 19:493-502.

Schweich, D., and M. Sardin. 1981. Adsorption, partition, ion exchange and chemical reaction in batch reactors or columns. A review. J. Hydrol. 50:1-33.

Selim, H.M., J.M. Davidson, and R.S. Mansell. 1976. In Proceedings of the 1976 Summer Computer Simulation Conference, Washington, D.C.

Serna, C.J., J.L. White, and S.L. Hem. 1977. Anion-aluminum hydroxide gel interaction. Soil Sci. Soc. Am. J. 41:1009-1013.

Singh, B.R. 1984. Sulfate sorption by acid soils: 4. Kinetics and effects of temperature and moisture. Soil Sci. 138:440-447.

Singh, B.R., G. Abrahamsen, and A. Stuanse. 1980. Effects of simulated acid rain on sulfate movement in acid forest soils. Soil Sci. Am. J. 44:75-80.

Tanji, K.K. 1970. A computer analysis of the leaching of boron from stratified soil columns. Soil Sci. 110:44-51.

Tanji, K.K., L. D. Doneen, and J.L. Paul. 1967. III. The quality of water percolating through stratified substrata, as predicted by computer analyses. Hilgardia. 38:319-347.

Thomas, G.W. 1960. Effects of electrolyte imbibition upon cation-exchange behavior of soils. Soil Sci. Soc. Am. Proc. 24:329-332.

Thomas, G.W. 1982. Exchangeable cations. In A.L. Page (ed.) Methods of soil analysis. Part 2. Chemical and microbiological properties, 2nd ed. American Society of Agronomy, Inc., Madison, Wis.

Valocchi, A.J., R.L. Street and P.V. Roberts. 1981. Transport of ion-exchange solutes in groundwater: Chromatographic theory and field simulations. Water Resour. Res. 17:1517-1527.

Van Ommen, H.C. 1985. The "mixing-cell" concept applied to transport of non-reactive and reactive components in soils and groundwater. J. Hydrol. 78:201-213.

Wolt, J.D. 1981. Sulfate retention by acid sulfate polluted soils in the copper basin area of Tennessee. Soil Sci. Soc. Am. J. 45:283-287.

APPENDIX A

ANION SORPTION DATA

Table A-1. Sulfate and Cl^- sorption data for Cecil topsoil and subsoil. Solution concentration in $mol(-)/m^3$ and sorbed phase concentration in $cmol(-)/kg$.

Topsoil

Solution SO_4^{2-}	Solution H^+	Sorbed SO_4^{2-}	Solution Cl	Solution H^+	Sorbed Cl
0.08	0.05	0.10	0.02	0.05	0.02
0.08	0.05	0.09	0.02	0.05	0.01
0.41	0.16	0.15	0.37	0.18	0.03
0.38	0.16	0.16	0.37	0.17	0.03
0.77	0.37	0.29	1.00	0.43	0.00*
0.86	0.37	0.24	1.00	0.46	0.00*
1.64	0.81	0.39	1.82	0.94	0.08
1.71	0.87	0.35	1.92	0.94	0.03*
5.76	2.98	0.47	5.35	3.43	0.23
5.78	3.19	0.47	5.39	3.51	0.21

*Not included in regression analysis

Subsoil

Solution SO_4^{2-}	Solution H^+	Sorbed SO_4^{2-}	Solution Cl	Solution H^+	Sorbed Cl^-
0.08	0.02	0.32	0.02	0.02	0.01
0.08	0.02	0.34	0.02	0.02	0.01
0.12	0.04	0.36	0.31	0.06	0.06
0.14	0.04	0.55	0.36	0.05	0.04
0.51	0.08	0.69	0.90	0.15	0.05
0.48	0.08	0.70	0.85	0.14	0.08
1.05	0.22	0.96	1.68	0.46	0.17
0.99	0.20	0.98	1.77	0.45	0.13
3.91	1.53	1.67	4.70	2.54	0.55
3.83	1.53	1.71	4.75	2.60	0.53

APPENDIX B

COLUMN LEACHING DATA

The following 16 tables contain the complete column leaching data. These tables fall into two groups. Tables B-1 through B-8 contain data for the topsoil leaching experiments and Tables B-9 through B-16 contain subsoil leaching data. Within each group the tables are presented in alphabetical order by name of ion species. Table B-1, for example, contains effluent concentration data for Al^{3+} leached by each of the six acid treatments.

Table B-1. Aluminum leaching data for the Cecil topsoil as concentration ($mol(+)/m^3$) versus pore volumes of effluent.

HNO3 pH 3.0		H2SO4 pH 3.0		HNO3 pH 3.7		H2SO4 pH 3.7		HNO3 pH 4.7		H2SO4 pH 4.7	
PV	C	PV	C	PV	C	PV	C	PV	C	PV	C
0.17	2.23	0.13	2.54	0.11	2.57	0.14	2.37	0.17	1.67	0.14	2.74
0.33	0.59	0.29	0.47	0.27	0.82	0.31	0.53	0.34	0.40	0.31	0.76
0.49	0.21	0.45	0.19	0.42	0.34	0.47	0.21	0.51	0.18	0.48	0.30
0.82	0.16	0.60	0.15	0.74	0.14	0.80	0.13	0.85	0.13	0.81	0.16
1.15	0.14	0.76	0.14	1.05	0.11	1.13	0.10	1.18	0.12	1.14	0.14
1.65	0.13	0.91	0.13	1.52	0.09	1.62	0.09	1.69	0.11	1.64	0.12
2.47	0.13	1.22	0.12	3.08	0.08	3.26	0.07	3.38	0.11	3.29	0.11
3.30	0.17	1.53	0.11	4.64	0.06	4.90	0.06	5.07	0.10	4.95	0.10
4.95	0.29	2.31	0.11	7.77	0.06	8.18	0.05	8.46	0.09	8.26	0.09
6.60	0.48	3.09	0.11	10.89	0.06	11.46	0.05	15.23	0.08	14.88	0.09
8.25	0.60	4.64	0.18	14.02	0.06	14.74	0.05	21.99	0.08	21.51	0.08
9.90	0.69	6.20	0.28	17.15	0.07	18.02	0.06	28.76	0.07	28.13	0.08
11.55	0.81	7.75	0.42	20.27	0.07	21.30	0.06	35.52	0.07	34.76	0.07
13.20	0.88	9.31	0.55	23.40	0.07	24.58	0.07	42.29	0.07	41.05	0.07
14.85	0.89	10.86	0.61	26.52	0.07	27.86	0.08				
16.50	0.91	12.41	0.66	29.65	0.06	31.15	0.07				
18.15	0.89	13.97	0.77	32.77	0.07	34.43	0.07				
19.80	0.87	15.52	0.81	35.90	0.07	37.71	0.07				
21.44	0.92	17.08	0.83	39.02	0.08	46.99	0.08				
23.09	0.88	18.63	0.88								
24.74	0.92	20.19	0.86								
26.39	0.93	21.74	0.93								
28.04	0.93	23.30	0.94								

Table B-1. continued

HNO3 pH 3.0		H2SO4 pH 3.0		HNO3 pH 3.7		H2SO4 pH 3.7		HNO3 pH 4.7		H2SO4 pH 4.7	
PV	C	PV	C	PV	C	PV	C	PV	C	PV	C
29.69	0.96	24.85	0.94								
31.34	0.91	26.40	0.96								
32.99	0.86	27.96	0.95								
34.64	0.83	29.51	0.95								
36.29	0.84	31.07	0.96								
37.94	0.93	32.62	0.97								
39.92	0.91	34.18	0.97								
		35.73	0.89								
		37.28	0.92								
		38.84	0.91								

Table 8-2. Ammonium leaching data for the Cecil topsoil as concentration ($\mathrm{mol}(+)/m^{3}$) versus pore volumes of effluent.

HNO_3 pH 3.0		H_2SO_4 pH 3.0		HNO_3 pH 3.7		H_2SO_4 pH 3.7		HNO_3 pH 4.7		H_2SO_4 pH 4.7	
PV	C	PV	C	PV	C	PV	C	PV	C	PV	C
0.16	5.69	0.13	5.82	0.11	5.66	0.14	5.25	0.17	4.49	0.14	5.13
0.33	2.56	0.29	1.93	0.27	2.72	0.31	2.17	0.34	1.88	0.37	2.44
0.49	1.26	0.45	1.11	0.42	1.60	0.47	1.27	0.51	1.19	0.48	1.39
0.66	1.13	0.60	1.13	0.58	1.11	0.63	0.74	0.68	0.73	0.64	1.04
0.91	0.95	0.83	0.74	0.81	0.68	0.88	0.62	0.93	0.61	0.89	0.68
1.32	0.78	0.91	0.71	0.89	0.64	0.96	0.57	1.02	0.57	0.97	0.64
1.57	0.69	1.22	0.62	1.21	0.52	1.29	0.46	1.35	0.45	1.30	0.48
1.98	0.54	1.46	0.57	1.52	0.43	1.62	0.38	1.69	0.36	1.64	0.38
2.80	0.33	1.84	0.49	1.83	0.36	1.95	0.32	2.03	0.30	1.97	0.31
3.63	0.17	2.62	0.39	2.61	0.27	2.77	0.24	2.88	0.21	2.79	0.21
4.45	0.10	3.40	0.31	3.39	0.21	3.59	0.19	3.72	0.16	3.62	0.15
5.28	0.08	4.18	0.25	4.17	0.18	4.41	0.16	4.57	0.12	4.45	0.13
6.93	0.08	4.95	0.17	4.96	0.17	5.23	0.15	5.41	0.11	5.28	0.12
8.58	0.09	6.51	0.10	6.52	0.12	6.87	0.11	7.11	0.10	6.93	0.10
10.23	0.08	8.06	0.09	8.08	0.10	8.51	0.11	8.80	0.09	8.59	0.09
13.53	0.06	9.92	0.08	9.64	0.08	10.15	0.10	10.49	0.08	10.25	0.08
16.83	0.05	12.72	0.07	12.77	0.05	13.43	0.08	13.87	0.06	13.56	0.06
20.12	0.04	15.83	0.05	15.90	0.05	16.71	0.06	17.26	0.05	16.87	0.05
23.42	0.04	18.94	0.04	19.02	0.05	19.99	0.05	20.64	0.04	20.18	0.04
26.72	0.03	22.05	0.03	22.15	0.04	23.27	0.04	24.02	0.04	23.49	0.05
30.02	0.02	25.16	0.03	25.27	0.03	26.55	0.04	27.40	0.03	26.81	0.03
33.32	0.02	28.27	0.03	28.40	0.03	29.83	0.03	30.79	0.03	30.12	0.02
36.62	0.01	31.38	0.02	31.52	0.02	33.11	0.03	34.17	0.02	33.43	0.02
39.92	0.01	34.49	0.01	34.65	0.02	32.40	0.03	37.55	0.01	36.74	0.02
		38.84	0.01	39.02	0.01	40.99	0.02	42.29	0.01	41.38	0.01

Table B-3. Calcium leaching data for the Cecil topsoil as concentration (mol(+)/m^3) versus pore volumes of effluent

HNO3 pH 3.0		H2SO4 pH 3.0		HNO3 pH 3.7		H2SO4 pH 3.7		HNO3 pH 4.7		H2SO4 pH 4.7	
PV	C	PV	C	PV	C	PV	C	PV	C	PV	C
0.08	6.60	0.06	8.80	0.03	7.20	0.06	7.30	0.08	7.10	0.06	6.80
0.25	2.50	0.21	2.08	0.19	2.60	0.22	1.95	0.26	1.52	0.23	2.25
0.58	0.64	0.37	0.50	0.35	0.88	0.39	0.48	0.42	0.44	0.39	0.56
0.74	0.33	0.52	0.26	0.66	0.22	0.55	0.22	0.59	0.22	0.56	0.27
1.24	0.28	0.83	0.18	0.97	0.14	0.88	0.14	0.93	0.12	0.89	0.15
1.81	0.26	1.15	0.15	1.44	0.10	1.21	0.10	1.27	0.10	1.22	0.10
2.14	0.29	1.69	0.14	3.08	0.06	1.54	0.08	1.61	0.08	1.55	0.07
2.64	0.34	2.16	0.16	4.64	0.06	2.27	0.05	2.37	0.04	2.30	0.04
3.30	0.38	3.09	0.24	6.21	0.06	3.26	0.04	3.38	0.03	3.29	0.03
3.79	0.46	3.87	0.30	7.77	0.06	4.90	0.04	5.08	0.02	4.95	0.02
4.12	0.48	4.64	0.32	9.33	0.06	6.54	0.04	8.46	0.02	8.26	0.02
4.62	0.48	5.58	0.32	10.58	0.06	8.18	0.04	14.89	0.02	14.55	0.01
4.95	0.48	6.20	0.32	12.46	0.06	9.82	0.05	21.65	0.01	21.18	0.01
5.94	0.46	7.75	0.30	13.71	0.06	11.13	0.06	28.42	0.01	27.80	0.01
6.60	0.40	9.31	0.28	16.83	0.05	13.10	0.06	35.19	0.01	34.42	0.01
8.25	0.36	10.55	0.26	19.96	0.05	14.41	0.06	42.29	0.01	41.05	0.01
9.90	0.31	12.41	0.20	23.08	0.05	16.38	0.07				
11.22	0.22	13.66	0.18	26.21	0.05	17.69	0.06				
12.54	0.12	15.52	0.11	32.46	0.05	19.66	0.06				
14.52	0.06	16.77	0.08	39.02	0.06	20.98	0.06				
17.82	0.04	18.01	0.06			24.26	0.06				
21.11	0.04	19.88	0.05			27.54	0.06				
24.41	0.03	22.98	0.04			34.10	0.06				
27.71	0.02	26.09	0.03			40.99	0.05				
34.31	0.02	32.31	0.02								
39.59	0.02	38.53	0.02								

Table B-4. Hyrodgen ion leaching data for the Cecil topsoil as concentration (mol(+)/m^3) versus pore volumes of effluent.

HNO3 pH 3.0		H2SO4 pH 3.0		HNO3 pH 3.7		H2SO4 pH 3.7		HNO3 pH 4.7		H2SO4 pH 4.7	
PV	C	PV	C	PV	C	PV	C	PV	C	PV	C
0.08	0.240	0.06	0.300	0.03	0.210	0.06	0.270	0.08	0.270	0.06	0.260
0.25	0.170	0.21	0.170	0.19	0.160	0.22	0.150	0.25	0.130	0.23	0.150
0.41	0.100	0.37	0.100	0.35	0.100	0.39	0.083	0.42	0.071	0.39	0.087
0.74	0.072	0.68	0.060	0.66	0.055	0.72	0.050	0.76	0.038	0.72	0.049
1.07	0.066	0.99	0.054	0.97	0.035	1.04	0.041	1.10	0.032	1.06	0.041
1.40	0.066	1.30	0.050	1.67	0.028	1.78	0.028	1.86	0.021	1.80	0.019
1.81	0.066	1.69	0.048	2.30	0.022	2.44	0.021	2.54	0.018	2.46	0.018
2.47	0.066	2.31	0.050	3.08	0.021	3.26	0.016	3.38	0.012	3.29	0.019
3.30	0.079	3.09	0.052	4.64	0.025	4.90	0.021	5.07	0.018	4.95	0.017
4.12	0.095	3.87	0.055	6.21	0.027	6.54	0.021	8.46	0.009	8.26	0.010
4.95	0.110	4.64	0.069	7.77	0.019	8.18	0.018	11.84	0.006	11.57	0.008
5.94	0.130	5.58	0.093	9.33	0.023	9.82	0.017	15.22	0.009	14.88	0.009
6.60	0.140	6.20	0.100	10.89	0.027	11.46	0.017	18.61	0.008	18.20	0.011
8.25	0.170	7.75	0.120	14.02	0.024	14.74	0.021	21.99	0.008	21.51	0.010
9.90	0.170	9.31	0.130	17.15	0.031	18.02	0.030	25.37	0.008	24.82	0.010
13.20	0.190	12.41	0.150	20.27	0.036	21.30	0.034	28.76	0.008	28.13	0.010
16.50	0.200	15.52	0.170	23.40	0.038	24.58	0.036	32.14	0.008	31.44	0.010
19.80	0.200	18.62	0.190	26.52	0.043	27.86	0.045	35.52	0.009	34.76	0.011
23.09	0.220	21.74	0.210	29.65	0.038	31.15	0.049	38.91	0.008	38.07	0.008
26.39	0.210	24.85	0.200	32.77	0.040	34.43	0.054	42.29	0.011	41.30	0.010
29.69	0.230	27.96	0.200	35.90	0.045	37.71	0.056				
32.99	0.230	31.07	0.200	39.02	0.048	40.99	0.060				
36.29	0.250	34.18	0.220								
39.92	0.240	37.28	0.210								
		38.84	0.230								

Table B-5 Potassium leaching data for the Cecil topsoil as concentration (mol(+)/m^3) versus pore volumes of effluent.

HNO3 pH 3.0		H2SO4 pH 3.0		HNO3 pH 3.7		H2SO4 pH 3.7		HNO3 pH 4.7		H2SO4 pH 4.7	
PV	C	PV	C	PV	C	PV	C	PV	C	PV	C
0.08	1.304	0.06	1.483	0.11	1.069	0.14	0.985	0.08	1.407	0.06	1.330
0.25	0.665	0.21	0.573	0.19	0.729	0.22	0.614	0.25	0.494	0.23	0.596
0.41	0.332	0.37	0.284	0.35	0.355	0.39	0.266	0.42	0.263	0.39	0.312
0.58	0.251	0.52	0.215	0.50	0.223	0.55	0.187	0.59	0.197	0.56	0.217
0.74	0.230	0.68	0.192	0.66	0.184	0.72	0.161	0.76	0.169	0.72	0.179
1.07	0.212	0.99	0.166	0.97	0.146	1.04	0.128	1.10	0.133	1.06	0.138
1.40	0.194	1.30	0.153	1.52	0.100	1.62	0.092	1.69	0.095	1.64	0.092
1.81	0.174	1.69	0.151	2.30	0.077	2.44	0.069	2.54	0.061	2.46	0.058
2.47	0.141	2.31	0.130	3.08	0.068	3.26	0.058	3.38	0.049	3.29	0.043
3.30	0.107	3.09	0.110	4.64	0.048	4.90	0.048	5.08	0.034	4.95	0.031
4.12	0.082	3.87	0.097	6.21	0.042	6.54	0.040	8.46	0.025	8.26	0.023
4.95	0.070	4.64	0.087	7.77	0.037	8.18	0.036	11.84	0.020	11.57	0.019
6.60	0.048	6.20	0.063	10.89	0.028	11.46	0.030	15.22	0.017	14.88	0.016
8.25	0.036	7.75	0.049	14.02	0.022	14.74	0.025	18.61	0.014	18.20	0.015
9.90	0.027	9.31	0.037	17.15	0.018	18.02	0.021	21.99	0.012	21.51	0.013
11.55	0.019	10.86	0.028	20.27	0.016	21.30	0.017	28.76	0.009	28.13	0.008
13.20	0.012	12.41	0.023	23.40	0.014	24.58	0.013	35.52	0.006	34.76	0.006
14.85	0.009	13.97	0.016	26.52	0.012	27.86	0.012	42.29	0.005	41.05	0.004
18.15	0.006	17.08	0.011	32.77	0.008	34.43	0.008				
21.44	0.004	20.19	0.006	39.02	0.005	40.99	0.005				
24.74	0.005	23.30	0.005								
28.04	0.003	26.40	0.004								
31.34	0.003	29.51	0.003								
34.64	0.002	32.62	0.002								
37.94	0.002	35.73	0.002								
39.92	0.002	38.84	0.001								

Table 6-6. Magnesium leaching data for the Cecil topsoil as concentration (mol(+)/m^3) versus pore volumes of effluent

HNO3 pH 3.0		H2SO4 pH 3.0		HNO3 pH 3.7		H2SO4 pH 3.7		HNO3 pH 4.7		H2SO4 pH 4.7	
PV	C	PV	C	PV	C	PV	C	PV	C	PV	C
0.08	3.621	0.06	4.543	0.11	2.426	0.14	2.146	0.08	3.786	0.06	3.786
0.25	1.091	0.21	0.938	0.19	1.383	0.22	1.016	0.25	0.815	0.23	1.218
0.41	0.283	0.37	0.186	0.35	0.465	0.39	0.226	0.42	0.199	0.39	0.284
0.58	0.120	0.52	0.091	0.50	0.155	0.55	0.095	0.59	0.092	0.56	0.118
0.74	0.107	0.68	0.070	0.66	0.092	0.72	0.067	0.76	0.061	0.72	0.077
0.91	0.100	0.99	0.058	0.97	0.056	1.04	0.044	1.10	0.044	1.06	0.049
1.40	0.103	1.30	0.052	1.52	0.035	1.61	0.028	1.69	0.027	1.64	0.028
1.81	0.117	1.69	0.053	2.30	0.026	2.44	0.019	2.54	0.017	2.46	0.016
2.14	0.125	2.00	0.067	3.08	0.024	3.26	0.016	3.38	0.013	3.29	0.012
2.47	0.128	2.31	0.080	4.64	0.025	4.90	0.016	5.07	0.009	4.95	0.008
2.80	0.123	2.78	0.081	6.21	0.023	6.54	0.020	8.46	0.006	8.26	0.007
3.30	0.118	3.09	0.079	7.77	0.022	8.18	0.021	15.22	0.005	14.88	0.005
4.12	0.110	3.87	0.075	9.33	0.022	9.82	0.021	21.99	0.004	21.57	0.004
4.95	0.094	4.64	0.075	10.89	0.019	11.46	0.020	28.76	0.004	28.13	0.004
5.95	0.046	6.20	0.077	14.02	0.014	14.74	0.018	35.52	0.004	34.76	0.004
6.60	0.021	7.75	0.061	17.15	0.012	18.02	0.016	42.29	0.004	41.30	0.004
8.25	0.003	9.31	0.025	20.27	0.013	21.30	0.015				
11.58	0.001	10.86	0.009	26.52	0.012	24.58	0.015				
14.85	0.001	13.97	0.003	32.77	0.010	27.86	0.014				
18.15	0.000	17.08	0.002	39.02	0.007	34.43	0.011				
21.44	0.000	20.19	0.002			40.99	0.009				
28.04	0.000	26.40	0.001								
34.64	0.000	32.62	0.001								
39.92	0.000	38.84	0.001								

Table 8-7. Sodium leaching data for the Cecil topsoil as concentration (mol(+)/m^3) versus pore volumes of effluent.

HNO3 pH 3.0		H2SO4 pH 3.0		HNO3 pH 3.7		H2SO4 pH 3.7		HNO3 pH 4.7		H2SO4 pH 4.7	
PV	C	PV	C	PV	C	PV	C	PV	C	PV	C
0.08	1.543	0.06	1.804	0.11	1.004	0.14	0.952	0.08	1.552	0.06	1.511
0.25	0.500	0.21	0.426	0.19	0.589	0.22	0.426	0.25	0.365	0.23	0.465
0.41	0.157	0.37	0.139	0.35	0.209	0.39	0.130	0.42	0.130	0.39	0.170
0.58	0.094	0.52	0.090	0.50	0.079	0.55	0.080	0.59	0.081	0.56	0.097
0.74	0.064	0.68	0.069	0.66	0.058	0.72	0.058	0.76	0.057	0.72	0.063
1.07	0.034	0.99	0.037	0.97	0.032	1.04	0.028	1.10	0.028	1.06	0.031
1.40	0.019	1.30	0.022	1.52	0.012	1.62	0.013	1.69	0.017	1.64	0.013
1.81	0.016	1.69	0.011	3.08	0.005	3.26	0.006	3.38	0.007	3.29	0.007
2.47	0.013	2.31	0.006	4.64	0.004	4.90	0.003	8.46	0.004	8.26	0.004
3.30	0.005	3.09	0.007	7.77	0.003	8.18	0.002	15.22	0.003	14.88	0.003
4.95	0.005	4.64	0.005	14.02	0.003	14.74	0.002	21.99	0.002	21.57	0.003
8.25	0.004	7.75	0.003	20.27	0.002	21.30	0.001	28.76	0.002	28.13	0.003
11.55	0.004	10.86	0.002	26.52	0.001	27.86	0.003	35.52	0.002	34.76	0.005
14.85	0.003	17.08	0.003	32.77	0.001	34.43	0.002	42.29	0.002	41.30	0.005
18.15	0.002	23.30	0.003	39.02	0.002	40.99	0.002				
21.44	0.003	29.51	0.002								
24.74	0.002	35.73	0.002								
28.04	0.003	38.84	0.002								
31.34	0.002										
34.64	0.002										
37.94	0.003										
39.92	0.002										

Table B-8. Sulfate leaching data for the Cecil topsoil as concentration (mol(+)/m^3) versus pore volumes of effluent.

HNO3 pH 3.0		H2SO4 pH 3.0		HNO3 pH 3.7		H2SO4 pH 3.7		HNO3 pH 4.7		H2SO4 pH 4.7	
PV	C	PV	C	PV	C	PV	C	PV	C	PV	C
0.18	0.25	0.13	0.21	0.11	0.18	0.14	0.17	0.17	0.22	0.14	0.19
0.33	0.40	0.29	0.60	0.27	0.49	0.31	0.73	0.34	0.73	0.31	0.51
0.49	0.64	0.52	1.28	0.50	0.86	0.55	1.02	0.59	0.98	0.56	1.03
0.82	0.72	0.76	1.25	0.74	0.85	0.80	0.98	0.85	0.93	0.81	1.05
1.07	0.56	0.99	1.18	0.97	0.81	1.04	0.80	1.10	0.76	1.06	0.89
1.32	0.43	1.30	0.98	1.28	0.58	1.37	0.82	1.44	0.54	1.39	0.61
1.65	0.34	1.53	0.93	1.67	0.36	1.78	0.46	1.86	0.37	1.80	0.40
2.14	0.19	2.00	0.80	1.99	0.31	2.11	0.39	2.20	0.32	2.13	0.33
2.97	0.09	2.78	0.83	2.77	0.19	2.93	0.30	3.05	0.21	2.98	0.22
3.79	0.07	3.55	0.85	3.55	0.11	3.75	0.24	3.89	0.14	3.79	0.14
5.28	0.04	4.95	0.85	4.96	0.07	5.23	0.22	5.41	0.10	5.28	0.12
8.58	0.04	8.08	0.91	8.08	0.04	8.51	0.21	8.80	0.06	8.59	0.06
15.18	0.01	14.28	0.97	14.33	0.03	15.07	0.19	15.58	0.04	15.21	0.03
21.77	0.01	20.50	1.00	20.58	0.02	21.63	0.19	22.33	0.02	21.84	0.03
28.37	0.04	26.72	0.99	26.84	0.04	28.19	0.19	29.10	0.02	28.48	0.03
34.97	0.03	32.93	1.03	33.09	0.03	34.75	0.19	35.62	0.02	35.09	0.03
39.92	0.02	38.84	1.01	39.02	0.03	40.99	0.18	42.29	0.01	41.30	0.03

Table 8-9. Aluminum leaching data for the Cecil subsoil as concentration (mol(+)/m^3) versus pore volumes of effluent

HNO3 pH 3.0		H2SO4 pH 3.0		HNO3 pH 3.7		H2SO4 pH 3.7		HNO3 pH 4.7		H2SO4 pH 4.7	
PV	C	PV	C	PV	C	PV	C	PV	C	PV	C
0.15	0.04	0.14	0.05	0.08	0.03	0.07	0.05	0.12	0.02	0.08	0.05
0.30	0.03	0.28	0.04	0.30	0.03	0.29	0.04	0.40	0.02	0.37	0.04
0.45	0.03	0.42	0.03	0.90	0.02	0.88	0.02	0.69	0.01	0.66	0.02
0.75	0.02	0.70	0.02	1.65	0.02	1.62	0.03	1.26	0.02	1.24	0.02
1.05	0.02	0.99	0.02	3.14	0.02	3.09	0.02	1.97	0.01	1.97	0.02
1.66	0.02	1.55	0.02	4.79	0.02	4.71	0.02	3.40	0.01	3.42	0.03
2.26	0.02	2.11	0.01	6.28	0.03	6.18	0.02	4.83	0.01	4.89	0.02
3.01	0.02	2.82	0.01	7.78	0.03	7.65	0.02	7.41	0.01	7.78	0.01
4.57	0.02	4.22	0.02	9.28	0.03	9.12	0.02	10.55	0.02	10.69	0.02
6.02	0.02	5.63	0.02	12.27	0.02	12.06	0.02	16.27	0.01	16.51	0.01
7.53	0.02	7.04	0.02	15.26	0.02	15.00	0.02	21.99	0.01	22.32	0.02
9.03	0.03	8.45	0.02	21.24	0.03	20.89	0.02	27.71	0.01	28.14	0.02
10.54	0.03	9.86	0.02	27.23	0.02	26.77	0.02	33.43	0.02	33.95	0.02
12.04	0.03	11.27	0.02	33.21	0.03	32.65	0.03	39.72	0.01	40.49	0.02
13.55	0.05	12.68	0.02	39.50	0.03	39.49	0.03				
15.05	0.12	14.08	0.02								
16.56	0.20	15.49	0.02								
18.06	0.30	16.90	0.03								
19.57	0.36	18.31	0.09								
21.07	0.44	19.72	0.12								
22.58	0.47	21.13	0.14								
24.08	0.53	22.53	0.14								

Table B-9. continued

HNO3 pH 3.0		H2SO4 pH 3.0		HNO3 pH 3.7		H2SO4 pH 3.7		HNO3 pH 4.7		H2SO4 pH 4.7	
PV	C	PV	C	PV	C	PV	C	PV	C	PV	C
25.59	0.53	23.94	0.17								
27.09	0.52	25.35	0.20								
28.60	0.57	26.76	0.25								
30.10	0.53	28.17	0.29								
31.61	0.57	29.58	0.32								
33.11	0.62	30.98	0.34								
34.62	0.69	32.39	0.35								
36.12	0.71	33.80	0.38								
37.63	0.73	35.21	0.43								
39.14	0.73	36.62	0.45								
40.64	0.73	38.03	0.52								
42.07	0.73	39.44	0.56								

Table 8-10. Ammonium leaching data for the Cecil subsoil as concentration (mol(+)/m^3) versus pore volumes of effluent

HNO3 pH 3.0		H2SO4 pH 3.0		HNO3 pH 3.7		H2SO4 pH 3.7		HNO3 pH 4.7		H2SO4 pH 4.7	
PV	C	PV	C	PV	C	PV	C	PV	C	PV	C
0.15	0.11	0.14	0.11	0.15	0.10	0.15	0.19	0.19	0.12	0.08	0.19
0.30	0.07	0.28	0.11	0.30	0.09	0.29	0.17	0.33	0.10	0.15	0.16
0.45	0.09	0.42	0.10	0.45	0.13	0.44	0.13	0.47	0.09	0.30	0.13
0.60	0.14	0.56	0.09	0.60	0.11	0.59	0.10	0.62	0.07	0.44	0.10
0.83	0.14	0.70	0.12	0.90	0.12	0.88	0.09	0.76	0.07	0.59	0.10
0.90	0.14	0.84	0.11	1.20	0.09	1.18	0.09	1.04	0.06	0.73	0.08
1.05	0.15	0.99	0.11	1.50	0.13	1.47	0.10	1.40	0.06	1.03	0.07
1.20	0.12	1.13	0.11	1.95	0.08	1.91	0.08	2.12	0.06	1.39	0.07
1.50	0.10	1.41	0.10	2.69	0.07	2.65	0.07	2.83	0.04	2.12	0.06
1.81	0.10	1.69	0.09	3.44	0.06	3.38	0.06	4.26	0.04	2.84	0.06
2.11	0.10	1.97	0.09	4.49	0.07	4.41	0.07	5.69	0.04	4.30	0.05
2.56	0.09	2.39	0.08	5.98	0.07	5.88	0.06	7.12	0.04	5.75	0.05
3.31	0.09	3.10	0.08	7.48	0.06	7.35	0.06	9.98	0.05	7.20	0.05
4.06	0.08	3.80	0.07	10.47	0.08	10.30	0.06	12.84	0.06	10.11	0.05
4.82	0.08	4.57	0.07	13.46	0.06	13.24	0.06	15.70	0.05	13.02	0.05
6.32	0.09	5.91	0.07	16.46	0.06	16.18	0.05	18.56	0.05	15.93	0.04
7.83	0.08	7.32	0.08	19.45	0.06	19.12	0.05	21.42	0.04	18.83	0.04
9.33	0.07	8.73	0.08	22.44	0.05	22.06	0.06	24.28	0.04	21.74	0.03
12.34	0.06	11.55	0.07	25.43	0.05	25.00	0.06	27.14	0.03	24.65	0.03
15.35	0.05	14.36	0.07	28.42	0.05	27.95	0.06	30.00	0.03	27.55	0.03
18.36	0.05	17.18	0.07	31.42	0.05	30.89	0.05	32.86	0.03	30.46	0.02
21.37	0.04	20.00	0.06	34.41	0.05	33.83	0.04	35.72	0.03	33.37	0.02
24.38	0.04	22.82	0.05	37.40	0.05	36.77	0.04	39.72	0.03	36.28	0.02
27.39	0.04	25.63	0.05	39.50	0.05	39.49	0.04			40.49	0.02

Table B-10. continued

HNO3 pH 3.0		H2SO4 pH 3.0		HNO3 pH 3.7		H2SO4 pH 3.7		HNO3 pH 4.7		H2SO4 pH 4.7	
PV	C	PV	C	PV	C	PV	C	PV	C	PV	C
30.40	0.04	28.45	0.05								
34.02	0.04	31.27	0.05								
36.43	0.03	34.08	0.05								
39.44	0.04	36.90	0.05								
42.07	0.04	39.44	0.04								

Table 8-11. Calcium leaching data for the Cecil subsoil as concentration (mol(+)/m^3) versus pore volumes of effluent

HNO_3 pH 3.0		H_2SO_4 pH 3.0		HNO_3 pH 3.7		H_2SO_4 pH 3.7		HNO_3 pH 4.7		H_2SO_4 pH 4.7	
PV	C	PV	C	PV	C	PV	C	PV	C	PV	C
0.08	2.40	0.07	1.80	0.08	1.30	0.07	2.65	0.04	1.88	0.01	2.66
0.38	1.08	0.35	1.02	0.22	1.35	0.22	1.05	0.19	0.98	0.15	1.62
0.68	0.98	0.63	0.49	0.52	0.90	0.52	0.86	0.47	0.62	0.44	0.69
1.13	0.86	1.06	0.43	0.82	0.56	0.81	0.52	0.76	0.48	0.73	0.42
1.96	0.78	1.34	0.26	1.12	0.49	1.10	0.39	1.12	0.36	1.03	0.31
3.46	0.70	2.11	0.18	1.50	0.39	1.47	0.30	1.40	0.30	1.39	0.25
5.12	0.70	2.82	0.18	2.24	0.32	2.21	0.22	1.97	0.24	1.97	0.20
6.62	0.63	4.22	0.22	2.99	0.28	2.94	0.17	2.83	0.19	2.70	0.15
8.13	0.64	5.63	0.28	4.49	0.24	4.41	0.17	4.12	0.17	4.15	0.16
9.63	0.65	7.04	0.33	5.98	0.22	7.06	0.17	6.84	0.16	6.91	0.12
11.44	0.62	8.45	0.39	7.48	0.21	10.30	0.16	9.70	0.14	9.82	0.12
12.64	0.64	10.14	0.42	10.47	0.20	13.24	0.14	12.56	0.12	12.73	0.10
14.45	0.61	11.27	0.43	13.46	0.14	16.18	0.14	15.41	0.10	15.63	0.09
15.65	0.56	12.96	0.46	16.46	0.14	19.12	0.12	18.27	0.08	18.54	0.07
16.86	0.54	14.08	0.46	19.45	0.14	22.06	0.12	21.13	0.06	21.45	0.06
18.06	0.48	15.21	0.48	22.44	0.16	27.95	0.12	23.99	0.06	24.36	0.06
19.86	0.38	16.90	0.48	25.43	0.14	33.83	0.11	26.85	0.05	27.26	0.05
21.07	0.35	18.03	0.48	28.42	0.14	39.49	0.11	29.71	0.05	30.17	0.04
22.88	0.30	19.72	0.44	31.42	0.14			32.57	0.05	33.08	0.04
24.08	0.28	21.41	0.40	34.41	0.14			35.43	0.04	35.98	0.04
25.89	0.26	22.53	0.37	37.40	0.14			38.29	0.02	38.89	0.02
27.09	0.24	24.22	0.36	39.50	0.16			39.72	0.02	40.49	0.02
28.90	0.22	27.04	0.32								

Table B-11. continued

HNO3 pH 3.0		H2SO4 pH 3.0		HNO3 pH 3.7		H2SO4 pH 3.7		HNO3 pH 4.7		H2SO4 pH 4.7	
FV	C	FV	C	FV	C	FV	C	FV	C	FV	C
30.10	0.20	29.86	0.30								
32.81	0.18	32.67	0.27								
34.92	0.16	35.49	0.23								
37.33	0.12	39.44	0.20								
42.07	0.11										

Table 8-12. Hydrogen leaching data for the Cecil subsoil as concentration (mol(+)/m^3) versus pore volumes of effluent

HNO3 pH 3.0		H2SO4 pH 3.0		HNO3 pH 3.7		H2SO4 pH 3.7		HNO3 pH 4.7		H2SO4 pH 4.7	
PV	C	PV	C	PV	C	PV	C	PV	C	PV	C
0.08	0.051	0.07	0.047	0.08	0.046	0.07	0.056	0.12	0.042	0.08	0.056
0.22	0.046	0.21	0.044	0.30	0.041	0.29	0.045	0.26	0.035	0.23	0.045
0.37	0.042	0.35	0.035	0.52	0.032	0.52	0.031	0.34	0.030	0.37	0.035
0.53	0.001	0.49	0.023	0.75	0.002	0.74	0.023	0.69	0.021	0.66	0.026
0.75	0.001	0.70	0.000	1.50	0.000	1.47	0.000	1.40	0.006	0.95	0.010
1.50	0.000	1.41	0.000	3.14	0.003	3.09	0.001	2.83	0.005	1.53	0.003
2.26	0.000	2.11	0.000	4.79	0.005	4.71	0.001	4.26	0.008	2.84	0.004
3.01	0.001	2.82	0.001	7.78	0.007	7.65	0.003	7.12	0.003	4.30	0.007
4.57	0.006	4.22	0.002	10.77	0.002	10.59	0.002	9.98	0.005	7.20	0.003
7.53	0.019	7.04	0.003	13.76	0.002	13.53	0.002	12.84	0.005	10.11	0.007
10.54	0.016	9.56	0.004	16.76	0.001	16.47	0.001	15.70	0.006	13.02	0.007
13.55	0.019	12.68	0.009	19.75	0.001	19.42	0.001	18.56	0.002	15.92	0.007
16.56	0.056	15.49	0.011	22.74	0.001	22.36	0.001	21.42	0.001	18.83	0.004
19.57	0.078	18.31	0.010	25.73	0.002	25.30	0.001	24.28	0.001	21.74	0.002
22.58	0.091	21.13	0.027	28.72	0.002	28.24	0.001	27.14	0.001	24.65	0.001
25.59	0.095	23.94	0.031	31.72	0.001	31.18	0.001	30.00	0.001	27.55	0.002
28.60	0.098	26.76	0.036	34.71	0.002	34.12	0.001	32.86	0.001	30.46	0.001
31.61	0.102	29.58	0.045	37.10	0.002	37.06	0.001	35.72	0.001	33.37	0.002
34.62	0.115	32.39	0.050	39.50	0.002	39.49	0.001	39.72	0.001	36.28	0.002
37.63	0.115	35.21	0.058								
40.49	0.002										
40.64	0.129	38.03	0.078								
42.07	0.117	39.44	0.078								

Table B-13. Potassium leaching data for the Cecil subsoil as concentration (mol(+)/m^3) versus pore volumes of effluent.

HNO3 pH 3.0		H2SO4 pH 3.0		HNO3 pH 3.7		H2SO4 pH 3.7		HNO3 pH 4.7		H2SO4 pH 4.7	
PV	C	PV	C	PV	C	PV	C	PV	C	PV	C
0.08	0.141	0.07	0.192	0.08	0.118	0.07	0.174	0.12	0.146	0.08	0.205
0.23	0.120	0.21	0.151	0.22	0.105	0.22	0.143	0.19	0.120	0.15	0.161
0.38	0.110	0.35	0.115	0.37	0.092	0.37	0.115	0.33	0.100	0.23	0.178
0.53	0.105	0.49	0.090	0.52	0.082	0.52	0.086	0.47	0.084	0.44	0.100
0.68	0.097	0.63	0.077	0.82	0.063	0.81	0.063	0.76	0.067	0.73	0.074
0.83	0.095	0.77	0.067	1.12	0.055	1.10	0.053	1.04	0.057	1.03	0.062
1.13	0.092	1.06	0.056	1.50	0.050	1.47	0.045	1.40	0.050	1.39	0.053
1.50	0.089	1.41	0.049	2.24	0.043	2.21	0.034	2.12	0.039	2.12	0.042
2.26	0.084	2.11	0.040	2.99	0.039	2.94	0.032	2.83	0.035	2.84	0.036
3.01	0.082	2.82	0.042	4.49	0.036	4.41	0.031	4.26	0.032	4.30	0.035
4.57	0.072	3.52	0.043	7.48	0.032	7.35	0.030	7.12	0.029	7.20	0.032
6.02	0.069	4.22	0.046	10.47	0.028	10.30	0.027	9.98	0.028	10.11	0.029
7.53	0.063	5.07	0.050	13.46	0.022	13.24	0.026	12.84	0.027	13.02	0.025
9.03	0.055	5.63	0.054	16.46	0.019	16.18	0.025	15.41	0.021	15.63	0.021
10.54	0.052	6.48	0.055	19.45	0.017	19.12	0.021	18.27	0.017	18.54	0.017
13.55	0.042	7.04	0.058	22.44	0.015	22.06	0.019	21.13	0.015	21.45	0.014
16.56	0.030	8.45	0.058	25.43	0.014	25.00	0.018	23.99	0.013	24.86	0.012
19.57	0.020	9.86	0.057	28.42	0.013	27.95	0.015	26.85	0.011	27.26	0.012
22.58	0.017	11.27	0.050	34.41	0.011	33.83	0.014	32.57	0.009	33.08	0.007
25.59	0.013	12.68	0.047	39.50	0.010	39.49	0.011	39.72	0.007	40.49	0.006
31.61	0.010	14.08	0.043								
37.63	0.007	15.49	0.039								
42.07	0.006	18.31	0.031								

Table 8-13 continued

HNO3 pH 3.0		H2SO4 pH 3.0		HNO3 pH 3.7		H2SO4 pH 3.7		HNO3 pH 4.7		H2SO4 pH 4.7	
PV	C	PV	C	PV	C	PV	C	PV	C	PV	C
		21.13	0.028								
		23.94	0.023								
		29.58	0.015								
		35.21	0.012								
		39.44	0.008								

Table 8-14. Magnesium leaching data for the Cecil subsoil as concentration (mol(+)/m^3) versus pore volumes of effluent.

HNO3 pH 3.0		H2SO4 pH 3.0		HNO3 pH 3.7		H2SO4 pH 3.7		HNO3 pH 4.7		H2SO4 pH 4 7	
PV	C	PV	C	PV	C	PV	C	PV	C	PV	C
0.08	0.481	0.07	0.746	0.08	0.453	0.07	0.823	0.04	0.461	0.01	0.778
0.38	0.420	0.21	0.581	0.22	0.479	0.22	0.672	0.19	0.299	0.15	0.556
0.68	0.344	0.35	0.385	0.37	0.363	0.37	0.444	0.33	0.224	0.30	0.358
0.98	0.326	0.49	0.222	0.52	0.262	0.52	0.253	0.47	0.184	0.44	0.231
1.28	0.319	0.63	0.166	0.67	0.218	0.66	0.184	0.62	0.156	0.59	0.179
1.66	0.306	0.77	0.133	0.82	0.185	0.81	0.146	0.76	0.135	0.73	0.132
2.26	0.249	1.06	0.090	1.12	0.141	1.10	0.103	1.04	0.101	1.03	0.095
3.01	0.238	1.41	0.070	1.50	0.119	1.47	0.079	1.40	0.080	1.39	0.075
4.52	0.235	2.11	0.042	2.24	0.083	2.21	0.049	2.12	0.055	2.11	0.054
6.02	0.229	2.82	0.043	2.99	0.071	2.94	0.042	2.83	0.044	2.84	0.047
7.53	0.226	4.22	0.063	4.49	0.062	4.41	0.038	4.26	0.043	4.30	0.044
9.03	0.216	5.63	0.085	7.48	0.054	7.35	0.038	7.12	0.038	7.20	0.040
10.54	0.215	7.04	0.109	10.47	0.049	10.30	0.035	9.98	0.033	10.11	0.035
12.04	0.190	8.45	0.127	13.46	0.039	13.24	0.030	12.84	0.029	13.02	0.030
13.55	0.164	9.86	0.142	16.46	0.034	16.18	0.028	15.41	0.023	15.63	0.026
15.05	0.125	11.27	0.147	19.45	0.035	19.12	0.026	18.27	0.020	18.54	0.021
16.56	0.108	12.68	0.147	22.44	0.036	22.06	0.026	21.13	0.016	21.45	0.018
18.06	0.088	14.08	0.143	24.43	0.035	25.00	0.024	26.85	0.013	27.26	0.015
19.57	0.076	15.49	0.143	28.42	0.035	27.95	0.025	32.57	0.011	33.08	0.012
22.58	0.055	16.90	0.130	31.42	0.031	30.89	0.024	39.72	0.009	46.34	
25.59	0.045	18.31	0.123	34.41	0.035	33.83	0.024				
28.60	0.030	19.72	0.107	37.40	0.034	36.77	0.025				
31.61	0.020	21.13	0.095	39.50	0.034	39.42	0.024				

Table B-14. continued

HNO3 pH 3.0		H2SO4 pH 3.0		HNO3 pH 3.7		H2SO4 pH 3.7		HNO3 pH 4.7		H2SO4 pH 4.7	
PV	C	PV	C	PV	C	PV	C	PV	C	PV	C
34.62	0.010	22.53	0.084								
37.63	0.005	23.94	0.079								
40.64	0.003	26.76	0.065								
42.07	0.002	29.58	0.052								
		32.39	0.043								
		35.21	0.035								
		39.44	0.028								

Table B-15. Sodium leaching data for the Cecil subsoil as concentration (mol(+)/m^3) versus pore volumes of effluent

HNO3 pH 3.0		H2SO4 pH 3.0		HNO3 pH 3.7		H2SO4 pH 3.7		HNO3 pH 4.7		H2SO4 pH 4.7	
PV	C	PV	C	PV	C	PV	C	PV	C	PV	C
0.08	0.346	0.07	0.446	0.06	0.617	0.07	0.843	0.04	0.539	0.01	0.761
0.23	0.274	0.21	0.322	0.22	0.443	0.22	0.557	0.19	0.409	0.16	0.513
0.38	0.230	0.35	0.187	0.37	0.352	0.37	0.313	0.33	0.326	0.30	0.322
0.53	0.174	0.49	0.126	0.52	0.243	0.52	0.174	0.47	0.261	0.44	0.217
0.68	0.122	0.63	0.093	0.67	0.165	0.66	0.125	0.62	0.209	0.59	0.196
0.98	0.046	0.92	0.060	0.62	0.115	0.81	0.096	0.76	0.165	0.73	0.119
1.28	0.024	1.20	0.039	1.12	0.065	1.10	0.063	1.04	0.107	1.03	0.074
1.66	0.014	1.55	0.025	1.50	0.030	1.47	0.037	1.40	0.063	1.39	0.044
2.26	0.010	2.11	0.015	2.24	0.010	2.21	0.013	2.12	0.020	2.12	0.022
3.01	0.010	2.82	0.011	2.99	0.004	2.94	0.007	2.83	0.010	2.64	0.013
4.52	0.006	4.22	0.008	4.49	0.001	4.41	0.003	4.26	0.003	4.30	0.006
7.53	0.005	7.04	0.007	7.46	0.002	7.35	0.003	7.12	0.001	7.20	0.003
10.54	0.004	9.86	0.006	10.47	0.001	10.30	0.001	9.98	0.001	10.11	0.001
16.56	0.004	15.49	0.003	13.46	0.001	13.24	0.000	12.84	0.003	13.02	0.001
22.58	0.003	21.13	0.003	19.45	0.000	19.12	0.000	18.27	0.001	18.54	0.000
28.60	0.006	26.76	0.007	25.43	0.000	25.00	0.000	23.99	0.000	24.36	0.000
34.62	0.004	32.39	0.010	31.42	0.000	30.89	0.000	29.71	0.001	30.17	0.003
39.14	0.004	36.62	0.006	39.50	0.000	39.49	0.000	35.43	0.000	35.98	0.000
42.07	0.004	39.44	0.004					39.72	0.000	40.49	0.000

Table B-16. Sulfate leaching data for the Cecil subsoil as concentration (mol(+)/m^3) versus pore volumes of effluent.

HNO3 pH 3.0		H2SO4 pH 3.0		HNO3 pH 3.7		H2SO4 pH 3.7		HNO3 pH 4.7		H2SO4 pH 4.7	
PV	C	PV	C	PV	C	PV	C	PV	C	PV	C
0.23	0.04	0.21	0.02	0.52	0.02	0.22	0.03	0.26	0.05	0.52	0.03
0.53	0.05	0.49	0.02	1.12	0.04	0.52	0.03	0.47	0.05	1.10	0.06
1.13	0.04	1.06	0.05	1.80	0.07	1.10	0.08	1.12	0.08	1.68	0.11
1.81	0.03	1.69	0.13	3.29	0.10	1.77	0.13	1.69	0.11	2.41	0.15
3.37	0.03	3.10	0.26	5.39	0.10	2.50	0.18	2.40	0.15	3.13	0.17
4.82	0.03	4.51	0.37	7.18	0.11	3.24	0.20	3.12	0.17	4.15	0.17
6.32	0.04	5.91	0.47	8.68	0.11	3.97	0.21	5.12	0.17	5.46	0.17
7.83	0.03	7.32	0.55	11.67	0.10	5.30	0.22	6.55	0.17	6.91	0.16
13.85	0.03	10.14	0.66	14.66	0.10	6.77	0.20	7.98	0.17	8.66	0.15
19.87	0.02	12.96	0.68	17.35	0.07	8.24	0.21	9.12	0.16	9.82	0.13
25.89	0.02	15.77	0.73	20.35	0.06	11.18	0.19	10.84	0.15	11.56	0.11
31.91	0.02	18.59	0.74	26.33	0.04	14.12	0.17	13.70	0.13	14.47	0.10
37.93	0.02	21.41	0.73	32.31	0.03	17.06	0.15	16.56	0.11	17.38	0.08
42.07	0.02	24.22	0.78	39.50	0.02	20.00	0.15	19.42	0.08	20.29	0.06
		27.04	0.79			22.94	0.14	25.14	0.06	26.10	0.05
		29.86	0.77			25.89	0.14	30.86	0.04	31.92	0.03
		32.67	0.81			28.83	0.14	39.72	0.03	40.49	0.03
		35.49	0.84			31.77	0.14				
		39.44	0.91			34.71	0.14				
						39.49	0.13				

APPENDIX C

COMPUTER PROGRAM

The mixing-cell transport model and the two-site chemical submodel are listed below. The chemical model includes pH-dependent anion sorption. The transport model includes a section of code to handle the initial wetting phase (transient flow) of leaching for soil columns. Both this section of the transport model and the additional parameters and dimensions in both the transport and chemical models needed for inclusion of nonequilibrium adsorption may be deleted to give code applicable to steady flow and equilibrium exchange. Variables used are defined for both the transport and chemical models.

```
C
C MIXING-CELL TRANSPORT MODEL
C
C VARIABLE LIST:
C  ARRAYS-
C   C(I,K) IS THE SOLUTION CONCENTRATION ARRAY WHERE I=1,9
C    REFERS TO SPECIES (I=1, NH4; I=2, K; I=3, NA; I=4 CA;
C    I=5, MG; I=6, AL, I=7, H; I=8, SO4, AND I=9, MONOVALENT
C    ANIONS), AND K=1,11 REFERS TO CELL NUMBER ( CELL
C    NO. 1 IS OUTSIDE THE COLUMN AND CONTAINS THE INPUT
C    SOLUTION)
C   X(I,J,K) IS THE SORBED PHASE ARRAY.  DIMENSIONS I AND K
C    ARE AS ABOVE.  DIMENSION J=1,2 REFERS TO EQUILIBRIUM OR
C    KINETIC SITES, RESPECTIVELY
C   POWER(I) STORES VALENCES OF THE SEVERAL SPECIES
C   BEGIN(I) STORES INITIAL QUANTITIES OF THE SEVERAL SPECIES
C   AMOUNT(I) STORES RESIDUAL QUANTITIES OF THE SEVERAL
C    SPECIES REMAINING IN THE COLUMN AT CESSATION OF LEACHING
C   SIGMA(I) STORES THE TOTAL QUANTITIES OF IONS LEACHED
C   CONC AND ENTER(I) ARE USED TO HOLD RESIDENT
C    CONCENTRATIONS OF AND INPUT CONCENTRATIONS TO A CELL,
C    RESPECTIVELY, DURING A FLOW STEP
C   CEC(J) ARE THE EXCHANGE CAPACITIES FOR EQUILIBRIUM AND
C    KINETIC SITES
C  SINGLE VARIABLES-
C    VOLUME IS THE SOLUTION VOLUME OF A CELL
C    RK1, RK2, RK3, R4, R5, AND R6 ARE GAINES-THOMAS
C    SELECTIVITY COEFFICIENTS FOR H EXCHANGE FOR NH4, K, NA
C    CA, MG, AND AL, RESPECTIVELY
C   R IS THE RATIO XAL/(XH**3)
C   COEF1 AND COEF2 ARE COEFFICIENTS OF THE SORPTION
C    ISOTHERMS FOR SO4 AND MONOVALENT ANIONS
C   EX1, EX2, EX3, AND EX4 ARE THE EXPONENTS IN THESE
C    ISOTHERMS
C   FACT1 IS f, EQS. [12] AND [13]
C   FACT2 IS (1-f)
C   ZT IS (RII)T, EQS. [43] AND [45]
C   PV IS PORE VOLUME
C   NSEG IS THE NUMBER OF CELLS
C   NSTOP IS THE TOTAL NUMBER OF FLOW STEPS, BEYOND THE
C    WETTING PHASE, LEACHING OCCURS
C   N, NCOUNT, NN, AND NCOUNT ARE USED TO INDICATE WHERE
C    AND HOW MANY TIMES THE EQUILIBRIUM CRITERIA IN THE
C    CHEMICAL SUBROUTINE WERE NOT MET
C   OTHER VARIABLES ARE DEFINED AND USED LOCALLY
C
```

```
      DIMENSION C(9,11),X(9,2,11),POWER(9), AMOUNT(9),
     $ BEGIN(9),ENTER(9),CEC(2), $ SIGMA(9)
      OPEN(UNIT=10,FILE='NPTSUB',STATUS='OLD')
      OPEN(UNIT=12,FILE='BTCSUB',STATUS='NEW')
      READ(10,*) NSEG,NSTOP,CEC(1),CEC(2), VOLUME
      READ(10,*) FACT1,FACT2,ZT, COEF1, COEF2
      DO 101 I=1,9
       READ(10,*) C(I,2),X(I,1,2),POWER(I)
       IF(I .GE. 8) THEN
        X(I,2,2)=0.0
       ELSE
        X(I,2,2)=X(I,1,2)
       ENDIF
  101 CONTINUE
      DO 102 I=1,9
       READ(10,*) C(I,1),X(I,1,1)
       C(I,2,1)=C(I,1,1)
       X(I,2,1)=X(I,1,1)
  102 CONTINUE
      DO 103 I=1,9
       DO 104 J=3,NSEG
        C(I,J)=C(I,2)
        X(I,1,J)=X(I,1,2)
        X(I,2,J)=X(I,2,2)
  104  CONTINUE
  103 CONTINUE
      DO 105 I=1,7
       BEGIN(I)=C(I,2)*VOLUME*POWER(I)+
     $ X(I,1,2)*(CEC(1)+CEC(2))
       BEGIN(I)=(FLOAT(NSEG-1))*BEGIN(I)
  105 CONTINUE
      DO 106 I=8,9
       BEGIN(I)=C(I,2)*VOLUME*POWER(I)+X(I,1,2)
       BEGIN(I)=(FLOAT(NSEG-1))*BEGIN(I)
  106 CONTINUE
      NCOUNT=0
      MCOUNT=0
      DO 3 I=2,NSEG
       DO 4 J=1,9
        ENTER(J)=C(J,1)
        DO 44 K=2, I
         IF(K .EQ. I) THEN
          C(J,K)=ENTER(J)+C(J,K)
         ELSE
          CONC=C(J,K)
          C(J,K)=ENTER(J)*FACT1+CONC*FACT2
          ENTER(J)=ENTER(J)*FACT2+CONC*FACT1
         ENDIF
   44   CONTINUE
    4  CONTINUE
       DO 5 L=2,I
         CALL GETRED(C(1,L),X(1,1,L),X(1,2,L),C(2,L),(2,1,L),
     $    X(2,2,L),C(3,L),X(3,1,L),X(3,2,L),C(4,L),X(4,1,L),
     $    X(4,2,L),C(5,L),X(5,1,L),X(5,2,L),C(6,L),X(6,1,L),
   $     X(8,2,L),C(7,L),X(7,1,L),X(7,2,L),C(8,L),C(8,1,L),
   $     C(9,L),X(9,1,L),CEC(1),CEC(2),VOLUME,
   $     RK1,RK2,RK3,R4,R5,R6,R,
   $     COEF1,COEF2,EX1,EX2,EX3,EX4,ZT,N,NN)
        IF(N .EQ. 100) NCOUNT=NCOUNT+1
        IF(NN .EQ. 100) MCOUNT=MCOUNT+1
  5   CONTINUE
  3  CONTINUE
     DO 10 I=1,9
      SIGMA(I)=0.0
 10  CONTINUE
     DO 11 I=1,NSTOP
      DO 13 J=1,9
       ENTER(J)=C(J,1)
       DO 133 K=2,NSEG
        CONC=C(J,K)
        C(J,K)=ENTER(J)*FACT1+CONC*FACT2
         ENTER(J)=ENTER(J)*FACT2+CONC*FACT1
133     CONTINUE
 13    CONTINUE
       PV=FLOAT(I)/FLOAT(NSEG-1)
       PPV=FLOAT(2*I/(NSEG-1))
       IF(PPV .EQ. 2.0*PV) WRITE(12,1000) PV,
     $  ENTER(1)*1000.0,ENTER(2)*1000.0,ENTER(3)*1000.0,
     $  ENTER(4)*2000.0,ENTER(5)*2000.0,ENTER(6)*3000.0,
     $  ENTER(7)*1000.0,ENTER(8)*2000.0,ENTER(9)*1000.0
       DO 40 NN=1,9
        SIGMA(NN)=SIGMA(NN)+ENTER(NN)*VOLUME*POWER(NN)
 40    CONTINUE
       DO 14 L=2,NSEG
        CALL GETRED(C(1,L),X(1,1,L),X(1,2,L),C(2,L),X(2,1,L),
     $   X(2,2,L),C(3,L),X(3,1,L),X(3,2,L),C(4,L),X(4,1,L),
     $   X(4,2,L),C(5,L),X(5,1,L),X(5,2,L),C(6,L),X(6,1,L),
     $   X(6,2,L),C(7,L),X(7,1,L),X(7,2,L),C(8,L),C(8,1,L),
     $   C(9,L),X(9,1,L),CEC(1),CEC(2),VOLUME,
     $   RK1,RK2,RK3,R4,R5,R6,R,
     $   COEF1,COEF2,EX1,EX2,EX3,EX4,ZT,N,NN)
         IF(N .EQ. 100) NCOUNT=NCOUNT+1
         IF(NN .EQ. 100) MCOUNT=MCOUNT+1
 14    CONTINUE
 11   CONTINUE
      DO 50 I=1,7
       AMOUNT(I)=0.0
       DO 51 J=2,NSEG
        AMOUNT(I)=AMOUNT(I)+C(I,J)*VOLUME*POWER(I)
     $   +(X(1,1,J)*CEC(1)+X(I,2,J)*CEC(2))
 51    CONTINUE
 50   CONTINUE
      DO 52 I=8,9
       AMOUNT(I)=0.0
       DO 53 J=2,NSEG
        AMOUNT(I)=AMOUNT(I)+C(I,J)*VOLUME*POWER(I)+X(I,1,J)
 53    CONTINUE
```

```
  52  CONTINUE
     DO 54 I=1,9
      WRITE(12,2000) SIGMA(I)*1000.0,AMOUNT(I)*1000.0,
    $  BEGIN(I)*1000.0
  54 CONTINUE
     WRITE(12,*) NCOUNT
     WRITE(12,*) MCOUNT
1000 FORMAT(X,F5.2,9F7.3)
2000 FORMAT(X,3F7.3)
     STOP
     END
```

```
C
C CHEMICAL EQUILIBRIUM MODEL
C
C VARIABLE LIST:
C  CNH4,...,CCL ARE THE SOLUTION CONCENTRATIONS OF THE
C   SEVERAL SPECIES
C  CTOT IS THE TOTAL CONCENTRATION, IN EQUIVALENTS, OF
C   CATIONS
C  XNH4,...,XH ARE THE EQUIVALENT FRACTIONS OF CATIONS ADSORBED
C   ONTO EQUILIBRIUM EXCHANGE SITES
C  XNH42,...,XH2 ARE THE EQUIVALENT FRACTIONS OF CATIONS
C   ADSORBED ONTO RATE DEPENDENT EXCHANGE SITES
C  SORB1 IS SORBED SO4
C  SORB2 IS SORBED MONOVALENT ANIONS
C  T1T,...,T5T ARE TOTAL EQUIVALENTS OF BASIC CATIONS
C   NH4,...,MG IN THE CELL
C  T1,...,T5 ARE TOTAL EQUIVALENTS OF BASIC CATIONS
C   NH4,...,MG IN SOLUTION AND ADSORBED ONTO EQUILIBRIUM
C    EXCHANGE SITES
C  T8 AND T9 ARE TOTAL EQUIVALENTS OF SO4 AND MONOVALENT
C   ANIONS, RESPECTIVELY
C  TAT IS TOTAL ACIDITY IN THE CELL
C  TA IS TOTAL ACIDITY IN SOLUTION AND ADSORBED ONTO
C   EQUILIBRIUM SITES
C  SK1 AND SK2 ARE THE ION PAIR CONSTANTS FOR CASO4 AND
C   MGSO4, RESPECTIVELY
C  CSO4E1 AND CSO4E2 ARE ESTIMATES OF THE CONCENTRATION OF
C   SO4 EXCLUSIVE OF THE ABOVE ION PAIRS
C  A AND B ARE COEFFICIENTS OF THE SORPTION ISOTHERMS FOR
C   SO4 AND MONOVALENT ANIONS, RESPECTIVELY
C  SIONIC IS THE IONIC STRENGTH
C  GAMMA1, GAMMA2, AND GAMMA3 ARE ACTIVITY COEFFICIENTS
C   CALCULATED FROM THE DAVIES EQUATION
C  CHECK, RELATV, TEST, EST, COMP, AND DELTA ARE USED TO
C   EXAMINE WHETHER CERTAIN CRITERIA ARE SATISFIED
C  K AND LL INDICATE WHETHER EQUILIBRIUM CRITERIA HAVE BEEN
C   MET AND COMMUNICATE THIS INFORMATION TO THE MAIN PROGRAM
C  OTHER VARIABLES ARE DEFINED AND USED LOCALLY
C
```

```
 SUBROUTINE GETRED (CNH4,XNH4,XNH42,CK,XK,XK2,CNA,XNA,XNA2,
$ CCA,XCA,XCA2,CMG,XMG,XMG2,CAL,XAL,XAL2,CH,XH,XH2,CSO4,
$ SORB1,CCL,SORB2,Q,Q2,V,RK1,RK2,RK3,R4,R5,R6,R,A,B,EX1,
$ EX2,EX3,EX4,ZT,K,LL)
 REAL CNH4,XNH4,XNH42,CK,XK,XK2,CNA,XNA,XNA2,CCA,XCA,XCA2,
$ CMG,XMG,XMG2,CAL,XAL,XAL2,CH,XN,XN2,CSO4,SORB1,CCL,
$ SORB2,Q,Q2,V,RK1,RK2,RK3,R4,R5,R6,R,A,B,EX1,EX2,EX3,EX4,
$ ZT,ALPHA,TEST,Y,DY,HIGH,AMED,ALOW,CHECK,F1,F2,RELATV,
$ T1,T2,T3,T4,T5,TA,T1T,T2T,T3T,T4T,T5T,TAT,SK1,SK2,CSO4E1,
$ CSO4E2,COMP,SIONIC,FACTOR,GAMMA1,GAMMA2,GAMMA3,RATIO1,
$ RATIO2,DELTAX,COEF1,COEF2,CTOT,Z,DZ,EST,DELTA,T8,T9,RK4,
$ RK5,RK6
 INTEGER K,M,N,LL,J,LNM
 SK1=2.04E+02
 SK2=1.70E+02
 T1=CNH4*V+XNH4*Q
 T2=CK*V+XK2*Q
 T3=CNA*V+XNA2*Q
 T4=2.0*CCA*V+XCA*Q
 T5=2.0CMG*V+XMG*Q
 TA=(CH+3.0*CAL)*V+(SORB1+SORB2)+(XN+XAL)*Q
 T8=2.0*CSO4*V+SORB1
 T9=CCL*V+SORB2
 T1T=T2+XNH42*Q2
 T2T=T2+XK2*Q2
 T3T=T3+XNA2*Q2
 T4T=T4+XCA2*Q2
 T5T=T5+XMG2*Q2
 TAT=TA+(XN2+XAL2)*Q2
 LNM=0
 DO 200 MMM=1,2
 DO 100 NN=1,2
  LL=0
  COEF1=A*(CH**EX2)
  HIGH=T8/(2.0*V)
  ALOW=0.0
  AMED=HIGH/2.0
  DO 20 I=1,100
   CSO4=AMED
   SORB1=T8-CSO4*2.0*V
   F1=COEF1*(CSO4**EX1)-SORB1
   IF(SORB1 .LT. 1.00E-30) GO TO 21
   CHECK=F1/SORB1
   IF(ABS(CHECK) .LT. 0.001) GO TO 21
   IF(CHECK .LT. 0.0) THEN
    HIGH=HIGH
    ALOW=AMED
    AMED=(HIGH+ALOW)/2.0
   ELSE
    HIGH=AMED
    ALOW=ALOW
    AMED=(HIGH+ALOW)/2.0
```

```
      ENDIF
 20   CONTINUE
      LL=100
 21   COEF2=B*(CH**EX4)
      HIGH=T9/V
      ALOW=0.0
      AMED=HIGH/2.0
      DO 30 I=1,100
       CCL=AMED
       SORB2=T9-CCL*V
       F2=COEF2*(CCL**EX3)-SORB2
       IF(SORB2 .LT. 1.00E-30) GO TO 31
       RELATV=F2/SORB2
       IF(ABS(RELATV) .LT. 0.001) GO TO 31
       IF(RELATV .LT. 0.0) THEN
        HIGH=HIGH
        ALOW=AMED
        AMED=(HIGH+ALOW)/2.0
       ELSE
        HIGH=AMED
        ALOW=ALOW
        AMED=(HIGH+ALOW)/2.0
       ENDIF
 30    CONTINUE
      LL=100
 31   CTOT=2.0*CSO4+CCL
      SIONIC=0.5*(CNH4+CK+CNA+4.0*CCA+4.0*CMG+9.0*CAL+CH+4.0*
     $ CSO4+CCL)
      FACTOR=-0.5*(SQRT(SIONIC)/(1.0+SQRT(SIONIC))-0.3*SIONIC)
      GAMMA1=10.0**FACTOR
      GAMMA2=10.0**(4.0*FACTOR)
      GAMMA3=10.0**(9.0*FACTOR)
      RATIO1=GAMMA1*GAMMA1/GAMMA2
      RATIO2=GAMMA1*GAMMA1*GAMMA1/GAMMA3
      RK4=RATIO1*R4
      RK5=RATIO1*R5
      RK6=RATIO2*R6
      Y=CH+3.0*RK6*R*CH*CH-CTOT
      TEST=ABS(Y)
      N=0
      DO WHILE(TEST .GE. CTOT/1000.0 .AND. N .LE. 99)
       DY=1.0+9.0*RK6*CH*CH
       CH=(DY*CH-Y)/DY
       Y=CH+3.0*RK6*CH*CH*CH-CTOT
       TEST=ABS(Y)
       N=N+1
      ENDDO
      HIGH=CH
      ALOW=0.0
      AMED=HIGH/2.0
      K=0
      DO 10 I=1,100
     K=K+1
     CH=AMED
     ALPHA=(TA-(CH+3.0*RK6*CH*CH*CH)*V-(SORB1+SORB2))/Q
     Z=XH+R*XH*XH*XH-ALPHA
     EST=ABS(Z)
     M=0
     DO WHILE(EST .GE. ALPHA/100000.0 .AND. M .LE. 99)
     DZ=1.0+3.0*R*XH*XH
     XH=(DZ*XH-Z)/DZ
     Z=XH+R*XH*XH*XH-ALPHA
     EST=ABS(Z)
     M=M+1
    ENDDO
    CNH4=(T1*RK1*CH/XH)/(Q+RK1*V*CH/XH)
    CK=(T2*RK2*CH/XH)/(Q+RK2*V*CH/XH)
    CNA=(T3*RK3*CH/XH)/(Q+RK3*V*CH/XH)
    CSO4E1=0.0
    IF(CSO4 .LT. 1.00E-20) GO TO 40
    CSO4E1=CSO4/(1.0+GAMMA2*GAMMA2*(SK1*CCA+SK2*CMG))
    COMP=1.0
    J=0
    DO WHILE(COMP .GT. 0.001 .AND. J .LE. 99)
     CCA=T4/(2.0*V*(1.0+GAMMA2*GAMMA2*SK1*CSO4E1)+Q*XH*XH/
   $  (RK4*CH*CH))
     CMG=T5/(2.0*V*(1.0+GAMMA2*GAMMA2*SK2*CSO4E1)+Q*XH*XH/
   $  (RK5*CH*CH))
     CSO4E2=CSO4/(1.0+GAMMA2*GAMMA2*(SK1*CCA+XK2*CMG))
     COMP=ABS(1.0-CSO4E2/CSO4E1)
     CSO4E1=CSO4E2
     J=J+1
    ENDDO
    CAL=RK6*R*CH*CH*CH
    CCA=CCA+GAMMA2*GAMMA2*SK1*CSO4E1*CCA
    CMG=CMG+GAMMA2*GAMMA2*SK1*CSO4E1*CMG
    DELTA=CNH4+CK+CMA+2.0*CMG+3.0*CAL+CH-CTOT
    IF(ABS(DELTA) .LT. CTOT/1000.0) GO TO 100
    IF(DELTA .LT. 0.0) THEN
     HIGH=HIGH
     ALOW=AMED
     AMED=(HIGH+ALOW)/2.0
    ELSE
     HIGH=AMED
     ALOW=ALOW
     AMED=(HIGH+ALOW)/2.0
    ENDIF
 10 CONTINUE
100 CONTINUE
    XNH4=T1/Q-CNH4*V/Q
    XK=T2/Q-CK*V/Q
    XNA=T3/Q-CNA*V/Q
    XCA=T4/Q-2.0*CCA*V/Q
    XMG=T5/Q-2.0*CMG*V/Q
```

```
      XAL=R*XH*XH*XH
      IF(LMN .EQ. 1) RETURN
      XNH42=SORBED(T1T,RK1,XH,XH2,CH,Q,Q2,V,1.0,XNH42,ZT)
      XK2=  SORBED(T2T,RK2,XH,XH2,CH,Q,Q2,V,1.0,XK2,ZT)
      XNA2= SORBED(T3T,RK3,XH,XH2,CH,Q,Q2,V,1.0,XNA2,ZT)
      XCA2= SORBED(T4T,RK4,XH,XH2,CH,Q,Q2,V,2.0,XCA2,ZT)
      XMG2= SORBED(T5T,RK5,XH,XH2,CH,Q,Q2,V,2.0,XMG2,ZT)
      DELTAX=1.0-(XNH42+XK2+XNA2+XCA2+XMG2)
      Z=XH2+R*XH2*XH2*XH2-DELTAX
      EST=ABS(Z)
      M=0
      DO WHILE(EST .GE. DELTAX/100000.0 .AND. M .LE. 99)
      DZ=1.0+3.0*R*XH2*XH2
      XH2=(DZ*XH2-Z)/DZ
      Z=XH2+R*XH2*XH2*XH2-DELTAX
      EST=ABS(Z)
      M=M+1
      ENDDO
      XAL2=DELTAX-XH2
      T1=T1T-XNH42*Q2
      T2=T2T-XK2*Q2
      T3=T3T-XNA2*Q2
      T4=T4T-XCA2*Q2
      T5=T5T-XMG2*Q2
      TA=TAT-DELTAX*Q2
      LNM=1
  200 CONTINUE
      END
     C
     C  THIS FUNCTION CALCULATES CATION ADSORPTION/
     C   DESORPTION FOR THE KINETIC SITES ACCORDING TO
     C   EQ[45]
     C
      FUNCTION SORBED(T,RK,SH1,SH2,CONCH,CHARG1,CHARG2,VOL,
     $ POW,XSTART,ZZ)
      REAL T,RK,SH1,SH2,CONCH,CHARG1,CHARG2,VOL,POW,XSTART,
     $ ZZ,A,B,C
      A=(T*(1.0/RK)*((SH2/CONCH)**POW))/
     $ (VOL+CHARG1*(1.0/RK*((SH1/CONCH)**POW))
      B=1.0+(CHARG2*(1.0/RK)*((SH2/CONCH)**POW))/
     $ (VOL+CHARG1*(1.0/RK)*((SH1/CONCH)**POW))
      C=(1.0/RK)*((SH2/CONCH)**POW)
      SORBED=(1.0/B)*(A-(A-B*XSTART)*EXP(-B*ZZ/C))
      RETURN
      END
```

BIOGRAPHICAL SKETCH

The little guy who came to be called Lewis Gaston was made sometime in the spring of 1953 and he waited until the day after Christmas to be born. He lived with his parents, Madge and Erskin, in Shreveport, Louisiana, where he later attended primary and secondary schools. He received an equivalency degree from Byrd High in 1972. He attended Louisiana State University where he studied chemistry. He received a BA from that institution in 1977. Subsequently he worked in private industry but returned to college later for further study. He earned an MS in agronomy from Louisiana State University in 1982. During that same year he then began study and research at the University of Florida toward a PhD in soil science. About the time he came to the University of Florida he married Cathy Figg. Two children, Mary, then Peter, have since been born to him and his wife.

I certify that I have read this study and that in my opinion it conforms to acceptable standards of scholarly presentation and is fully adequate, in scope and quality, as a dissertation for the degree of Doctor of Philosophy.

Robert S. Mansell

Robert S. Mansell, Chairman
Professor of Soil Science

I certify that I have read this study and that in my opinion it conforms to acceptable standards of scholarly presentation and is fully adequate, in scope and quality, as a dissertation for the degree of Doctor of Philosophy.

R D Rhue

R. Dean Rhue, Cochairman
Associate Professor of Soil Science

I certify that I have read this study and that in my opinion it conforms to acceptable standards of scholarly presentation and is fully adequate, in scope and quality, as a dissertation for the degree of Doctor of Philosophy.

PSC Rao

P. Suresh C. Rao
Professor of Soil Science

I certify that I have read this study and that in my opinion it conforms to acceptable standards of scholarly presentation and is fully adequate, in scope and quality, as a dissertation for the degree of Doctor of Philosophy.

Allen R. Overman
Allen R Overman
Professor of Agricultural
Engineering

I certify that I have read this study and that in my opinion it conforms to acceptable standards of scholarly presentation and is fully adequate, in scope and quality, as a dissertation for the degree of Doctor of Philosophy.

William W. McFee
William W. McFee
Professor of Soil Science

This dissertation was submitted to the Graduate Faculty of the College of Agriculture and to the Graduate School and was accepted as partial fulfillment of the requirements for the degree of Doctor of Philosophy

August 1987

G.L. Zachariah
Dean, College of Agriculture

Dean, Graduate School